

Removal of Organic Foulants from Capillary Ultrafiltration Membranes by Use of Ultrasound

AM Nel

Thesis presented in partial fulfilment of the requirements for the degree of Master
of Engineering at the university at the University of Stellenbosch.



Study leader: C Aldrich

December 2005

Declaration

I, the undersigned, hereby declare that the work contained in this thesis is my own original work and that I have not previously in its entirety or in part submitted it at any university for a degree.

Signature:

Date:

Summary

Fouling is a serious problem in membrane filtration, caused by pore plugging and adsorption of rejected macromolecules or other solutes in the membrane system. This requires periodic cleaning of membranes, which can add considerably to the overall cost of plant operation owing to lost productivity related to down-time, the cost of the chemicals used in cleaning, higher pressures and associated pumping costs to maintain membrane productivity, as well as reduced lifetime of the membranes.

Ultrasound has recently been suggested as a promising approach to combating fouling in membranes. In principle it can be used on-line and may even eliminate the use of chemical cleaning or alternative measures completely, which could lead to major advances in the development and implementation of membrane technology. The objective of this investigation was therefore to assess the feasibility of using ultrasound to mitigate fouling in capillary ultrafiltration systems applied to water containing natural organic matter.

Experimental work was conducted with a small laboratory-scale capillary membrane module. Ultrasound was introduced into the system by means of an ultrasonic probe operating at a fixed frequency of approximately 30 kHz, generating a maximum acoustic power density of 130 W/cm² with a nominal power output of 50 W (IKA Labortechnik Staufen, United Kingdom, U50).

Five systems were investigated, viz. aqueous solution of Congo Red dye, ultrapure water, coloured ground water from the George region, water from the Steenbras dam, as well as an aqueous solution of dextran. In most cases, ultrasonication resulted in an increase in the permeate flux. This increase could partly be attributed to an increase in the temperature and thus a decrease in the viscosity of the fluid and partly to enhanced mass and energy transfer due to sonication. Based on experiments done with the Congo Red dye and ultrapure water, no damage as a result of ultrasonication could be discerned in the membrane filter, except when there was direct contact between the ultrasonic probe and the membrane materials. Permeate quality analyses confirmed that sonication does not damage the membrane material – no degradation of permeate quality was found specifically during sonication intervals.

In conclusion, ultrasound indeed appeared to be an effective approach to remove foulants associated with natural organic matter from membranes. However, an issue not addressed by this study, but apparent from the literature, is that the effect of ultrasound is strictly local and this has major implications for the scale-up of such ultrasound systems.

Opsomming

Die blokkasie van membrane is 'n ernstige probleem in membraanfiltrasie, as gevolg van die verstopping van die porieë van die membraan en die adsorpsie van verwerpte makromolekules of ander opgeloste stowwe in the membraanstelsel. Dit vereis periodieke skoonmaak van die membrane, wat beduidend kan bydra tot die algehele bedryfskoste van aanlegte, as gevolg van verlore bedryfstyd, die koste van chemikalieë benodig vir skoonmaak, hoë drukke en die pompkoste benodig om membraanproduktiwiteit te handhaaf, sowel as 'n verkorting van die leeftyd van die membrane.

Die gebruik van ultraklank is onlangs voorgestel as 'n benadering om membraanverstopping te beveg. Dit kan in beginsel aanlyn gebruik word en mag selfs die gebruik van chemiese skoonmaking of alternatiewe benaderings heeltemal uitskakel. Dit kan lei tot groot vordering in the ontwikkeling en implementering van membraantegnologie. Hierdie studie was derhalwe 'n ondersoek na die uitvoerbaarheid van die gebruik van ultraklank om verstopping teen te werk in kapillêre ultrafiltrasiestelsels met water wat natuurlike organiese partikels bevat.

Eksperimentele werk is gedoen in 'n klein laboratoriumskaal kapillêre membraan-module. Ultraklank is tot die stelsel toegevoeg deur 'n ultrasoniese probe wat bedryf is by 'n vaste frekwensie van 30 k, wat 'n maksimum akoestiese drywingsdigtheid van 130 W/cm^2 gelewer het, met 'n nominale drywingsuitset van 50 W (W (IKA Labortechnik Staufen, Verenigde Koninkryk, U50) Vyf stelsels is ondersoek, te wete waterige oplossings van Kongo Rooi kleurstof, ultrasuiwer water, gekleurde grondwater van die George-streek, water van die Steenbras dam, sowel as 'n waterige oplossing van dextran. In meeste gevalle het blootstelling aan ultraklank gelei tot 'n verbetering in die permeaatvloed. Die verhoging kon deels verklaar word deur die verhoging in temperatuur en dus verlaging in die viskositeit van vloeistof en deels deur verhoogde massa- en energie-oordrag effek veroorsaak deur die ultraklank. Gebaseer op eksperimente met die Kongo Rooi en ultrasuiwer water, kon geen skade as gevolg van ultrasonikasie aan die toerusting waargeneem word nie, behalwe waar die ultrasoniese probe in kontak was met die membraanmateriale. Hierdie waarneming is bevestig deur analyses van die permeaat-produk – geen verswakking in produk-kwaliteit is gevind spesifiek gedurende intervalle waar ultraklank tot die stelsel toegevoeg is nie.

Ten slotte, ultraklank kan inderdaad doeltreffend aangewend word om membraanverstopping te bekamp. 'n Kwessie wat egter nie hier bestudeer is nie, maar wat wel duidelik geblyk het uit die literatuurstudie, is dat die effek van ultraklank hoogs lokaal is en dit kan groot implikasies hê vir die opskalering van sulke ultraklankstelsels.

Table of Contents

Declaration.....	i
Summary.....	ii
Chapter 1	1
Introduction.....	1
1.1 History of Membranes.....	2
1.2 Membrane filtration processes.....	3
1.2.1 Reverse Osmosis	6
1.2.2 Nanofiltration	7
1.2.3 Ultrafiltration	7
1.2.4 Microfiltration.....	8
1.2.5 Electrodialysis	9
1.3 Membrane modules.....	9
1.3.1 Tubular modules.....	9
1.3.2 Spiral Wound Modules	10
1.3.3 Hollow fibre modules.....	10
1.3.4 Capillary Modules	11
1.3.5 Plate and Frame Modules.....	11
1.4 Membrane Performance.....	11
1.5 Concentration polarisation.....	12
1.6 Membrane fouling.....	12
1.6.1 Biological fouling.....	13
1.6.2 Particle and Colloid Fouling	14
1.6.3 Crystalline Fouling.....	14
1.7 Membrane Life	14
1.8 Conventional Membrane Cleaning Methods.....	15
1.8.1 Biological fouling.....	15
1.8.2 Particle and Colloid Fouling	15
1.8.3 Crystalline Fouling.....	16
1.8.4 Disadvantages of Conventional Membrane Cleaning Methods.....	16
1.9 Preventing and Reducing Membrane Fouling	16
1.9.1 Pretreatment.....	17
1.9.2 Design	17
1.9.3 Operation	17
1.9.4 Alternative methods for the prevention of fouling.....	18
1.10 Objectives of the thesis	19
Chapter 2	20
Literature Review of Ultrasonic Cleaning of Membranes	20
2.1 Ultrasound	20
2.1.1 Cavitation.....	21
2.1.2 Effects of cavitation	22
2.1.3 Chemical and mechanical effects of ultrasound.....	24
2.2 Ultrasonic Equipment.....	25
2.2.1 Transducers	25
2.2.2 General considerations regarding ultrasonic equipment	25
2.2.3 Laboratory equipment.....	26
2.2.4 Large-scale equipment.....	26
2.3 Ultrasonically Assisted Filtration – Early Developments.....	27
2.4 Modern Applications	28
2.5 Enhanced Permeation via Ultrasonication.....	32
Chapter 3	33
Experimental Setup and Methods	33
3.1 Process description.....	33
3.2 Equipment	33
3.3 Membrane Preparation	35
3.4 Tests with Congo Red dye	35

3.5	Tests with Ultra-Pure Water	35
3.6	Tests with Coloured Ground Water from the George Region	36
3.7	Tests with Water from the Steenbras Dam.....	36
3.8	Tests with Dextran.....	37
Chapter 4	39
Results and Discussion	39
4.1	Visual Tests with Congo Red	39
4.1.1.	Visual Test 1.....	39
4.1.2.	Visual Test 2.....	39
4.1.3.	Visual Test 3.....	39
4.1.4.	Visual Test 4.....	40
4.1.5.	Visual Test 5.....	42
4.1.6.	Visual Test 6.....	42
4.2.	Tests with Ultra-Pure Water	44
4.2.1.	Milli-Q Water Test 1	44
4.2.2.	Milli-Q Water Test 2	45
4.2.3.	Milli-Q Water Test 3	47
4.3.	Tests with Coloured Ground Water from the George Region..	48
4.3.1.	First Experimental Run.....	48
4.3.2.	Second Experimental Run.....	52
4.4.	Tests with Water from the Steenbras Dam	57
4.4.1.	First Experimental Run.....	57
4.4.2.	Second Experimental Run.....	59
4.5.	Tests with Dextran	62
4.6.	Relationship between flux and temperature	65
4.7.	Observations on the Dynamics of Fouling.....	67
Chapter 5	69
Conclusions	69
References	72
Appendices	75
A.	Experimental Data	75
A.1	Visual Tests with Congo Red	75
A.2	Tests with Ultrapure Water.....	80
A.3	Tests with Coloured Ground Water from the George Region	83
A.4	Tests with Water from the Steenbras Dam.....	91
A.5	Tests With Dextran	97
A.6	Relationship between Temperature and Viscosity	100
B.	Experimental Set-up.....	102

List of Tables and Figures

Table 1-1. Characteristics of pressure driven membrane filtration processes

Figure 3-2. Diagram of the bench-scale capillary ultrafiltration module

Figure 3-3. Photograph of the bench-scale module and probe.

Table 3-1. Physicochemical characteristics of the natural organic water sample from Steenbras Dam (the data are average values of the samples taken over 3 weeks).

Figure 4-4. Effect of sonication on permeate temperature

Figure 4-5. Permeate flux of water containing 0.11 wt% Congo Red dye (visual test 4). Bands indicate sonication intervals.

Figure 4-6. Effect of sonication on temperature – temperatures only recorded during sonication intervals.

Figure 4-7. Permeate flux of water containing 0.11 wt% Congo Red dye (Visual Test 6). Bands indicate sonicated intervals.

Figure 4-8. Effect of sonication on temperature – temperatures only recorded during sonication intervals, as indicated in Figure 4-5.

Figure 4-9. Permeate flux of ultrapure water (Visual Test 1). Coloured bands indicate sonication intervals.

Figure 4-10. Effect of sonication on permeate temperature (Visual Test 1).

Figure 4-11. Permeate flux of ultrapure water.

Figure 4-12. Effect of sonication on permeate temperature (Visual Test 2).

Figure 4-13. Permeate flux of ultrapure water.

Figure 4-14. Effect of sonication on permeate temperature (Visual Test 3).

Figure 4-15. Membrane Preparation with Milli-Q Water

Figure 4-16. Prefouling with coloured ground water from the George region.

Figure 4-17. The effect of sonication on the permeate flux

Figure 4-18. Permeate Quality Analysis – Turbidity, Absorbency and pH

Figure 4-19. Permeate Quality Analysis – Conductivity and Apparent Colour test

Figure 4-20. Retentate Quality Analysis – Turbidity, pH and Conductivity

Figure 4-21. Membrane Preparation with Milli-Q Water

Figure 4-22. Prefouling with coloured ground water from the George region.

Figure 4-23. Effect of sonication on the permeate flux

Figure 4-24. Permeate Quality Analysis – Conductivity and Apparent Colour

Figure 4-25. Permeate Quality Analysis – Turbidity and pH

Figure 4-26. Retentate Quality Analysis – Turbidity and pH

Figure 4-27. Retentate Quality Analysis – Conductivity and Apparent Colour

Figure 4-28. Effect of sonication on temperature.

Figure 4-29. Membrane preparation with distilled water

Figure 4-30. Prefouling with Steenbras dam water.

Table 4-1. Effect of sonication on temperature.

Figure 4-311. Membrane preparation with distilled water.

Figure 4-322. Prefouling with Steenbras dam water

Figure 4-333. Effect of sonication on the permeate flux

Figure 4-344. Effect of sonication on temperature.

Figure 4-355. Membrane preparation with distilled water.

Figure 4-366. Effect of sonication on the permeate flux.

Figure 4-377. Effect of sonication on temperature.

Figure 4-38. Contribution of temperature effect to flux enhancement

Figure 4-39. Increase in temperature of the systems studied, as a function of nominal ultrasonic energy input per kg of fluid.

Figure 4-40. Incremental flux of George mountain water, corresponding to the data in Figure 4-20.

Figure 4-41. Incremental flux of George mountain water, corresponding to the data in Figure 4-20 – first hour only.

Table A-1. Experimental data

Table A-2. Experimental data

Table A-3. Experimental data

Table A-4. Experimental data

Table A-5. Experimental data

Table A-6. Experimental data

- Table A-7.** Experimental data
- Table A-8.** Experimental data
- Table A-9.** Experimental data
- Table A-10.** Permeate Quality Analysis for Experimental Run 1
- Table A-11.** Retentate Quality Analysis for Experimental Run 1
- Table A-12.** Membrane preparation with distilled water
- Table A-13.** Operating Data
- Table A-14.** Permeate Quality Analysis for Experimental Run 2
- Table A-15.** Retentate Quality Analysis for Experimental Run
- Table A-16.** Temperature data
- Table A-17.** Temperature statistics
- Table A-18.** Membrane preparation with distilled water
- Table A-19.** Prefouling of the membranes
- Table A-20.** Operating Data
- Table A-21.** Temperature data
- Table A-22.** Temperature Statistics
- Table A-23.** Membrane preparation with distilled water
- Table A-24.** Prefouling with Steenbras dam water
- Table A-25.** Operating data
- Table A-26.** Temperature data
- Table A-27.** Temperature statistics
- Table A-28.** Membrane preparation with distilled water
- Table A-29.** Operating Data
- Table A-30.** Temperature data
- Table A-31.** Temperature statistics
- Table A-32.** Density and Viscosity of pure water as a function of temperature at 100 kPa
- Table O-33.** Calculation of normalised temperature and flux
- Figure B-1.** Close-up of membrane module with ultrasonic probe
- Figure B-2.** The capillary ultrafiltration membranes – ends were epoxied into the 10 mm stainless steel tubing
- Figure B-3.** Close-up of the hollow fibres
- Figure B-4.** Lab-scale setup showing permeate collection and measurement via scale.

Chapter 1

Introduction

Membrane filtration is an increasingly popular separation and purification technology. It has revolutionised the separation of fine particle suspensions. Membrane filtration is utilized in many industries, for instance:

- Water treatment (desalination of sea water and purification of brackish water)
- Pharmaceuticals (clarification of fermentation products: antibiotics and vaccines)
- Biotechnology (cell concentration) and food processing (production of sauces and curds, esp. also the dairy industry)
- Beverage production (production of potable liquids: beer)
- Electronics (production of ultrapure water for manufacture of semi-conductors)

Unfortunately membrane fouling limits the success of ultrafiltration membranes in the processing of industrial wastewaters. Membrane fouling restricts membrane filtration economically: it can lead to reduced performance, higher energy consumption and even failure to meet product specifications.

Various pretreatment techniques and processes including prefiltration and backwashing are employed to prevent or reduce the rate of membrane fouling. Chemicals are added to prevent mineral scaling and biocides to combat biofouling. Unfortunately all these techniques have shown to be inefficient: periodic membrane cleaning is still unavoidable.

For membrane cleaning to take place, the unit needs to be shut down for a chemical or a mechanical cleaning, or both. The downtime is significant and the cleaning process is labour intensive. The cleaning chemicals may also reduce the lifetime and efficiency of the membrane modules. The whole process is cumbersome and economically unfavourable.

Ultrasonication can be introduced into a membrane module on-line. The unit need not be shut down or opened up. No additional labour is required and no chemicals are involved. Therefore ultrasonication as a membrane cleaning method seems ideal and merits further investigation.

From various publications and recent work done by the University of Stellenbosch, it seems possible that ultrasonication may be a viable means of preventing or reversing fouling of membranes. Laboratory-scale experiments were performed to determine the possibilities ultrasonication have for industrial membrane processes.

1.1 History of Membranes

The osmotic phenomenon was first observed by the French Cleric, Abbé Nollet in 1748. The first experimental work was conducted with membranes of animal and plant materials until 1867 when Traube prepared the first inorganic semi-permeable membrane: a gelatinous film of copper ferro-cyanide supported on a porous clay frit. The first references to pressure driven filtration appear at the end of the 19th century. In 1907 Bechold published a paper on what we call ultrafiltration today (Glater, 1998:298). Up until the 1930's very few polymeric materials were known to man – almost all plastics and films were derived from cellulose (a natural product). In 1937 Carothers developed nylon – the first synthetic polyamide. The polymeric membranes used for membrane filtration today originated with the first synthesis of Nylon. Shortly after World War II the United States government became interested in desalination and promoted research and development in this field. Hassler launched membrane research at the University of California in 1949 (Glater, 1998:299). In the 1950's Reid and Breton made valuable contributions to the research field especially regarding membrane transport mechanisms (Glater, 1998:304). In 1958 Loeb and Sourirajan developed the first practical reverse osmosis (RO) membrane (Glater, 1998:306). By 1961 the Loeb-Sourirajan membrane had entered the public domain and by the mid 1960's Dow and DuPont recognised the potential for large-scale membrane desalination (Glater, 1998:307-308). These first membranes were cellulose-acetate membranes with low fluxes and required high operating pressures (Membrane Processes and Ion Exchange, 2004).

Since the 1960's the membrane field has grown rapidly with the development of new and improved membrane materials. The use of membrane processes have diversified and the reliability has improved. The main contributing factors to the phenomenal growth in the membrane field are

- Increasingly stringent environmental legislation and regulations regarding water and effluent composition and the drive towards wastewater re-use.
- Continuously increasing fresh water demand in arid regions and developing countries.
- Rapid growth in research and development in the membrane field and the discovery of new applications for membranes e.g. membranes in bioreactors.

The main application for membrane processes in the water field remains desalination of sea water and brackish water. Membrane processes have proven to be a cost effective and reliable method for the treatment of waste and contaminated waters all over the world (Reith and Birkenhead, 1998: 203-204). The Middle East has the largest installed desalination capacity and the largest RO plants. The world's total installed desalination capacity (including distillation) was estimated at 32000 ML/d in 2002. From 2000-2002 new desalination plants were added at a rate of about 70% per year. This dramatic growth rate is specifically credited to the increased water demand in arid regions and desalination cost reduction.

South Africa is not counted among the foremost membrane countries of the world regarding installed desalination capacity, but South Africa is considered as one of the fore-runners in membrane treatment of saline effluents. The treatment and desalination of cooling water blow down, mine water and textile and paper mill effluents have been initiated and researched in South Africa. Innovative full scale plants have been installed at Sasol, Eskom, Mondi, Columbus Steel and various mines (Membrane Processes and Ion Exchange Course, 2004).

1.2 Membrane filtration processes

A membrane is defined as a selective barrier that permits the passage of certain components, whilst retaining others. Either the permeating stream or the retained phase is enriched in one or more components. (Cheryan, 1986)

Membrane processes can be classified in various ways: type of membrane, driving force or type of application. Classification according to driving force is a common method:

- Pressure driven – examples: reverse osmosis (RO), nanofiltration (NF), ultrafiltration (UF), microfiltration (MF). RO, NF, UF and MF are used in different applications, use different types of membranes, have different separation mechanisms, operate at different pressure ranges and their product qualities differ. All these processes rely on the application of a hydraulic pressure to speed up the transport process and the nature of the membrane controls which components will permeate and which will be retained.
- Electrical potential driven – examples: electrodialysis (ED) and electrodialysis with polarity reversal (EDR). ED operates by the application of an electric field across a stack of alternate cation and anion permeable membranes, allowing separation of ionic species from the feed stream. The separation mechanism is a charge-exclusion mechanism. The membranes are thicker and more robust than RO membranes and the process operates at low pressure – slightly higher than atmospheric

pressure. ED and EDR are used for desalination of brackish water and desalination of certain effluents.

- Activity or concentration driven – examples: dialysis, pervaporation or membrane distillation and gas diffusion. Two cells with solutions are separated by a membrane. If the active concentrations of the two cells differ, the solute will diffuse from the high concentration region, through the membrane to the low concentration region. The concentration gradient across the membrane is the driving force.

The membrane process splits the feed water into a high quality permeate (product) stream and a reject (brine or concentrate) stream.

The filtration process can be divided into 2 modes: dead-end and cross-flow filtration.

Dead-end filtration is used when dealing with suspensions with very low solids content – e.g. sterile filtration in the beverage and pharmaceutical industries.

Cross-Flow filtration is used for high concentrations. With cross-flow the tangential velocity is high enough to cause turbulence near the membrane surface. The turbulence disrupts concentration polarisation and inhibits fouling. Cross-flow limits the build-up of solids on the membrane surface. Cross-flow causes the pressure drop from the inlet to the outlet of the membrane module. Of the two, CF-filtration has a more stable filtration rate over time.

Pressure driven membrane processes usually consist of the following components:

- Membranes, contained in modules, which form the basis of the process.
- High pressure pumps to deliver the feed water to the module at the required pressure
- Pretreatment processes to ensure that the feed water will not damage the membranes
- Post-treatment processes to ensure that the product water is according to the specification of the downstream consumer
- Process control equipment, including the equipment and chemicals required for membrane cleaning - usually clean in place (CIP) systems.
- Energy recovery systems (usually only for large scale RO installations).
- Brine or concentrate and CIP waste disposal systems.

The process usually runs as follows: a pump transfers the pretreated feed water under pressure over the surface of a membrane of an appropriate chemical nature and physical configuration. A valve on the retentate line maintains a certain (back)pressure in the module. Permeate is drawn off at or near atmospheric pressure. Retentate is recycled, fed to a subsequent stage or disposed of.

The most important factors in membrane plant design are:

- Conversion (also called yield, recovery or concentration factor)
- Potential for scale formation by sparingly soluble salts (CaSO_4 or BaSO_4 are typical examples)
- Required product quality

The conversion is the ratio of the permeate flow from the module to the feed flow to the particular module whilst recovery refers to the total product to feed ratio and is recorded as a percentage.

The concentration factor indicates to which extent the feed is concentrated:

$$\text{Concentration factor} = 100 / (100 - \text{Recovery})$$

The pumping duty and the backpressure valve setting affect the conversion. It is preferable to work at a high conversion ratio as this results in lower pump and piping costs as well as poses an energy saving concerning retentate circulation. Still, a conversion factor resulting in a situation where the solubility product of compounds is exceeded or which causes an extremely high retentate viscosity, must be avoided.

A membrane plant has the following typical hierarchy:

- Membranes – to achieve an effective separation
- Modules – a housing for the membranes to enable the practical application
- Membrane system – consists of the sets of modules in a specific sequence and configuration
- Membrane plant – consists of the membrane system and all related processing units and equipment.

Pressure driven membrane processes are the most common processes and will be discussed in more detail.

Table 1-1. Characteristics of pressure driven membrane filtration processes.

Process	Pressure (kPa)	Flux range ($\text{l.m}^{-2}.\text{h}^{-1}.\text{bar}^{-1}$)	Size of reject (nm)
RO	1000-10000	0.5-1.4	0.1-1
NF	500-2000	1.4-12	0.5-5
UF	100-800	10-50	1-100
MF	10-20	>50	75-10000

1.2.1 Reverse Osmosis

RO is used in the desalination of sea water or brackish water and the removal of dissolved salts from high TDS effluents (e.g. mine water).

RO removes all particulate matter including bacteria and viruses, all organic macromolecules and most organic molecules with molecular mass larger than 150 Daltons (molecular weight units). RO product water (permeate) is of very high quality – even from low quality feed water.

RO membranes do not have distinct pores and the separation mechanism is not according to a sieve mechanism. The latest theory regarding the separation mechanism for RO is a solution diffusion mechanism (or more specifically selective dissolution and diffusion of the components in the membrane). The membrane has a much higher affinity for water than the solute and the water diffuses faster through the membrane than the solute – effecting the separation. The operating pressure depends on the osmotic pressure of the feed water, normally 5-10 MPa for sea water and 1-2.5 MPa for brackish water. The high operating pressures may require costly positive displacement pumps. RO processes are usually operated in cross-flow mode.

Reverse osmosis membranes are manufactured from materials like cellulose acetate and its variations di-acetate and tri-acetate, aromatic polyamide and also from different materials when composite membranes are manufactured.

The skin of an RO membrane is non-porous and must be hydrophilic. Also, for RO the flux of the permeate stream is inversely proportional to the membrane thickness. This necessitates the membrane to be as thin as possible. The development of anisotropic (non-symmetric) membranes with a very thin skin on an underlying porous support structure satisfies this constraint. The skin effects the separation and the porous support provides structural stability. The skin thickness is usually 1 percent of the thickness of the porous layer. Anisotropic membranes are either asymmetric or composite membranes.

Asymmetric membranes are cast as flat sheets or spun as hollow fibres with external diameter of 100 micron and internal diameter of 50 micron. The membrane consists of a very dense skin supported by a porous sub-layer of the same material.

The top layer of a composite membrane is made from a different material than the supporting structure. Composite membranes are typically manufactured by casting the skin layer, for instance polyamide, on top of a polysulphone ultrafiltration membrane.

RO membranes operate at high pressures and must be supported mechanically. This is accomplished by engineering the membrane material into a specially module. Different types of modules exist.

1.2.2 Nanofiltration

NF is similar to RO in the respect that the separation is effected by selective transport through a membrane. NF membranes are less "tight" than RO membranes, the size of the rejected species is larger and the membrane may even carry an electrical charge. Monovalent ions (Na^+ , Cl^-) are usually able to permeate the membrane (low rejections of 40-60%) whilst divalent ions, the larger hydrated ions (Ca^{2+} , SO_4^{2-}), and colloids and larger organic molecules are rejected (high rejections of 96-99%). The 99% cut-off rejection for organic molecules is in the range of 300-500 Daltons. The operating pressure is also lower than for RO – typically less than 1.5 MPa. NF is used in water softening.

1.2.3 Ultrafiltration

Ultrafiltration (UF) membranes are porous. The membrane pore sizes range from 5-50 nm. Colloidal and particulate material and macromolecules, including bacteria, viruses and high molecular mass soluble species are retained by a mechanism of size exclusion (sieve mechanism). It is also said the transport of the filtrate occurs by convective flow through the membrane pores. UF can be used for concentrating, fractionating or filtering dissolved or suspended constituents. Most dissolved ions and low molecular weight dissolved organic molecules are not removed and because of this ultrafiltration cannot be used for desalination. The molecular weight cut-off (MWCO) or molecular mass cut off (MMCO) determines the size of the retained particles.

Because UF is a low pressure process, non-positive displacement pumps can be used as well as synthetic system components (pipes and fittings) – reducing capital cost. Cross-flow is usually employed in UF processes to increase the flux.

UF membranes can be isotropic and porous. The pores are defined as follows:

- Macropores – diameter larger than 50 nm

- Mesopores – diameters of 2-50 nm
- Micropores – diameters smaller than 2 nm

UF membranes are classified according to their MWCO in stead of the particle size. The MWCO is a specification used by membrane suppliers to describe the rejection properties of a membrane. It refers to the molecular mass of a macro-solute for which the membrane rejection is 90% or more. A 50 000 Dalton MWCO membrane will reject most compounds with a molecular mass greater than 50 000. The typical MWCO for UF membranes range from 1000-500000. UF membranes are typically characterized by their rejection of Dextran with molecular mass 5000-500000 Dalton or globular proteins with molecular mass 1000-70000 Dalton. Originally polyethylene glycols were also used to determine MWCO. The MWCO provides some information about the membrane pore dimensions. There is no sharply defined cut-off value because the conformation of the macro-molecules is not taken into account.

Like RO membranes, UF membranes can also have a discernible thin skin at the filtration surface. The skin thickness is typically 0.1-1.0 micron and it is supported by a more porous substructure. The skin has a high permeability for water, but rejects suspended and dissolved solids via a sieve mechanism (size exclusion). The minimum diameter of the pores are at the skin – this ensures that once a solute enters a pore it will be transported with the filtrate and will not be trapped in the membrane.

UF membrane material does not have to be hydrophilic. Typical materials include polysulphone (PS) polyethersulphone (PES), polypropylene, polycarbonate, polyethylene and Teflon. Some UF membrane materials, especially polysulphone, have good chemical and thermal resistances and can be used at high temperatures and over a wide pH-range – an advantage over the less robust RO membranes. Most UF membranes are hydrophobic, which requires wet storage. If the membranes are allowed to dry out the membrane structure might collapse and irreversible flux loss can occur.

UF membranes can also be manufactured from ceramics (TiO_2 and Al_2O_3). These membranes have very high chemical and thermal resistances and can be subjected to rigorous membrane cleaning procedures. They are available in tubular and capillary form in a large range of pore sizes, but their major disadvantage is the cost.

1.2.4 Microfiltration

Microfiltration (MF) is very similar to UF, the differences being in pore size (pores are 50 nm and larger), operating pressure and permeate quality. Mostly particulate matter is removed by MF.

MF processes can display rejection properties in the UF range. This occurs due to the dynamic membrane that forms on the membrane surface (filter cake).

1.2.5 Electrodialysis

ED membranes are charged polymeric membranes made from ion exchange resins. There are two types of membranes for ED: cationic and anionic. The membrane consists of cross-linked polymer chains with positive ions freely dispersed in the voids between them. There are fixed negative ions on the chains. ED membranes are thicker than RO membranes. The membrane thickness has a negligible effect on ion passage. Resistance to ion passage is determined by the degree of cross-linking between the polymer chains. If the cross-linking is too low it may have a negative effect on the structural stability as well as ion transport.

1.3 Membrane modules

A membrane module is an operational unit which consists of membranes, pressure support structures and feed inlet ports, concentrate outlet ports and permeate draw-off ports.

Membrane modules are designed to achieve three objectives:

- To ensure that at membrane level there is sufficient feed circulation to limit concentration polarisation and particle deposits.
- To produce a compact module – to achieve maximum packing density: membrane surface per unit volume.
- To avoid any leak between feed and permeate compartments.

Other requirements are concerned with ease of cleaning, ease of (dis)assembly and low hold-up volumes. Moreover, there are 5 major types of modules, viz. tubular, spiral wound, capillary, hollow fibre and plate and frame systems

1.3.1 Tubular modules

This is the simplest configuration. The membrane is cast inside the wall of a porous support tube. Internal diameters range from 6-40 mm. Individual tubes are housed inside stainless steel or PVC sleeves or the tubes are bunched together in bundles of 3-157 tubes in a cylindrical housing with suitable end plates.

Circulation velocities of up to 5 m/s are possible if highly turbulent flow is required. No extensive feed pretreatment is required and the modules are easy to clean. The disadvantage of this module is the low packing density which in turn increases the capital cost.

1.3.2 Spiral Wound Modules

To form a spiral wound membrane a sandwich of two flat-sheet membranes with a flexible spacer (permeate collector) in between is sealed on three of its edges. The open end is connected and rolled up onto a perforated tube which acts as the final permeate collector. Multiple membrane-and spacer constructs are fastened to one perforated tube and they are separated from each other by a feed spacer. The feed spacer supplies an open flow channel for feed and induces turbulence which in turn reduces concentration polarisation. The spacer can be a mesh or a corrugated spacer. The feed flow is parallel to the permeate tube axis.

The module can have a diameter of 300 mm and a length up to 1.5 m. Spiral wound modules are compact (packing density of 700-1000 m²/m³) and the pressure drop is lower than for tubular or plate-and-frame modules. High linear flow velocities can be achieved in spiral wound modules which limits severe concentration polarisation. The feed flow channel formed by the spacer clogs easily and therefore pretreatment is a requirement for spiral wound modules.

1.3.3 Hollow fibre modules

Membranes can be cast in the form of hollow fibres (HF's). The HF's are gathered in bundles of thousands or even millions. The feed flow can be inside the HF's (inside-out) configuration or on the outside (outside-in configuration).

For the inside-out configuration the feed and permeate is sealed off from each other via a potting resin which also forms a tube plate at the ends of the bundle. After the resin has hardened the bundle is cut, ensuring that the open ends of the HF's are exposed. The potting resin can also be used to seal the membrane bundle in the pressure housing (module), this negates the need for O-rings which are often the source of leaks in modules.

For the outside-in configuration the bundle is often arranged in a U-shape and the fibres are only sealed at one end.

Packing density is inversely proportional to diameter and therefore HF modules are very compact. The packing density range from 1000m²/m³ in UF modules to 10000 m²/m³ in RO modules.

The operating velocities in HF modules are usually very low and the modules can even be operated in dead-end mode. The flow in HF's is laminar, but because the flow channels are very small shear rates are high.

UF and MF HF's are self-supporting which enables back-flushing. During UF back-flushing the permeate pressure is raised above the feed pressure. The direction change of the flow through the fibre-wall lifts and detaches the particle deposits (cake) from the membrane surface. The cake is then removed from the module

with the circulating flow. Particles blocking the entry to the flow channel of the HF can also be removed thus. In MF the pores are larger and therefore air back-flushing is possible.

1.3.4 Capillary Modules

Capillary modules are similar to tubular modules, but the diameter is much smaller. The outside diameters range from 0.5-5mm and the inside diameters are usually 25-40% of the outside diameter. They are used for UF and MF.

Capillary membranes do not require pressure support because of their small dimensions and their low operating pressures. Despite this, the capillaries may have burst pressures of up to 2.5 MPa.

Capillary membranes are typically internally skinned with a finger-like or sponge-like porous substructure. Capillaries skinned on the outside or double-skinned are also available.

Capillary membranes are usually operated in cross-flow mode. It is common to use a shell-and-tube configuration where the feed flows inside the tubes (the membrane lumen) and permeate is collected from the shell side. If the membranes are skinned on the outside the feed may flow radially from or parallel to the membrane axis and permeate will be collected in the membrane lumen.

The pressure drop over a capillary membrane is large and limits the flow velocity in the membrane lumen. It also restricts the length of capillary membranes – they are usually not longer than 1.2 m.

1.3.5 Plate and Frame Modules

The modules are very much like a plate and frame filter press. They are constructed from stacked flat-sheet membranes and support plates. Feed flows between the membranes of two adjacent plates. The packing density for these modules is 100-400 m²/m³. Module arrangement is very versatile – series or parallel feed circulation or a combination is possible. The units are easy to assemble and disassemble, which aids manual cleaning and membrane replacement.

1.4 Membrane Performance

Membrane performance is generally measured by the flux.

The membrane flux (J_w) is expressed in volume or mass per area per unit time, typically g/cm²/s or cm³/cm²/s or cm/s.

The module flux refers to the average permeate flux for a module and is expressed as l/m²/h or l/m²/d.

The solute rejection can be calculated from the feed and product solute concentrations from $R = (C_{\text{Feed}} - C_{\text{Product}}) / C_{\text{Feed}} * 100$.

1.5 Concentration polarisation

Concentration polarization leads to reduced membrane permeability and alters the retention characteristics of the membrane – adversely affecting the flux of the ultrafiltration operation.

The flux limitation is due to either an increased thermodynamic boundary layer – the polarization boundary layer, or an increased hydrodynamic barrier – the “gel layer” polarization model. The interactions between solute macromolecules and the membrane surface as well as between the macromolecules within the polarization layer also affect membrane fouling.

In the membrane filtration process certain zones can be identified:

- Bulk feed region (high pressure or feed side) – the concentration remains fairly constant in this area
- Boundary layer (high pressure side) – the concentration of the reject increases sharply near the membrane surface due to concentration polarisation. An infinite build-up of the reject is prevented by back diffusion to the bulk region.
- Membrane – for RO membranes the solute concentration is much lower in the membrane skin than at the membrane surface, whilst the porous support region does not affect overall solute rejection. The porous layer adds some hydraulic resistance.
- Boundary layer (low pressure side) – no concentration polarisation, the concentration in the membrane is practically the same as the in the bulk permeate.
- Bulk permeate region (low pressure side) – the concentration remains constant.

At a low pressure, low feed concentration and high feed velocity the effects of concentration polarisation are minimal.

1.6 Membrane fouling

In a pressure driven membrane system the flux declines due to membrane fouling which is a direct result of concentration polarization, cake formation and pore fouling. The performance loss manifests itself as a decrease in permeate flux.

In membrane filtration the permeate flux decreases with time as retained particles and solutes accumulate on the membrane surface and in the porous structure of the membrane. This is referred to as fouling. The fouling material can be inorganic, precipitates of sparingly soluble salts or colloidal material or it can be organic colloids, macromolecules and even micro-organisms.

Particle build up on the membrane surface is referred to as external fouling or cake formation, and is usually reversible. Deposition of and adsorption of particles within the membrane pores, internal fouling, is irreversible. The observed flux decline in membrane filtration is due to the increase in membrane resistance caused by the development of these additional resistances.

Pore blocking increases the membrane resistance and cake formation creates another layer of resistance for permeate. Pore blocking and cake formation is regarded as two mechanisms of membrane fouling.

Membrane fouling can be classified in three main groups:

- Biological fouling. (Adhesion and accumulation of micro-organisms forming bio films)
- Particle and colloid fouling.
- Crystalline fouling, also called mineral scaling.

1.6.1 Biological fouling

Proteins, dissolved macromolecules and other biological, colloidal and particular matter can foul the membrane.

Biological fouling occurs when there is a formation of a bio-growth (bio-film) on the membrane surface. The bio-film is the habitat of micro-organisms. It increases the hydraulic resistance of the membrane, lowering the flux. Examples are iron reducing bacteria, sulphur reducing bacteria, mycobacteria and pseudomonas. Biological fouling acts gradually and can cause a major loss of production, a moderate decrease in rejections and a possible moderate increase in transmembrane pressure.

Organic fouling occurs when organic species attach to the membrane surface. Examples are poly-electrolytes, oil and grease. When the membrane surface is exposed to the solution, solute molecules adsorb at the membrane surface because of physico-chemical interactions. Organic fouling causes a rapid and major loss of production. It is also accompanied by a stable or moderate increase in salt rejection and trans-membrane pressure

Membrane fouling by proteins occurs in 2 separate steps:

- Protein adsorption/deposition (mainly on pore walls and mouths).
- Cake formation on membrane surface (because of deposition and formation of aggregates)

Colloids and particulates narrow and plug pores.

Extra cellular polysaccharides excreted by micro-organisms also contribute to the fouling layer (Williams and Wakeman, 2000: 4-5).

1.6.2 Particle and Colloid Fouling

Suspended matter (colloidal clays or silt) agglomerates on the membrane surface. Silt is able to clog the membrane surface. This increases the hydraulic resistance causing a reduction in permeate flux. Finer particles in the feed can enter the internal pore structure and block pores internally. Examples are SiO_2 , $\text{Fe}(\text{OH})_3$, $\text{Al}(\text{OH})_3$ and FeSiO_3 . This type of fouling causes a rapid increase in trans-membrane pressure, a moderate loss in production and rejection and the effects usually occur in the first stage of a multi-stage membrane process.

1.6.3 Crystalline Fouling

This is also known as scaling. Sparingly soluble salts (minerals) are deposited on the membrane surface due to the concentration of the salts in the feed/brine solution during its passage across the membrane surface. The retentate becomes increasingly concentrated until the solubility product is exceeded and precipitation starts. Nucleation of crystals commences and the crystals grow on the membrane surface as a scale. Examples are CaCO_3 , $\text{CaSO}_4 \cdot \text{H}_2\text{O}$, BaSO_4 , SrSO_4 , and SiO_2 . Scaling causes a major decrease in salt rejection, a moderate increase in trans-membrane pressure, a slight loss of production and the effects usually manifest in the final stage of a multi-stage membrane process.

1.7 Membrane Life

The normal life of polymeric membranes is typically 3-5 years; some thin film composite membranes that are less susceptible to hydrolysis reactions carry 5 year warranties. Where membrane systems are properly operated and managed membrane life can exceed the normal lifetime, but incorrect operation, incorrect feed pretreatment and/or cleaning procedures can necessitate membrane replacements in less than one year and void membrane warranties.

Membrane replacement typically represents 30-60% of the cost of producing a cubic meter of ultra filtered water.

1.8 Conventional Membrane Cleaning Methods

Membranes must be cleaned regularly during their operating life. The frequency and type of cleaning is determined by the feed water quality. There are a variety of solutions and chemicals for membrane cleaning. The membrane manufacturers usually recommend cleaning procedures and conditions including temperature, pH, frequency and duration of cleaning.

Cleaning in place methods are most often used for membrane cleaning. This is usually a chemical cleaning process, but other methods can also be employed – large diameter tubular membranes can be cleaned mechanically using sponge-balls.

Cleaning solutions are usually circulated through the membrane unit at a pressure lower than the operating pressure to prevent foulants from penetrating deeper into the membrane material. The CIP-loop is usually fitted with a filter to remove particulates from the circulating CIP-chemical mixture.

The choice of cleaning solution is determined by the type of foulant and the compatibility of the membrane material with the particular cleaning solution at the cleaning temperature (Williams and Wakeman, 2000: 10) .

1.8.1 Biological fouling

Removal of a bio-film is not easily achieved. Rigorous cleaning is required and cleaning chemicals are used which can impair the performance of the membrane after cleaning. Biological fouling is cleaned with Biz-type (17.6% phosphorous, the original cleaner found to be effective with RO-membranes by Procter & Gamble, USA) detergents or ethylene diamine tetraacetic acid (EDTA) based solutions at high pH; or a shock disinfection program with formaldehyde, hydrogen peroxide or peracetic acid.

Sodium hydroxide-based cleaners with, or without hypochlorite can be used to solubilise fats and proteins.

Cleaning of organic fouling is rarely successful, but isopropanol or proprietary solutions have had some success. (Membrane Processes and Ion Exchange Course, 2004).

1.8.2 Particle and Colloid Fouling

Deposits like elemental sulphur and colloidal clays are almost impossible to remove. Colloidal clays and silt are usually cleaned with EDTA, sodium triphosphate (STP) or Biz-type detergents at high pH. Silicate-based foulants can be cleaned with ammonium bifluoride-based solutions.

1.8.3 Crystalline Fouling

Salt precipitates and mineral scalants can be treated by membrane cleaning with citric acid, mineral acids, sodium hexametaphosphate, polyacrylates or EDTA-based solutions (Williams and Wakeman, 2000: 10). Phosphoric acid is used to remove inorganic deposits like calcium carbonate.

1.8.4 Disadvantages of Conventional Membrane Cleaning Methods

- Harsh cleaning regimes often shorten membrane life.
- Membrane cleaning chemicals and the effluent from the cleaning process has to be disposed of.
- Residual cleaning chemicals in the membrane system may have a detrimental effect on downstream processes.
- Membrane cleaning procedures are time consuming
- Manual membrane cleaning procedures are labour-intensive.

Since labour is one of the most costly process resources, manual cleaning is a costly operation. Clean in place procedures (CIP) and manual cleaning also requires the membrane unit to be taken offline. This imposed downtime results in a loss of production. This can impact on upstream and downstream processes and can also be a loss of income for the processing unit. The shutdown and subsequent start-up of a membrane unit is time-consuming – during start-up the pressure in and feed flow to the membrane module is built up gradually. Shut down, CIP and subsequent start-up can result in downtime of 2-3 8hour shifts.

1.9 Preventing and Reducing Membrane Fouling

Membrane fouling cannot be completely avoided, but its impact can be limited by various techniques. The avoidance of fouling can improve filtration rates and eases membrane cleaning. This also limits the need for a harsh cleaning regime and has the potential to prolong the life of polymeric membranes.

The conventional approach to limit the impact of membrane fouling is by careful management of fouling of the membrane. This is achieved via pretreatment, design and operation (Williams and Wakeman, 2000: 4-14). Avoiding fouling improves filtration rates and makes membrane cleaning easier. It can also reduce the need for harsh cleaning regimes and thus prolong the membrane life of polymeric membranes.

1.9.1 Pretreatment

Membrane fouling can be controlled to a certain extent by pretreatment. Pretreatment minimise fouling by removing micro-organisms and fine suspended solids from the feed material. It enables operation at higher flux and extends the cleaning interval (Reith and Birkenhead, 1998: 205). It can involve either physical (prefiltration, centrifugation) or chemical processes (precipitation, coagulation, flocculation and addition of anti-scalants or disinfectants).

The most simple of pretreatment is cartridge filtration and pH adjustment. Depending on the fouling potential of the feed it may become more complex and include pH adjustment, chlorination, addition of coagulants, sedimentation, clarification, dechlorination, addition of complexing agents and/or anti-scalants, pH adjustment and final polishing.

Biological fouling can be controlled by sodium bisulphite addition and chlorination with or without activated carbon prefiltration. Organic fouling is controlled by prefiltration through granulated activated carbon (GAC). The deposition of colloidal clays or silt can be alleviated by prefiltration, charge stabilisation, higher feed-brine flows and operating at lower recoveries. Scaling is controlled by lowering recoveries, adjusting the pH and using anti-scalants. Unfortunately pretreatment chemicals (such as anti-scalants and disinfectants) may have a negative impact on downstream processes and necessitate intricate and costly separation-steps.

1.9.2 Design

Careful selection of membrane materials, membrane surface modification as well as module configuration can reduce fouling tendencies.

The effect of the membrane material on fouling is by preferentially adsorbing certain solutes. Only the initial rates of adsorption or deposition is affected – after a fouling layer has formed the membrane material has no further effect, until after membrane cleaning.

1.9.3 Operation

Fouling can be reduced by limiting trans-membrane pressure (production rate), maintaining a high cross-flow velocity, periodical hydraulic and mechanical cleaning as well as the choice of cleaning chemicals and the frequency of cleaning procedures.

Flows of up to 4 m/s have been utilized to limit polarization. The high velocity increases the shear rate and subsequently transfers material away from the membrane surface. High cross flow velocities have two great disadvantages: high

energy consumption of the process and large resulting pressure drop over the length of the membrane module.

1.9.4 Alternative methods for the prevention of fouling

One way to reduce fouling is by enhancing the local shear near the membrane surface – this increases the mass transfer of accumulated materials back into the bulk feed (Williams and Wakeman, 2000: 4-15), (Dekker and Boom, 1995: 129-131) and controls concentration polarization and cake formation. The local shear rate near the membrane surface can be increased by:

- Inducement of Dean or Taylor vortices
- Rotating membranes
- Vibrating membrane modules
- Use of corrugated (or grooved) membranes
- Use of scouring particles

Dean or Taylor vortices shorten the path length along the membrane surface for a particle that might be retained. These vortices can be obtained by screw thread or helical inserts in tubular membranes. By shortening the path, the chance that the particle will attach to the membrane is reduced (Dekker and Boom, 1995: 130).

Another method is to remove the materials accumulated at the membrane surface by a periodical flow-reversal (backflushing, pulsing and shocking). Filtrate is pumped back through the membrane to give a periodic backwash to lift the accumulated material off the membrane surface. In the case of high frequency backpulsing (0.1 – 1 Hz) with short pulses (0.1s or less), it seems that the fouling layer remains loose and does not get the opportunity to compact. (Williams and Wakeman, 2000: 6-7), (Dekker and Boom, 1995: 129-131)

Pulsatile flow can also improve the flux. Oscillations and unsteady flows can be obtained by introducing pulsations into feed or filtrate channels (Williams and Wakeman, 2000: 7).

Gas sparging has been found to enhance ultrafiltration in the downward cross-flow operation. Gas is added to the process stream. This technique disrupts the concentration polarization layer. It does not seem to be as effective as vortex promoters and handling the gas injected to the membrane system poses a problem (Williams and Wakeman, 2000: 7).

Additional force fields could be used to enhance the permeate flux. Magnetic, electric, ultrasonic and centrifugal forces can be utilized. Combined electric and ultrasonic fields can also be utilized (Williams and Wakeman, 2000: 7-9).

Corrosion of electrodes and high power consumption limit the use of continuously applied electrical fields, but the use of pulsed electrical fields shows promise.

The application of ultrasound for membrane cleaning is a novel emerging technology. Ultrasonic defouling of ultrafiltration membranes in the form of capillary membranes was investigated.

1.10 Objectives of the thesis

As explained before, ultrasound is a potentially promising approach to combat fouling in membranes. In principle it can be used on-line and may even eliminate the use of chemical cleaning or alternative measures completely, which could lead to major advances in the development and implementation of membrane technology. However, these conclusions have been based on small-scale laboratory studies, which have not taken the economic feasibility of the approach into account. The objective of this investigation was therefore to assess the techno-economic feasibility of using ultrasound on a large-scale to alleviate fouling in membrane filtration plants.

The focus was on the application of ultrasound on capillary ultrafiltration systems and the following objectives were pursued.

- A literature review of the use of ultrasound to reduce or prevent fouling in membranes, or to otherwise enhance membrane performance.
- Experimental assessment of possible damage to membranes by sustained use of ultrasound in membrane systems, as some conflicting results are reported in the literature.
- Experimental work to determine the efficiency of ultrasound in the removal of foulants from membranes used in the treatment of water containing natural organic matter.

Chapter 2

Literature Review of Ultrasonic Cleaning of Membranes

2.1 Ultrasound

Ultrasound waves have a frequency range from 16 kHz to 10 MHz. It is above the human hearing range. Ultrasound can be divided further into three frequency ranges: power ultrasound (16-100 kHz), high-frequency ultrasound (100 kHz-1 MHz) and diagnostic ultrasound (1-10 MHz) (Crabb and D'Aquino, 1999: 26). Ultrasound waves, like all sound waves, consist of cycles of compression and expansion. Compression cycles exert a positive pressure on the liquid – pushing molecules together. Expansion cycles exert a negative pressure – pulling the molecules apart. An intense sound wave can generate cavities or bubbles during the expansion cycle – cavitation. The lower the frequency, the larger the bubble will be. The bubbles can oscillate stably in the sound field for numerous acoustic cycles or implode violently in less than a microsecond (such bubbles are called transient bubbles) (Suslick, 1989: 62).

Power ultrasound causes chemical and physical changes in a liquid via the generation (and subsequent implosion or destruction) of cavitation bubbles. Transient bubble collapse generates the energy for the chemical and mechanical effects: temperatures of up to 4000 K, extreme heating or cooling rates of 10^{10} K/s and pressures exceeding 100 MPa are observed in the transient bubbles while the bulk fluid remains at ambient temperature and pressure. The implosion happens with a collision density of 1.5 kg/cm² and pressure gradients of 2 TPa/cm with lifetimes shorter than 0.1 μ s (Mason and Cordemans, 1996: 511-512). Radiation forces create intense micro and macromixing with high shear forces which are utilised in emulsification, homogenization and fragmentation processes. Asymmetrical bubble oscillations in the vicinity of solid particles lead to liquid microjets and shock waves which are used in cleaning, dispersion, activation and even fragmentation of solid materials (Hoffmann et al., 2000).

The determination of local intensities and ultrasound devices are difficult and are usually characterised by calorimetric measurements (Hoffmann et al., 2000).

2.1.1 Cavitation

Sonication, the use of ultrasound, is the conventional approach for creating cavitation. The actual physical phenomenon behind the effect of ultrasound is cavitation. Cavitation can be defined as: the formation, growth, and implosive collapse of bubbles (Pandit and Moholkar, 1996: 57).

For a system to be affected by sonication, at least one component must be in the liquid phase so that cavitation can be induced. If the sound pressure in a liquid is high enough, voids or gas- and vapour-filled bubbles are created. The minimum pressure required for disruption is determined by the tensile strength of the liquid. Theoretical calculations put the acoustic pressure requirement to cause cavitation at about 100 MPa (Pandit and Moholkar, 1996: 57). Almost all liquids contain various nuclei such as dissolved gases, solid impurities and rough walls. These nuclei reduce the tensile strength of the liquid and enable cavitation to occur at lower sound pressures than are theoretically necessary.

There are two types of cavitation: stable and transient cavitation. There are various types of bubbles present in cavitating liquids: empty cavities (true cavitation), gas-filled cavities, vapour-filled cavities or mixtures of gas and vapour. The type of bubble formed depends on the applied sound pressure, static pressure, temperature and the nature of the bulk liquid. Some of the bubbles disappear because of dissolution of their contents under the sound pressure, some oscillate stably over several acoustic cycles and others collapse violently – followed by the creation of smaller bubbles.

Cavitating voids can be classified according to the nature of the motion: stable cavitation, rectified diffusion, dissolving bubbles and transient cavitation.

Very small bubbles will dissolve. Bubbles larger than a certain threshold radius will oscillate stably in the sound field and can survive several acoustic cycles. A stable oscillating bubble can collect gas from the liquid and grow in size – rectified diffusion – the gas enters the bubble during the expansion cycle, but during the following compression cycle the bubble shrinks and the diffusion of the gas into the liquid is hindered by the smaller transfer area. For one sound cycle the bubble effectively expands a little more than it shrinks.

The growing bubble can reach the resonance radius where strong oscillations cause surface instabilities and generate smaller bubbles. Surface oscillations cause microstreaming near stable bubbles, which accelerates heat and mass transfer.

The growing bubble will reach a critical size where it will most efficiently absorb energy from the ultrasound. The critical size depends on the ultrasound frequency. At 20 kHz the critical bubble diameter is about 170 microns.

Once the bubble has experienced rapid growth (for instance: if the radius doubles in half an acoustic period) it can no longer absorb energy efficiently to sustain itself. The liquid will rush in and the bubble will collapse suddenly and disappear. These bubbles are called transient bubbles (Suslick, 1989: 63-64).

The intensity of cavitation can be affected by:

- Dissolved gas: liquids with a large amount of dissolved gas have larger numbers of cavitation nuclei and low cavitation thresholds
- Vapour Pressure: the vapour pressure of a liquid can cushion the bubble collapse. A high vapour pressure, near the boiling point of the liquid, can dampen cavitation efficiency to almost zero.
- Viscosity: the higher the liquid viscosity, the higher the cavitation threshold.
- Temperature: the temperature effect is via its effect on viscosity, gas solubility, vapour pressure and surface tension.
- Static Pressure: the static pressure in a sound field alters the thresholds for rectified diffusion, transient bubbles and other characteristics. It may even prevent the generation of bubbles by ultrasound.
- Frequency: frequency defines whether a bubble of a certain size is transient or stable. As the frequency is increased, the compression cycles shorten. At low frequencies (16 to 100 kHz, also called power ultrasound) the cavitation effects usually occur in heterogeneous systems and are micromixing, intense bubble motion, cleaning and mechanical action on the suspended solids. At high frequencies there are high temperatures and pressures in the cavitation bubbles which create a large number of radicals (sonochemical effects). In the megahertz region the duration of the expansion cycle is too short to generate bubbles and cavities.
- Ultrasound intensity: higher intensities create more and larger bubbles which may merge and lead to fewer transient effects (Hoffmann et al., 2000). The intensity can be increased by raising the amplitude or frequency of vibration of the ultrasonic device.

2.1.2 Effects of cavitation

- Bubble collapse near boundaries: A bubble will undergo symmetrical spherical oscillations and collapse in a sound field if undisturbed (in a liquid-only system). Disturbances such as suspended solids or reactor walls near a transient bubble will prevent spherical collapse. The presence of the surface distorts the pressure from the ultrasound field. Asymmetric

bubble wall motion leads to the formation of an involution which is directed towards the solid surface. During the last stages of transient (asymmetrical) bubble collapse, a liquid microjet will break through the remote bubble wall and impinge on the solid surface. The bubble is spherical at first and then shrinks rapidly. The jet develops opposite the solid surface and moves toward it. Liquid microjets can reach a velocity of 400 kilometers per hour (Suslick, 1989: 63-67) and are responsible for cavitation erosion on solids. These jets can increase mass and heat transfer to the surface by disruption of the interfacial boundary layers (disrupts the concentration polarization layer). The co-ordinated breakdown of a hemispherical transient bubble cloud can generate shock wave pressures and microjets with intensities orders of magnitude greater than that of a single bubble. At 20 kHz the collapsing bubble diameter will be around 150 μm ; solid particles smaller than this cannot cause microjet formation, only normal symmetrical spherical collapse will occur (Doktycz and Suslick, 1990: 1067).

- Shock waves: The implosion of a cavity sends shock waves through the liquid of which the Mach number can exceed unity.
- Streaming:
 - Acoustic streaming: absorption of the ultrasonic wave during its propagation in the cavitating liquid causes an energy gradient, which induces a macroscopic liquid flow. Momentum is absorbed in the direction of the sound field, initiating flow in this direction.
 - Acoustic microstreaming: small obstacles in a sound field create circulation by friction between their boundaries and the vibrating liquid particles. Microstreaming enhances mass and heat transfer and leads to shear forces on the obstacles.
- Radiation forces: the force experienced by objects in an acoustic field. Two types exist – the Rayleigh radiation force and the Langevin radiation force.
- Bjerknes forces: primary and secondary Bjerknes forces lead to the formation of structures called cavitation streamers. Clouds of oscillating micro-bubbles are formed and the lines of micro-bubbles are called microstreamers.
- Forces on small particles: small particles of which the radii is less than that of the cavitation bubbles are accelerated in the velocity and pressure gradients around oscillating bubbles. Shock waves increase the force on the particles. Particle velocities of up to 500 km/h can be reached (Hoffmann et al., 2000).

2.1.3 Chemical and mechanical effects of ultrasound

- Hot spot theory: very high temperatures and pressures are generated upon transient bubble collapse. Temperatures of 5000 K in the bubble, 2000 K in the liquid boundary layer and pressures of 50 MPa have been found in experiments. The heating and cooling rates are extreme: 10^5 K/s.
- Shock wave theory: compression of transient bubbles causes their bubble wall velocity to increase even up to the speed of sound in the liquid. During true transient cavitation, the bubbles vanish after collapse and create shock waves in the liquid. A steep pressure gradient is formed which accelerates particles and macromolecules. Collisions between high speed particles occur and cause mechanical damage to the particles.
- Supercritical water theory: the high temperatures and pressures effected during sonication of an aqueous medium may lead to conditions where supercritical water is formed.
- Charge theory: friction forces at the gas-liquid bubble boundary of an oscillating bubble undergoing rapid size changes can create charged species which can lead to side reactions in the bulk fluid.
- Promotion of single electron transfer (SET): ultrasound accelerate SET reactions, can alter reaction pathways and lead to different products.
- Cleaning: microstreaming, shock waves and liquid microjets near a solid boundary has a very efficient cleaning effect and has been put to industrial use for over forty years. The cleaning effect can remove insoluble layers of inorganic salts, polymers or liquids.
- Mechanical activation: high intensity ultrasound can remove passivating layers on solids and break solids like salts and metals.
- Enhanced mass and heat transfer: cavitation enhances micromixing which can accelerate heterogeneous reactions. Microstreaming is caused by oscillating and transient bubbles near suspended solid particles. Acoustic streaming and oscillating bubbles causes macromixing. The local mass transport coefficient is affected by the various types of mixing – the mass transfer coefficient in a sonicated fluid can be ten times higher than the coefficient measured under normal conditions (Hoffmann et al., 2000).

2.2 Ultrasonic Equipment

2.2.1 Transducers

Ultrasound transducers create the high frequency vibrations which are introduced into the liquid. There are two types of transducers used for liquids: liquid-driven and electromechanical.

The principle behind liquid driven transducers is that of a liquid whistle. The liquid is pumped through a small orifice and hits a blade. There is a sudden pressure drop in the orifice causing hydrodynamic cavitation. The blade generates ultrasonic vibrations and cavitation. Ultrasonic whistles are used in the food industry for mixing and homogenization.

Electromechanical transducers can either be magnetostrictive or piezoelectric. Both materials expand or contract (change shape) when placed in electromagnetic fields. Exposing the materials to a field alternating at an ultrasonic frequency produces ultrasound (Suslick, 1989: 65). Both types of transducers require a high frequency generator for electrical supply.

Magnetostrictive transducers are manufactured from ferromagnetic material like ferrite ceramics. High driving forces are achieved below 100 kHz. Magnetostrictive transducers display a broad frequency behaviour and poor efficiency.

Piezoelectric materials have a natural resonance frequency where the applied current produces the highest efficiency. Piezoelectric transducers are most often used in laboratory and industrial equipment. The transducers can be manufactured from barium titanate, lead metaniobate and lead zirconate titanate ceramics. Piezoelectric transducers usually have a fixed frequency as this enables operation at its highest efficiency. The transducers usually have a sandwich structure: two electrically opposed piezoceramics are fitted between two metal blocks. The length of the transducer is usually half a wavelength, it operates in compression mode and generates amplitudes up to 20 μm (Hoffmann et al., 2000).

2.2.2 General considerations regarding ultrasonic equipment

Scale-up for the industrial application of ultrasound is very difficult. For scale-up intensity, frequency, temperature and vessel geometry must be similar to that used under laboratory conditions to ensure reproducible results. The amplitude of the transducer, the ultrasonic intensity, the total power input, the specific power input per volume, the gas content and the local sound-energy distribution are the critical parameters for any sonication process (Hoffmann et al., 2000).

2.2.3 Laboratory equipment

The most common laboratory equipment is ultrasonic baths, high intensity disintegrator horns and cup-horn reactors.

Commercial ultrasonic baths can be used for low-intensity applications. Transducers are mounted at the bottom of a bath and are driven with the same frequency. A complicated standing wave field is created. The field intensity varies with location. The sample to be sonicated is immersed in the bath. Stirring is recommended.

Probe (also called ultrasonic immersion horn) systems are used for high intensity applications – up to 100 W/cm² at frequencies below 100 kHz. Use of a booster horn can increase the amplitude by a factor of ten. Only the vibrating tip of the horn is dipped into the liquid. This is the most effective method of introducing high power ultrasound into a liquid. Intense cavitation is created in the immediate vicinity of the horn. Ultrasound attenuates rapidly and only a few centimetres around the probe is subjected to the cavitation effect. As an ultrasonic probe generates acoustic streaming, external stirring is not required. The intense cavitation at the probe tip causes erosion and contaminates the sonicated liquid, frequent tip replacement is required (Pandit and Moholkar, 1996: 63). Power outputs from ultrasonic probes are quite high and the sonicated liquid may require cooling (Suslick, 1989: 65).

The cup-horn reactor is a variant of the probe system where a liquid is sonicated indirectly by submerging it in a sound-transmitting liquid (Hoffmann et al., 2000).

2.2.4 Large-scale equipment

Liquid-whistle reactors are used in homogenization emulsification and dispersion processes. The system is capable of high throughputs, stable operation and can be adapted to existing flow systems. The liquid-whistle is a low intensity device and is unsuitable for processes where more intense cavitation is required. The frequency is also fixed.

External or submersed rod or plate transducers can be fitted to tanks with a size of several cubic meters. Tube transducers can be retrofitted to existing plants. The use of these types of transducers enables quick scale-up. These types of transducers are low intensity devices.

A low intensity device transmits sound energy to a large liquid volume and the dimensions are larger than the liquid wavelength. At a frequency of 20 kHz and a diameter of 6 cm the typical power input is about 50 W per transducer.

When the dimensions of the sonicated volume are equal to or smaller than the liquid wavelength, high intensity devices are used. Probe systems can be used in

small flow cells – probes in series, which can be retrofitted. Gap reactors force liquids through the most active zone around an ultrasonic probe. The power input per transducer can reach 2 kW with a range of 10 cm.

Tube reactors are also used where high intensity ultrasound is required. The transducers are mounted on the outside of the tube and create intense cavitation in the centre. Hexagonal and heptagonal tubes to allow easier mounting of transducers are also used. Branson developed a reactor with a coupling fluid between the horn and reactor wall. The Sodeva sonitube consists of a stepped horn and a resonant collar which is mounted on a cylindrical pipe. Raiganis developed a tube reactor with axial cooling (Hoffmann et al., 2000).

2.3 Ultrasonically Assisted Filtration – Early Developments

In a Russian monograph published in 1965, (Nosov, 1965) ultrasound assisted filtration is mentioned – a filter for liquid slurries is described where the ultrasonic transducer is connected to the filter element.

In a patent by Harvey, (Harvey, 1965), an acoustic liquid whistle or ultrasound to produce cavitation to prevent clogging of the membrane and to remove concentration-polarization, was proposed.

A US patent of 1967 (Peterson, 1967) describes a process where a suspension of solids in a liquid is sieved and clogging of the sieve is prevented by ultrasonic vibrations by an ultrasonic probe placed in the fluid. The meshed sieve sizes were given to be 100 μm down to 5 μm .

A Russian publication about ultrasound in hydrometallurgy, published in 1969, describes experiments utilizing ultrasound to assist filtering (Agranat, 1969). An electrodynamic shaker operating at 100 Hz was used. The authors also found an increase in flow-rate with ultrasonic agitation and found that the reason for this was that deposits were not formed or were continuously removed from the filter element. The authors also gave various reasons why ultrasonically enhanced filters could not go beyond laboratory stage at the time.

In 1969 Howkins (Howkins, 1969: 129-130) investigated haemodialysis in artificial kidney machines and found that ultrasonic agitation of fluid layers near the membrane produced a major increase in dialysis rates.

In 1970 Semmelink (Semmelink, 1970), observed that the application of ultrasonic vibrations to the filtering of liquids leads to an increase in the flow-rate. The main reason for the increase in flow-rate with ultrasonic agitation was found to be the fact that a deposit of solid particles was continuously removed from the filter element. Without the ultrasonic agitation a filter deposit is formed and this deposit was found to be responsible for the rapid decline in flow-rate. Semmelink also found that a uniform removal of the deposit could be achieved by placing the

radiating face of the transducer close to the filter element, but not connecting it to the element. The transducer was placed 1 cm above the filter disk. The filter element was metal wire cloth with a nominal pore size of 8 μm . The electrical input to the transducer was 20 W at 20 kHz and the static pressure was 13 kPa, with Chicago tap water being the filtrant.

In a paper presented by Semmelink (Semmelink, 1973) the application of ultrasonic vibrations to the filtering of liquids and specifically by the reverse osmosis (RO) process was described. The project focused on was by the Central Acoustics Laboratory of the University of Cape Town. The project was aimed at determining the economics of ultrasound enhanced water purification processes, focusing on RO. A commercial transducer-generator combination was used. The operating frequency was fixed at 20 kHz; the maximum power output was 500 W. The radiating face was set just above the filter element. A Nuclepore plastic membrane and stainless steel wire cloth, both with nominal pore size of 5 μm were used. The static pressure was 5 kPa and Cape Town tap water was the filtrant. It was found that without ultrasonic irradiation, the flow-rate rapidly decreased. With ultrasonic irradiation the decrease was found to be much smaller and it approached a constant value after a few hours.

2.4 Modern Applications

A paper by Tarleton (Tarleton, 1988: 402-406) describes how electric and ultrasound fields can be used to reduce fouling in microfiltration. The experiments were carried out in dead-end filtration mode at constant pressure. A stainless steel filter cell consisting of a conventional leaf filter, electrodes and ultrasound transducers were used. The maximum power to the ultrasonic transducer was 600 W. Two ultrasound frequencies were used: 23 and 40 kHz. The authors found that the pH of the suspension affected the efficiency of the ultrasound. Ultrasound appeared to have a minimum effect when pH-levels corresponded to the points of zero and maximum zeta potential. It was also found that for certain suspensions, ultrasound has a detrimental effect on the permeate flux. It was suggested that the influence of ultrasound in filtration might be dependent on the surface properties of the particulates in suspension and also on particle shape and orientation.

Tarleton and Wakeman studied the effects of electrical and ultrasonic fields and the combined fields on crossflow microfiltration (MF), (Tarleton and Wakeman 1990: 192-194), (Wakeman and Tarleton, 1991: 386-397), (Tarleton and Wakeman, 1992: 428-432). Experiments were carried out at ultrasound frequencies of 23 and 40 kHz with maximum power output of 600 W. Different types of membranes were used. Crossflow velocities of 0 to 0.2 $\text{m}\cdot\text{s}^{-1}$ were used. They found that both fields can reduce membrane fouling by an amount dependent on applied field strength, acoustic frequency, suspension concentration, liquid viscosity, particle size and particle surface charge. The

combined fields had a synergistic effect. The authors also found that when the force fields are used in MF, lower crossflow velocities can be used, implying lowered energy consumption and reduced degradation of shear sensitive streams. The lower ultrasonic frequency gave a greater flux improvement. When the ultrasound source was brought closer to the membrane, the effect of ultrasound on improving filtration rates increased. It was found that at higher solids concentrations, the filtration rate enhancements possible with an ultrasonic field were reduced. It was observed that the application of ultrasound leads to a flux increase for smaller particles, but for larger particles it could lead to a reduced flux rate. It was also found that the application of an ultrasonic field led to a decrease in liquid viscosity. The authors also examined the power consumption of their setup, but did not optimize it.

Wakeman and Smythe, (Wakeman and Smythe, 2000: 125-135), (Wakeman and Smythe, 2000: 657-661), studied the effects of electric and acoustic fields on constant pressure filtration. The ultrasonic frequency was fixed at 23 kHz and the power input to the transducers was 275-300 W. The ultrasonic transducer was attached to one side of the filter cell and the ultrasonic energy was applied tangentially to the filter surface. Sartorius cellulose nitrate membranes with a pore size rating of 0.2 μm were used. Experiments were carried out at constant vacuum. In their experiments they observed a decrease in the filtration rate when the ultrasonic field was applied. They also found that acoustic fields have little effect on filtration rates close to the suspension isoelectric point (IEP). It produces a slight improvement in filtration rate at high pH, but has a deleterious effect at intermediate pHs. The combined fields exhibited a synergy closer to the IEP and high pHs. It was found that ultrasound enhances the effect of an applied electric field close to the IEP of the suspension by reducing the effective particle size and increasing electrophoretic velocities.

Muralidhara *et al.* (Muralidhara *et al.*, 1986: 351-353) developed an electro-acoustic process for the dewatering of a slurry. The process combines electrical and acoustic fields. The two applied fields have a synergistic effect and lead to higher dewatering rates and energy savings. An ultrasound frequency of 20 kHz was used.

Chai, Kobayashi and Fujii, (Chai *et al.*, 1998: 129-135) studied the ultrasound effect on cross-flow filtration of polyacrylonitrile (PAN) ultrafiltration (UF) membranes. The ultrasound effects on permeate flux and rejection of solids were investigated. Two types of PAN UF membranes reinforced with woven cloth were used. A 1 wt.% Dextran solution was used in the experiments and the applied pressure was fixed at 30 kPa throughout the UF experiments. The ultrasonic frequency was 45 kHz with input power of 248 W. The ultrasonic transducers were placed 50 mm from the membrane and the dense skin layer of the membrane faced the transmission direction of the ultrasound. Experiments were conducted with ultrasound on and off for alternating periods and also with

continuous ultrasound irradiation. They found that the sonication treatment increases permeate flux for Dextran solute, which is highly rejected by the PAN membrane. They observed no ultrasound effect for water and small effect for Dextran with low rejection by the membrane. The authors found evidence that the increase in permeate flux can be attributed to the enhancement of bulk mass transfer in the concentration polarization layer near the membrane.

In a different set of experiments Chai *et al.* (Chai *et al.*, 1999: 139-146) studied ultrasound-associated cleaning of various polymeric membranes for water treatment. Experiments were conducted with peptone solutions of 1, 2, 4 and 6 wt.%. An ultrasound cleaning technique was applied to remove fouling of UF and MF membranes. Polysulfone (PS), polyacrylonitrile (PAN) and polyvinylidene fluoride (PVDF) membranes were used. The ultrasonic frequency was 45 kHz and the power output 2.73 W.cm^{-2} . The feed flow-rate and operating pressure was fixed at 325 ml.min^{-1} and 30 kPa, respectively, throughout the experiments. The authors found that water cleaning under sonication is effective in cleaning polymeric membranes fouled by peptone solution. It was also found that a PS membrane fouled by high concentrations of peptone could be cleaned completely by this method and that an increase in the operating temperature showed a high cleaning efficiency by water cleaning under sonication.

In another set of experiments Kobayashi, Chai and Fujii studied ultrasound enhanced crossflow membrane filtration, (Kobayashi *et al.*, 1999: 31-40). The ultrasound effects on a permeate flux of Dextran solutions through PAN UF membranes were examined. Dextran solutions of 0.5, 1, 2, 3 and 5 wt.% were used. The ultrasonic frequencies were 28, 45 and 100 kHz and the power output 150 to 300 W. The effect of the ultrasound propagation direction was also examined. It was found that ultrasound with a frequency of 28 and 45 kHz enhanced the permeate flux of PAN UF membranes in crossflow filtration. It was also found that the enhancement of the permeate flux depended on ultrasound intensity and the irradiation direction relative to the membrane. Evidence was found that the ultrasound irradiation enhanced permeation by increasing mass transfer across the concentrated Dextran layer close to the membrane surface.

Band *et al.* investigated the enhancing effect of specially modulated ultrasound signals in water desalination by ion-exchange hollow fibers, (Band *et al.*, 1997: 303-313). The ultrasonic frequency was 45-49 kHz and the power output 23-61 W. It was found that, depending on the concentration of the solutions and hydrodynamic conditions, ultrasound enhanced different steps of the overall ion-exchange process. The effect also increased with temperature (in the range of 20-50 °C). It was found that the flux increase was proportional to the applied ultrasound power. The authors also found that acoustic cavitation may be controlled via appropriate amplitude modulation of the driving ultrasound.

Unpublished work done at Stellenbosch University used on-line ultrasonic cleaning to remove fouling from a polyamide RO membrane in crossflow filtration of CaSO₄, Fe³⁺ and carboxyl cellulose solutions. An ultrasonic bath with a frequency of 20 kHz and a power intensity of 2.8 W.cm⁻² was used. The flow-rate and pressure were maintained at 5 ml.min⁻¹ and 100 kPa respectively, throughout the experiments. When ultrasound was applied the permeate flux of the membrane increased with almost no decrease in rejection. Off-line ultrasonically assisted water cleaning was also effective and could restore the permeate flux with negligible change in rejection.

Simon *et al.* (Simon *et al.*, 2000: 183-186) studied the enhancement of dead-end ultrafiltration by ultrasound. The ultrasonic frequency was fixed at 20 kHz and the maximum power output was 40 W. The emitter was placed 14 mm from the membrane. Experiments were also done with a conventional mechanical stirrer. The authors concluded that low-frequency ultrasound could improve dead-end UF performance. The improvement is due to the removal of part of the boundary layer from the membrane surface. The removal of the boundary layer is effected by stirring – mechanical or ultrasonic. Higher permeate fluxes were achieved by either increasing stirrer speed or ultrasonic power – a virtual “ultrasonic stirrer” speed, depending on the ultrasonic power, was defined.

Masselin *et al.* (Masselin *et al.*, 2001: 213-220) studied the effect of ultrasound on polymeric membranes immersed in a water bath. The ultrasonic frequency they used was 47 kHz. Three different polymeric membranes were studied: Polyethersulfone (PES), polyvinylidene fluoride (PVDF) and polyacrylonitrile (PAN). The effect of ultrasonic irradiation on the polymeric structure was determined by the measurement of the water permeability and the ratio of surface porosity to thickness. The authors showed that only the PES membrane was affected over its entire surface, the PVDF and PAN membranes were more resistant – only the PAN50a and PVDF40 membranes were affected significantly and mainly at the edges of the membranes. The degradation of membrane surfaces under ultrasonic stress led to an increase in the pore radius for large pores, an overall increase in pore density and porosity and to the formation of large cracks, mainly at the edges of the membranes. The conclusion was that ultrasound should be used with care with membranes – the nature of the polymeric material, the ultrasonic frequency and intensity should be taken into account.

Li and Sanderson (Li, Sanderson and Jacobs, 2002: 247-257) used ultrasound and ultrasound coupled with water flushing to recover the permeate flux of flat sheet MF membranes fouled by Kraft paper mill effluent. The ultrasonic frequency used was 20 kHz and the power 375 W. The nylon membranes had a 0.2 μm average pore diameter. Forward-flushing, ultrasonic cleaning and ultrasonic cleaning coupled with forward-flushing was employed for membrane cleaning and the cleaning efficiencies were compared. The authors found that sonication coupled with water flushing was the most effective cleaning technique

and that a flushing velocity higher than the normal operating velocity is required. The authors showed that sonication was successful in removing the fouling layer, recovering the permeate flux and restoring the original structure of the membrane surface.

2.5 Enhanced Permeation via Ultrasonication

Lenart and Auslander, (Lenart and Auslander, 1980: 216), examined the effect of ultrasound on the diffusion of certain electrolytes through cellophane membranes. They used ultrasound with an intensity of $1.2-6 \text{ W.cm}^{-2}$ and a frequency of 1 MHz. They found accelerated diffusion with ultrasonic irradiation.

The patent by Kost and Langer, (Kost and Langer, 1988) uses ultrasound to enhance the permeability of molecules of small and large molecular weight in a membrane system irradiated with ultrasound of an intensity of $0.05-30 \text{ W.cm}^{-2}$ and a frequency between 10 kHz and 20 MHz for polymeric membranes and an intensity of $0.05-3 \text{ W.cm}^{-2}$ and a frequency of 1-3 MHz for biological membranes.

Li *et al.* (Li *et al.*, 1995: 2725-2729), (Li *et al.*, 1996: 3255-3258) investigated the influence of ultrasound on the diffusion of electrolytes through a cellophane membrane. They found that diffusion through the membrane with ultrasonic irradiation is faster than without ultrasound.

Chapter 3

Experimental Setup and Methods

3.1 Process description

The same approach as for pilot work was followed. The most common parameters during operation: temperature, start and stop times, pressures, in- and out-flows were recorded. Timed samples were collected and conductivity, pH, turbidity and absorbency were measured to quantify the feed, permeate and retentate quality. Flux, temperature and water quality versus operating time graphs could be constructed from the collected data. The permeate water quality and production rate (flux) was monitored closely.

It was attempted to construct a module corresponding to the basic unit of an industrial unit. The bench-scale process was also modelled on the typical industrial set-up. Permeate and retentate were collected, sampled and disposed of, not recycled to the feed reservoir.

3.2 Equipment

Experiments were conducted in a small cylindrical unit that housed polyether sulphone (PES) capillary tubes. A bench scale membrane module (Figure 3-1 and Figure 3-2) was designed to take the IKA U50 7 mm diameter ultrasonic probe. The operating frequency of the probe was fixed at 30 kHz and all experiments were run at full amplitude.

The module held 10 polyether sulphone hollow fibres, which were obtained from the Institute of Polymer Science at the University of Stellenbosch in South Africa. The fibres had a length of 345 mm and a diameter of 1.2 mm.

Permeate collected on the shell side of the module and was collected from the permeate port closest to the feed entrance. The ultrasonic probe was inserted at the central T junction shown in Figure 3-1. The first ½" of the T junction acted as the permeate port. Both the central T junction and the second ½" T were open to the atmosphere ensuring that the shell-side was at atmospheric pressure. The operating pressure of the hollow fibres was 100 kPa (g), while the maximum design pressure of the fibres was 200 kPa (g). The pressure was regulated via a backpressure valve on the retentate outlet. The hollow fibre bundle was 345 mm long (excluding the epoxied ends that were 70 mm in length each). The total

length of the module was 485 mm. A Watson-Marlow peristaltic pump was used to circulate the feed.

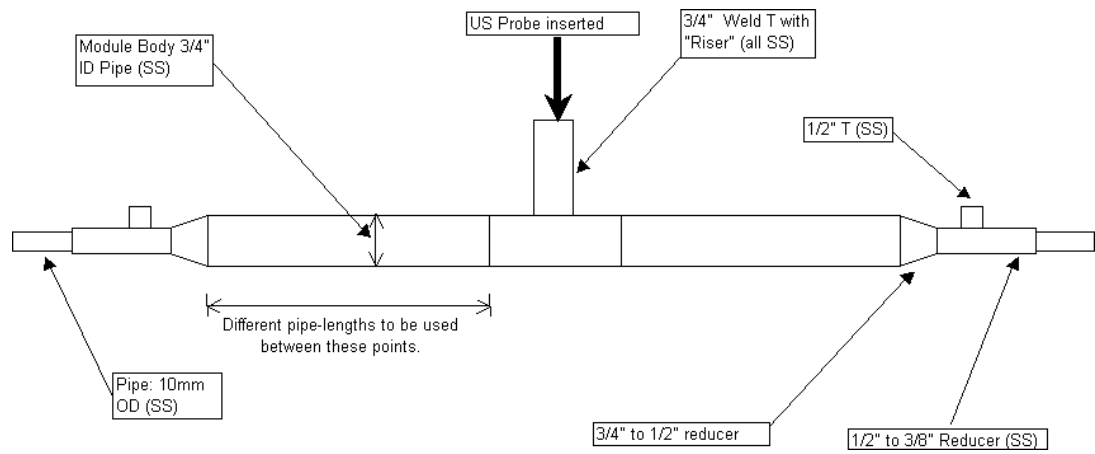


Figure 3-1. Diagram of the bench-scale capillary ultrafiltration module



Figure 3-2. Photograph of the bench-scale module and probe.

For later experiments permeate was collected in a large beaker set on an electronic scale. The scale was connected to a computer which logged the mass of permeate every ten seconds.

The temperature was measured at the second (unused) permeate port by inserting a thermometer or temperature probe.

3.3 Membrane Preparation

The hollow fibres were received in dry form and had to be prepared before any work could be done with them. Ultrapure water was pumped through the membrane at 50 kPa (g). The first 3 L of retentate was discarded as this contained organics that had been flushed out of the membrane. After 1 h the pressure was raised to 100 kPa (g) and ultrapure water was circulated through the membrane for up to 24 h.

After completion of the preparatory phase, permeate was collected for 1 h and the volume collected was used to calculate the clean water flux of the membrane in litres per meter squared per hour ($\text{Lm}^{-2}\text{h}^{-1}$). For the PES membranes, typical values ranged from 50 to 100 $\text{Lm}^{-2}\text{h}^{-1}$.

3.4 Tests with Congo Red dye

The feed was made up of approximately 9 L of distilled water with less than 0.01 g of Congo Red dye ($\text{C}_{32}\text{H}_{22}\text{N}_6\text{Na}_2\text{O}_6\text{S}_2$ – standard indicator, supplied by Fluka, molecular weight 696.68). This feed was pumped through the membrane module for 5 to 7 h, taking hourly flux and retentate flow rate measurements until the flux had become more or less stable. After this, the ultrasonic probe was inserted and sonication commenced. The bundle of hollow fibres was sonicated for a total of 6 h at the full amplitude and full cycle of the probe. Sonication was not applied continuously over the whole period of filtration, but was applied in intervals of one hour at a time during filtration. The feed temperature was measured at the start and finish of every sonication interval. Permeate and retentate temperatures were recorded every 10 minutes while sonication was taking place. Between sonication intervals, feed was circulated through the module for 30 minutes at a time. Whenever coloured permeate was observed the experiment was terminated, as coloured permeate was regarded as an indication of damage to the membrane. After the completion of each experimental run, the hollow fibre bundle was removed for further examination.

3.5 Tests with Ultra-Pure Water

Milli-Q water (distilled and deionized) was used as the feed. The water used in experimental runs was obtained from the Biochemistry department at the University of Stellenbosch. Feed was pumped through the membrane for 10-20 hours, taking hourly flux measurements until the flux had stabilized. After this,

the ultrasonic probe was inserted and sonication commenced. The bundle of hollow fibres was sonicated for a total of 6 hours at full amplitude and full cycle of the probe. As before, sonication took place over discrete time intervals during filtration. The feed temperature was measured at the start and end of every sonication interval and permeate temperatures were recorded every 10 minutes during sonication. Between each sonication interval, feed was circulated through the module for 30 minutes. An abnormal increase in permeate flux was regarded as an indication of damage to the membrane. After the completion of each experimental run the hollow fibre bundle was removed and the hollow fibres were examined under a microscope.

3.6 Tests with Coloured Ground Water from the George Region

The membranes were prepared with distilled water and prefouled with the coloured ground water until the flux stabilised. After this the probe was inserted and sonication commenced. Sonication was not applied continuously over the whole period of filtration, but was applied in intervals of one to two hours at a time during filtration. Each sonication interval was followed by a period of normal filtration of duration between one and two hours. The mass of permeate collected was recorded every ten seconds and this was used to calculate the flux. The permeate product and retentate were collected, measured, sampled and discarded after each filtration interval. For the second experimental run with the ground water from George the temperature was measured at the start and end of each sonication interval and also at 20-30 minute intervals during each filtration interval.

3.7 Tests with Water from the Steenbras Dam

The membranes were prepared with distilled water and then prefouled with Steenbras dam water until the flux stabilised. The ultrasonic probe was inserted and sonication commenced. As in the previous experiments, the sonication was not continuous. The general properties of the water are summarized in Table 3-1.

The sonication period was increased from 30 minutes to 90 minutes towards the end of the experimental run. Each sonication interval was followed by a normal filtration interval of duration 90-120 minutes. The probe immersion depth was between 25-32 mm (the water level in the riser varied slightly). The pump-speed was varied between 110 and 140 rpm to maintain the backpressure of 100 kPa. The feed temperature was measured at the tank at the start and end of each filtration interval. The module temperature was measured at the second (unused) permeate port at the start and end of each filtration interval. The retentate volume was measured after each filtration interval. The mass of permeate was recorded at 10 seconds intervals and used to calculate the flux. After each filtration interval the permeate product and retentate was discarded.

Table 3-1. Physicochemical characteristics of the natural organic water sample from Steenbras Dam (the data are average values of the samples taken over 3 weeks).

Category	Parameters	Values
Physical	Total dissolved solids mg/L	35
	Conductivity @ 20 °C, mS/m	6.5-7.1
	pH	5.24-5.63
	Turbidity, NTU	1.44-2.32
	Colour, Plat.std	60-80
Organic	UV-absorbancy, 254 nm	0.38-0.41
	PV4 @27 °C, mg/L	6.7-6.9
Hardness	Total, CaCO ₃ mg/L	7.2-8.1
Mineral	Alkalinity, CaCO ₃ mg/L	2.0
	Chloride , Cl mg/L	17-18
	Sulphate, SO ₄ mg/L	3.4-3.7
	Calcium, Ca mg/L	1.1-1.4
	Magnesium, Mg mg/L	1.06-1.16
	Sodium, Na mg/L	8.0-8.9
	Potassium, K mg/L	<0.50

3.8 Tests with Dextran

Dextran-solution was selected as the final test effluent. Dextran is a glucose polymer and various molecular weight ranges occur – $(C_6H_{10}O_5)_n$. Dextran molecules are round and solutions of Dextran of known molecular weight can be made up and used for determining the molecular weight cutoff (MWCO) of a particular membrane. The Institute of Polymer Science at the University of Stellenbosch uses poly ethylene glycol (PEG) for determining MWCO. PEG is an elongated molecule and due its non-symmetrical geometry it was decided to use Dextran for the investigation of the effect of sonication on permeate flux. For the PES membranes being used in the investigation Dextran with a molecular weight below 20 000 would be able to permeate through the membrane. Dextran with a molecular weight above 30 000 would not be able to be transported through the membrane at all.

It was decided to use Dextran with the threshold value of a molecular weight of 20 000. Dextran was purchased from Fluka: 15 000 – 20 000 M_r from *Leuconostoc ssp*, $(C_6H_{10}O_5)_n$ [9004-54-0]. A solution of 1 wt% Dextran was made up for the experimental run. The membranes were prefouled with Dextran solution for 2 hours. After 2 hours it was deemed that the flux-decline was sufficient so that sonication would have a noticeable impact. Sonication was not

done continuously. Sonication intervals of 30 and 60 minutes were used. Each sonication interval was followed by a normal filtration interval of 30 and 60 minutes. The temperature was monitored throughout the experimental run. The feed temperature was measured at the tank at the start and end of each filtration interval. The module temperature was measured at the second (unused) permeate port at the start and end of each filtration interval. The pump-speed was varied to maintain the backpressure of 100 kPa (g). The retentate volume was measured after each filtration interval. The mass of permeate was recorded at 10 seconds intervals and used to calculate the flux. After each filtration interval the permeate product and retentate was discarded. More details on the experiments can be found in Appendices A and B.

Chapter 4

Results and Discussion

4.1 Visual Tests with Congo Red

4.1.1. Visual Test 1

Feed was pumped through the module over a period of 5 hours, during which no sonication took place. After 5 hours, ultrasonication was introduced to the system, but the test was terminated 10 minutes after switching on the ultrasound when a hollow fibre ruptured. This occurred when the tip of the sonotrode touched the hollow fibre bundle. The damage to the membrane was visible to the naked eye and was in the middle of the strand in line with the insertion point of the sonotrode.

4.1.2. Visual Test 2

Feed was pumped through the module over a period of 5 hours, during which no sonication took place. This test was terminated 9.5 minutes after switching on the ultrasound when two hollow fibres were ruptured. This happened when the tip of the sonotrode touched the hollow fibre bundle. The damage to the hollow fibres was visible to the naked eye and was in the middle of the strands in line with the insertion point of the sonotrode.

4.1.3. Visual Test 3

As before, feed was pumped through the module over a period of 5 hours, during which no sonication took place. This was followed by sonication over a period of 7 hours. From Figure 4-1 it can be seen that during the first five hours (in the absence of sonication) the flux decreased with time. Within the first hour of sonication, the flux increased markedly, but then gradually decreased again, as indicated in Figure 4-1. Permeate and retentate temperatures were also recorded. The ultrasound caused a modest increase in these temperatures, never exceeding 4 °C, as indicated in Figure 4-2. All the permeate samples were clear and when the hollow fibres were examined under an optical microscope, no damage to the membranes surface could be observed.

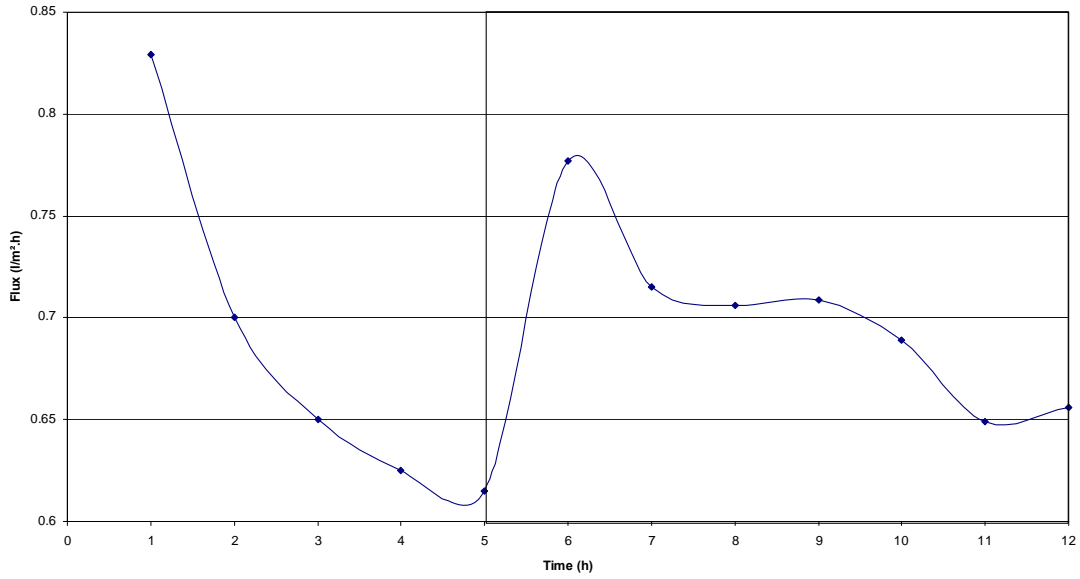


Figure 4-1. Permeate flux of water containing 0.11 wt% Congo Red dye. Coloured band indicates sonication interval.

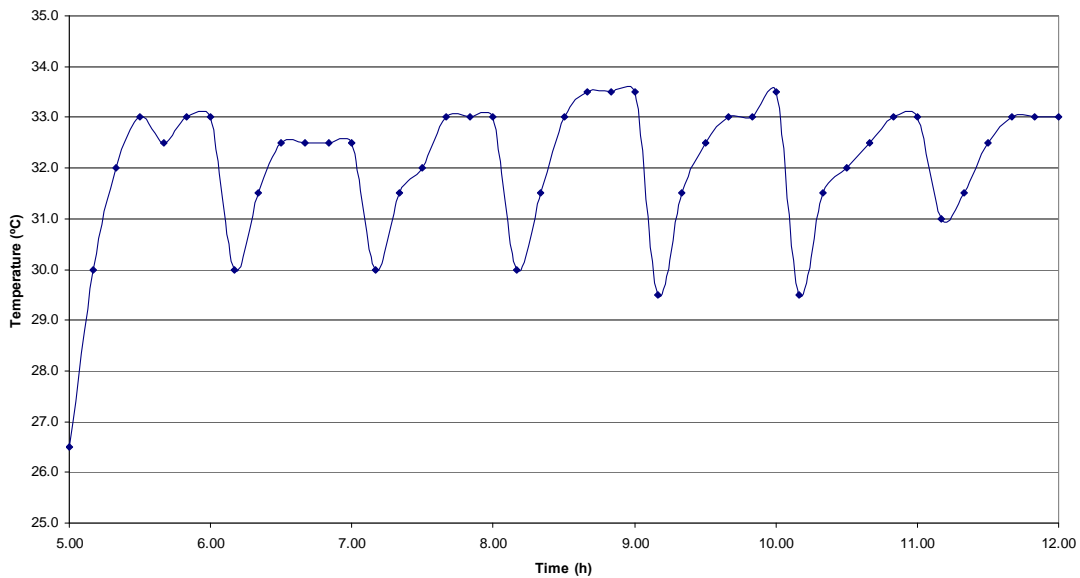


Figure 4-2. Effect of sonication on permeate temperature

4.1.4. Visual Test 4

Feed was pumped through the module in the absence of sonication for a total of 5 hours. This was followed by sonication in hourly intervals for a total time of 5 hours. Every sonication interval was followed by a 30 min interval where feed was pumped through the module in the absence of sonication. During the first 5 hours (in the absence of sonication) the flux was fairly constant at low values (Figure 4-3). During the first sonication-interval the flux increased markedly. During the 30-minute recovery period the flux decreased again, but not to the same level as

was recorded during the first 5 hours. Once the ultrasound was switched on again, the flux increased again. The sonicated flux values remained fairly constant.

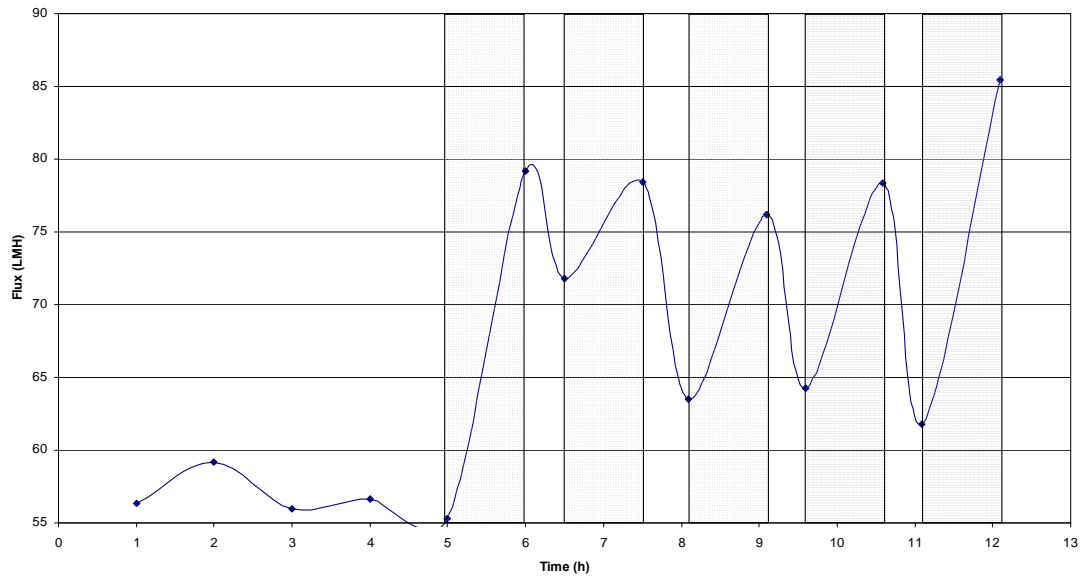


Figure 4-3. Permeate flux of water containing 0.11 wt% Congo Red dye (visual test 4). Bands indicate sonication intervals.

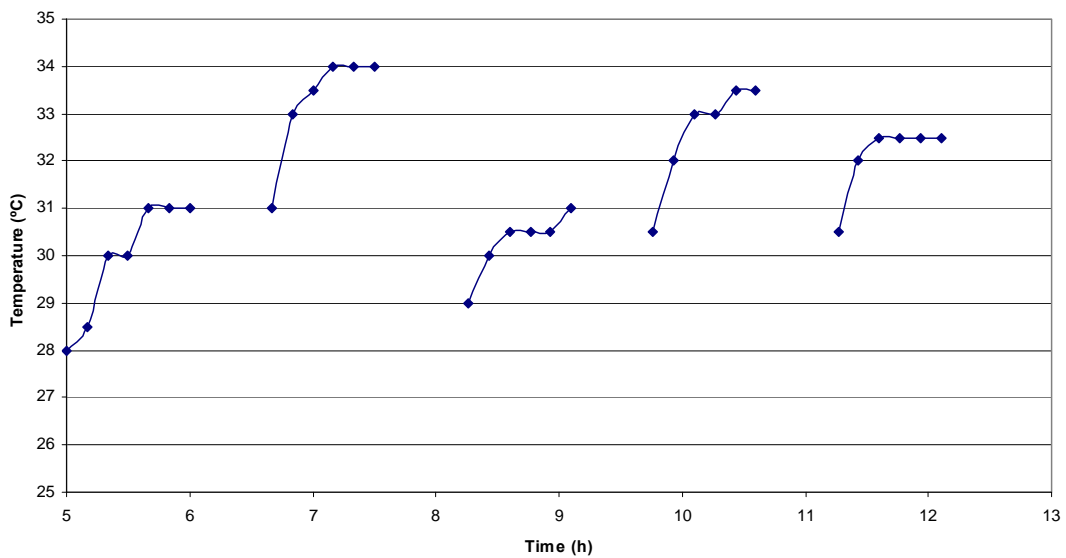


Figure 4-4. Effect of sonication on temperature – temperatures only recorded during sonication intervals.

Sonication appeared to have increased the permeate flux, as the average sonicated flux was 31% higher than the average unsonicated flux, and 40% higher than the average value of the unsonicated flux recorded during the first 5 hours. The last flux value is abnormally high – at this point coloured permeate was obtained, an indication of damage to the membrane, which was subsequently

confirmed by microscopic analysis. This damage again appears to have been caused by the sonotrode coming into contact with the fibre.

The temperature increase in the solution owing to the application of ultrasound is shown in Figure 4-4. The ultrasound caused a modest increase in temperature of approximately 3 °C in the permeate and less than 1.5 °C in the retentate. This minimal temperature increase indicates that temperature could not have been the only driving force behind the observed enhancement of the flux.

It appears as if phenomena other than defouling may also have occurred during sonication, since the generally higher flux values observed during sonication are not consistent with the effect expected with the removal of foulants from the membrane. Similar trends were identified in the other visual tests described here, as can be seen in Figure 4-3 as well.

4.1.5. Visual Test 5

Feed was pumped through the module in the absence of sonication for a total of 6 hours. This was followed by sonication for one hour followed by a 30 min interval where feed was pumped through the module in the absence of sonication. During the sonication interval the flux increased dramatically and at the end of the 30-minute recovery period coloured permeate was obtained. This was an indication that damage to the membrane occurred, again probably owing to contact made between the tip of the ultrasonic probe and the membrane material.

4.1.6. Visual Test 6

Feed was pumped through the module in the absence of sonication for a total of 8.5 hours. This was followed by sonication in hourly intervals for a total time of 6 hours. As with the previous test, each sonication interval was followed by a 30 minute interval where the feed was pumped through the module in the absence of sonication.

During the first 8.5 hours (in the absence of sonication) the flux varied with time, as indicated in Figure 4-5. During the first sonication interval the flux increased. During the 30-minute recovery period the flux decreased again, but not to the same level as was recorded during the first 8.5 hours. This pattern was repeated during subsequent cycles of ultrasonication and operation without ultrasound.

No indications of damage to the membrane could be observed from either the colour of the permeate or visual examination of the membrane fibres. At each cycle of one hour, the ultrasound increased the permeate and retentate temperatures to maximum values of 6 °C and 3 °C respectively, as indicated in Figure 4-6. Again, this was not sufficient to explain the increase in the observed flux enhancement. To elaborate on this point, compare the solution at 22 °C and 32 °C (the temperature extremes in Figure 4-6). Under these conditions, the

viscosities of the solutions range from approximately 0.94 mPa.s to 0.70 mPa.s. This translates into an increase in flow rate of approximately 20%, which would explain approximately half of the increase in the permeate flux when subjected to ultrasound.

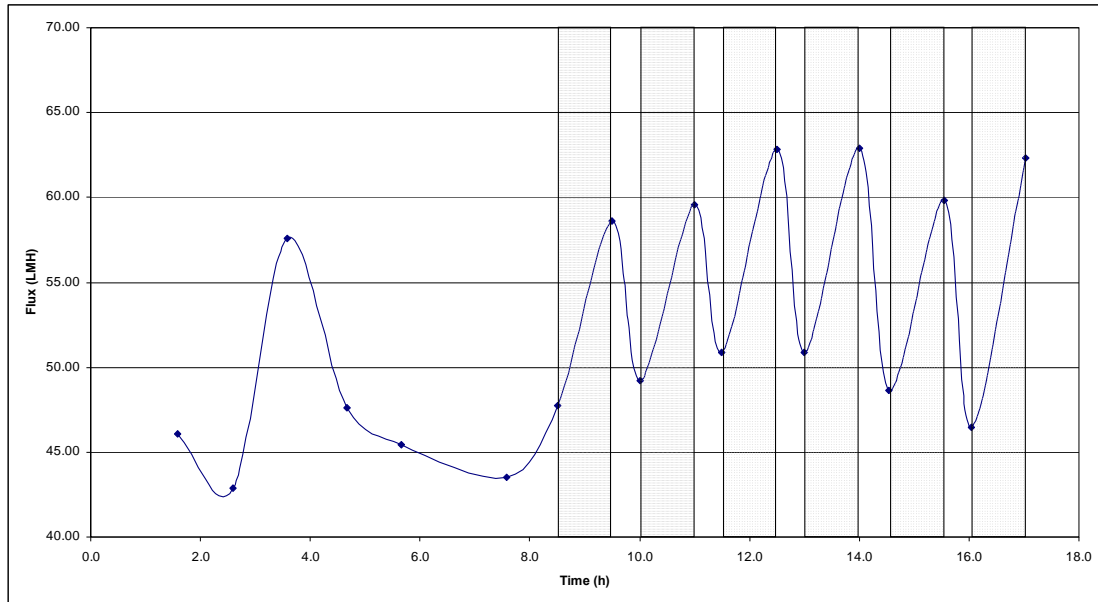


Figure 4-5. Permeate flux of water containing 0.11 wt% Congo Red dye (Visual Test 6). Bands indicate sonicated intervals.

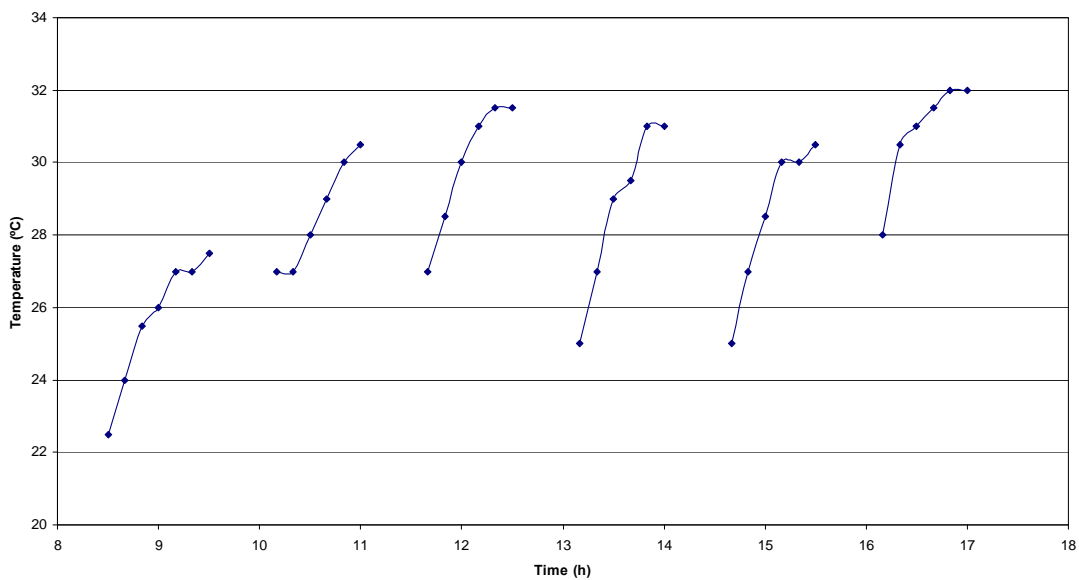


Figure 4-6. Effect of sonication on temperature – temperatures only recorded during sonication intervals, as indicated in Figure 4-5.

4.2. Tests with Ultra-Pure Water

Milli-Q water (distilled and deionized) was used as the feed. Generally, an abnormal increase in the permeate flux was regarded as an indication that damage to the membrane had occurred. Three experimental runs were carried out.

4.2.1. Milli-Q Water Test 1

Feed was pumped through the module in the absence of sonication for a total of 25 hours. This was followed by sonication in hourly intervals for a total time of 6 hours. Every sonication interval was followed by an approximately 30-minute interval where feed was pumped through the module in the absence of sonication.

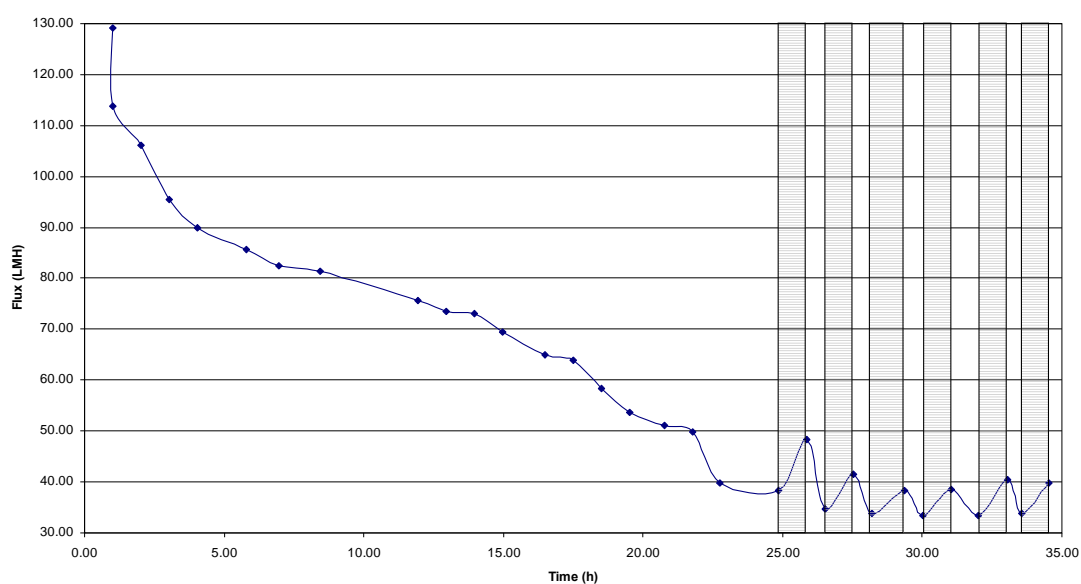


Figure 4-7. Permeate flux of ultrapure water (Visual Test 1). Coloured bands indicate sonication intervals.

The unsonicated flux decreased from approximately $56 \text{ Lm}^{-2}\text{h}^{-1}$ with time (possibly due to compaction of the membrane). Once sonication commenced, the flux stabilized, again showing the patterns of increase and decrease after sonication and in the absence of sonication respectively, but to a lesser extent than what was observed with the Congo Red dye.

No abnormal increases could be detected in the permeate flux. The increase in flux during sonication can only be attributed to minor cleaning, since ultrapure water was used as the feed. Even ultrapure water contains nanoparticles which can clog pores. The increase in flux could possibly be attributed to ultrasound having an enhancing effect on mass transfer. The permeate temperature was monitored during each experimental run, indicating a maximum increase of $3.5 \text{ }^{\circ}\text{C}$, which does not fully explain the observed increase in the permeate flux.

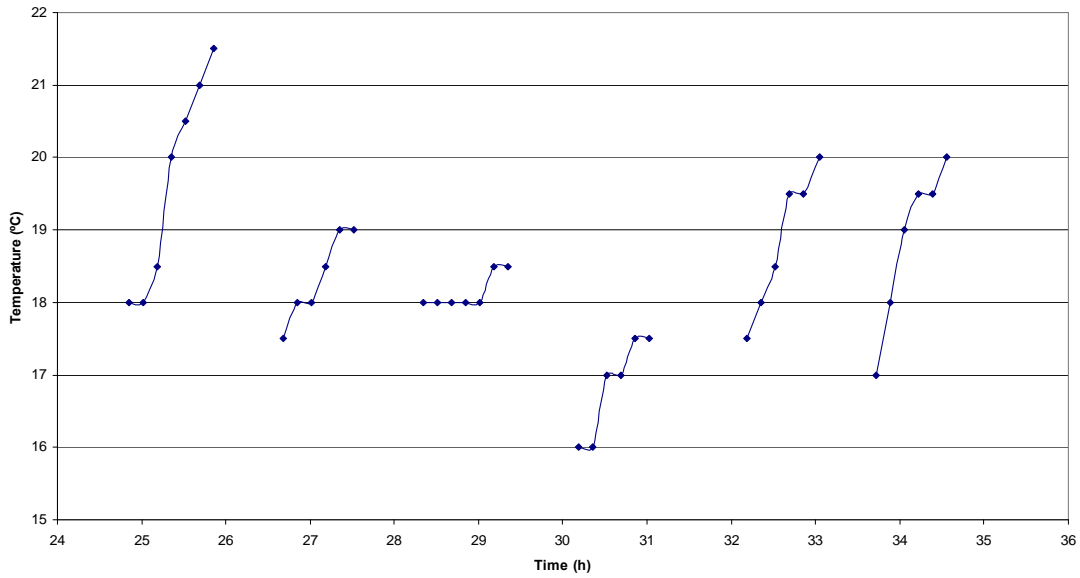


Figure 4-8. Effect of sonication on permeate temperature (Visual Test 1).

4.2.2. Milli-Q Water Test 2

Feed was pumped through the module in the absence of sonication for a total of 14.4 hours. This was followed by sonication in hourly intervals for a total time of 6 hours.

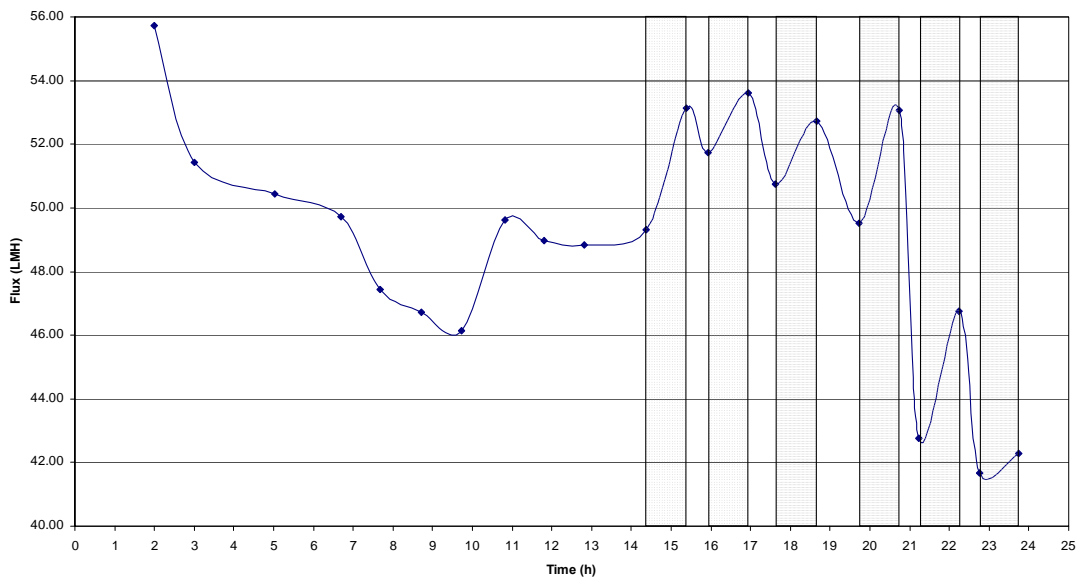


Figure 4-9. Permeate flux of ultrapure water.

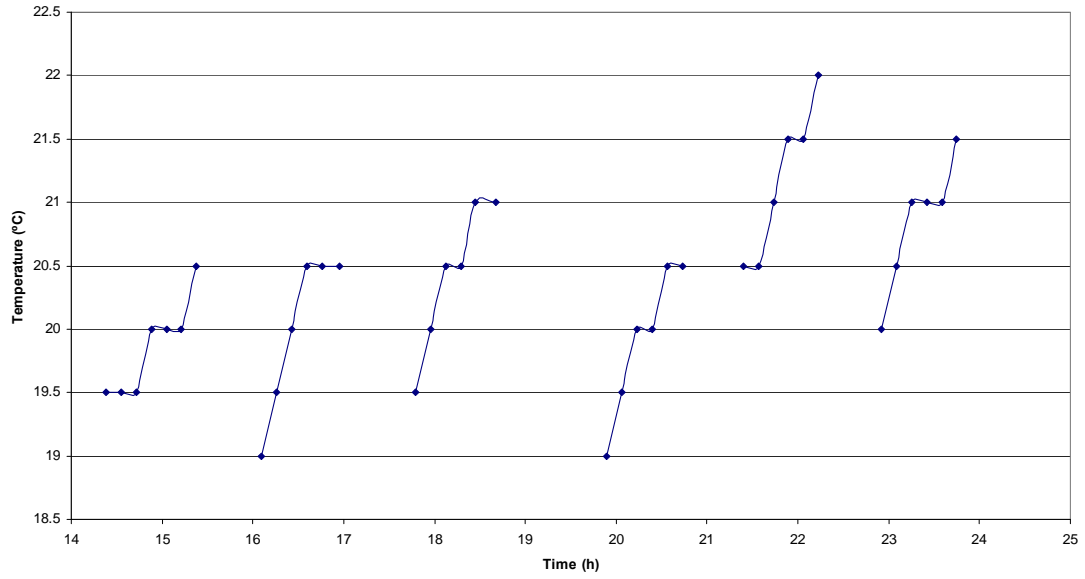


Figure 4-10. Effect of sonication on permeate temperature (Visual Test 2).

Every sonication interval was followed by a 30-60 minute interval, where feed was pumped through the module in the absence of sonication. Essentially the same effects were observed as was the case with Test 2.

4.2.3. Milli-Q Water Test 3

Feed was pumped through the module in the absence of sonication for a total of 10.3 hours. This was followed by sonication in hourly intervals for a total time of 6 hours. Every sonication interval was followed by a 30-90 minute interval where feed was pumped through the module in the absence of sonication. Again the same effects were observed as was the case with Tests 1 and 2.

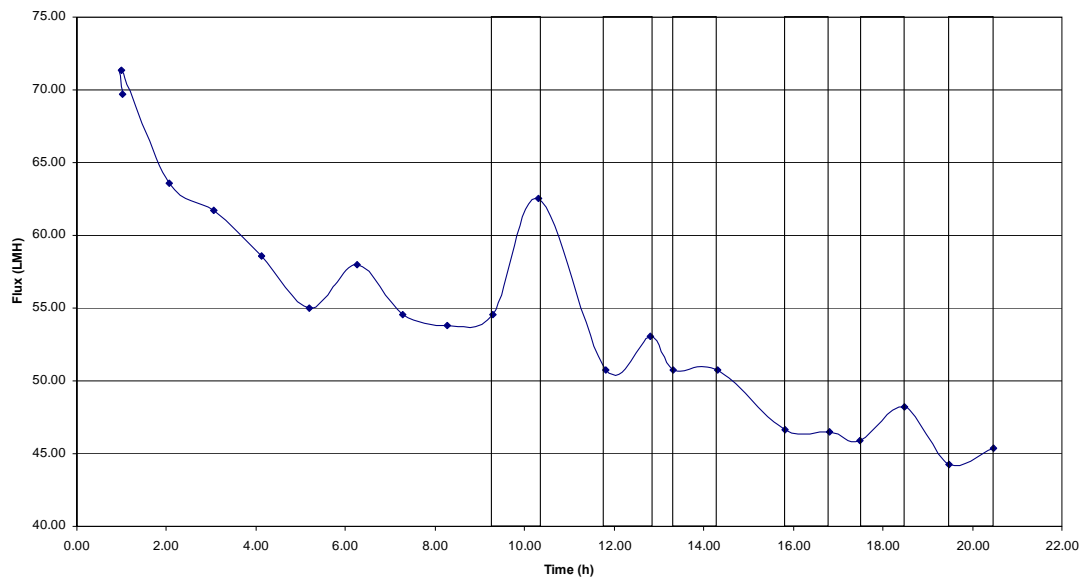


Figure 4-11. Permeate flux of ultrapure water.

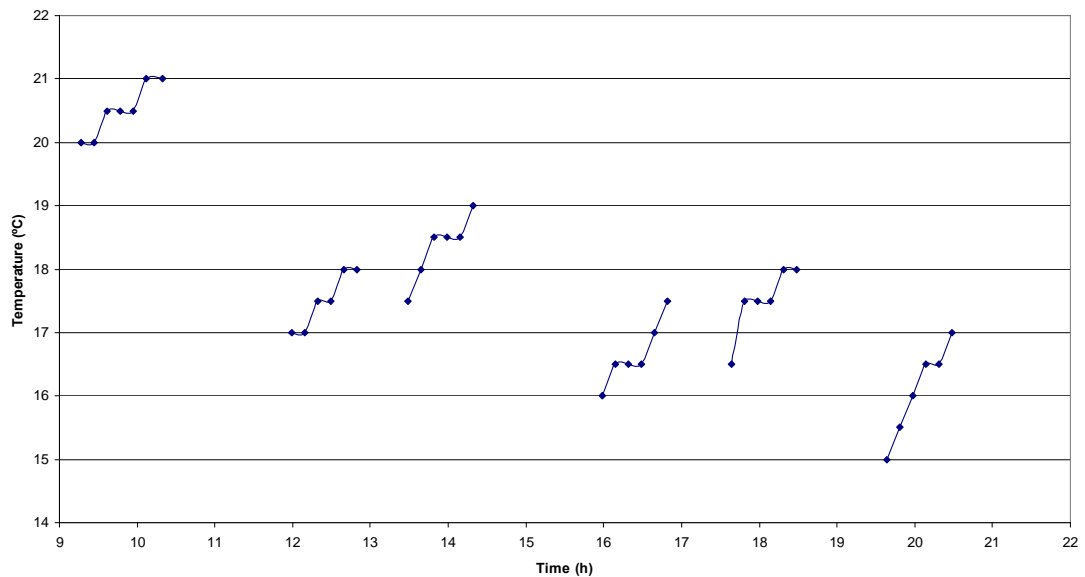


Figure 4-12. Effect of sonication on permeate temperature (Visual Test 3).

4.3. Tests with Coloured Ground Water from the George Region

4.3.1. First Experimental Run

The spikes in the graph represent times where the experiment was stopped for a brief interval. The membranes were prefouled with the ground water feed for 22 hours. After this time the flux seems to have stabilized around 16.5 kg/m².h.

During periods of sonication the flux increased by 39-54%. In no instance could the flux could be restored to the clean water flux (CWF) via sonication.

The flux obtained at the end of a sonication period has a decreasing trend. When the sonotrode was switched off, the flux decreased again, indicating that the effect of the ultrasound does not last after the sonotrode is switched off. The flux in the absence of sonication also shows a decreasing trend – decreases below the flux-value obtained at the end of the prefouling period.

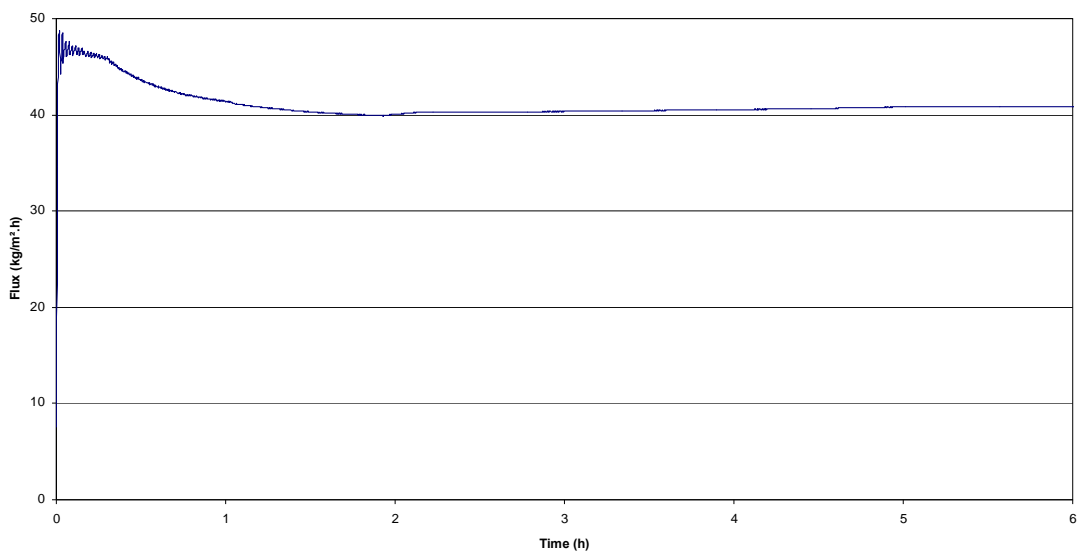


Figure 4-13. Membrane Preparation with Milli-Q Water

The clean water flux (CWF) was obtained from the membrane preparation process and has a value of 41 kg/m².h.

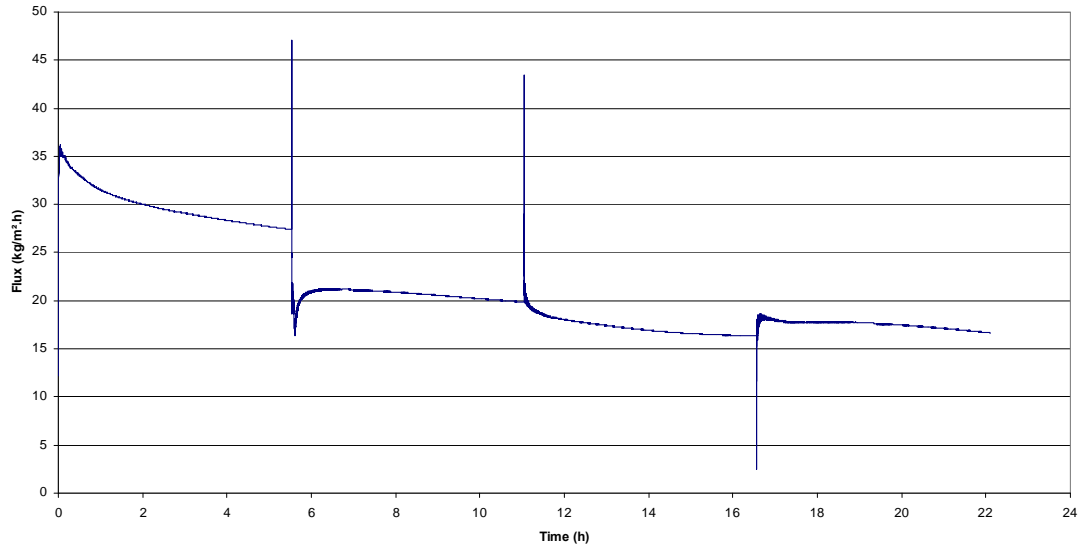


Figure 4-14. Prefouling with coloured ground water from the George region.

The spikes in the graph represent times where the experiment was stopped for a brief interval. The membranes were pre-fouled with the ground water feed for 22 hours. After this time the flux seems to have stabilized around 16.5 kg/m².h.

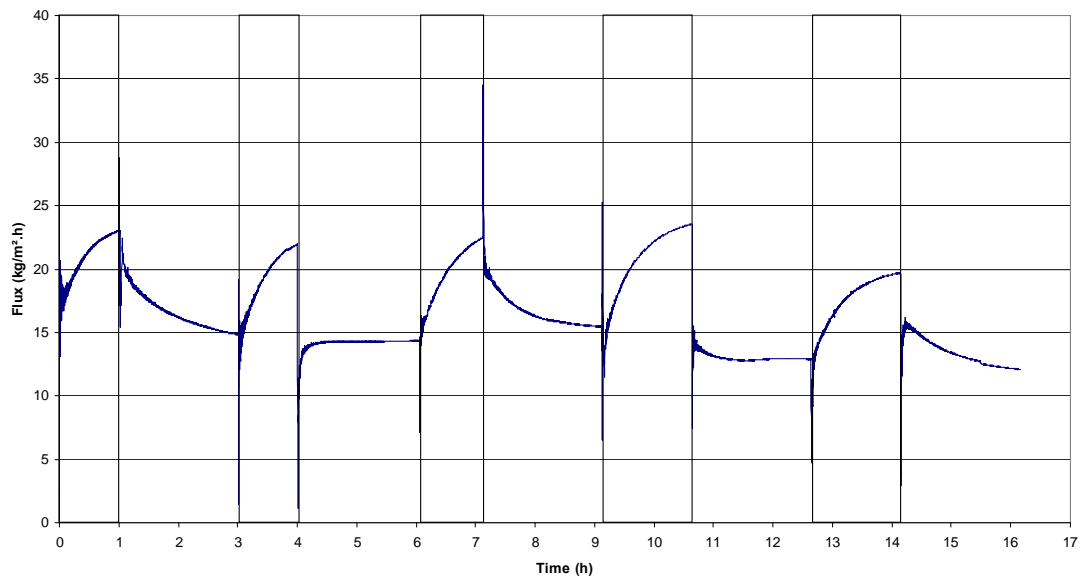


Figure 4-15. The effect of sonication on the permeate flux

During periods of sonication the flux increased by 39-54%. In no instance could the flux could be restored to the CWF via sonication.

The flux obtained at the end of an sonication period has a decreasing trend. When the sonotrode was switched off, the flux decreased again, indicating that

the effect of the ultrasound does not last after the sonotrode is switched off. The flux in the absence of sonication also shows a decreasing trend – decreases below the flux-value obtained at the end of the pre-fouling period.

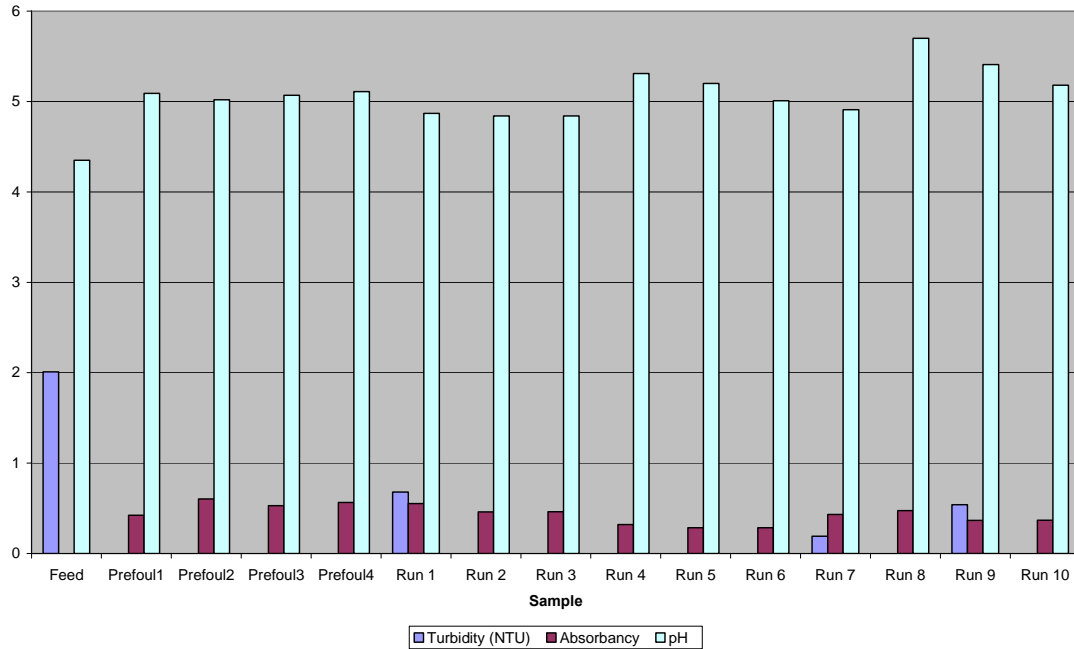


Figure 4-16. Permeate Quality Analysis – Turbidity, Absorbency and pH

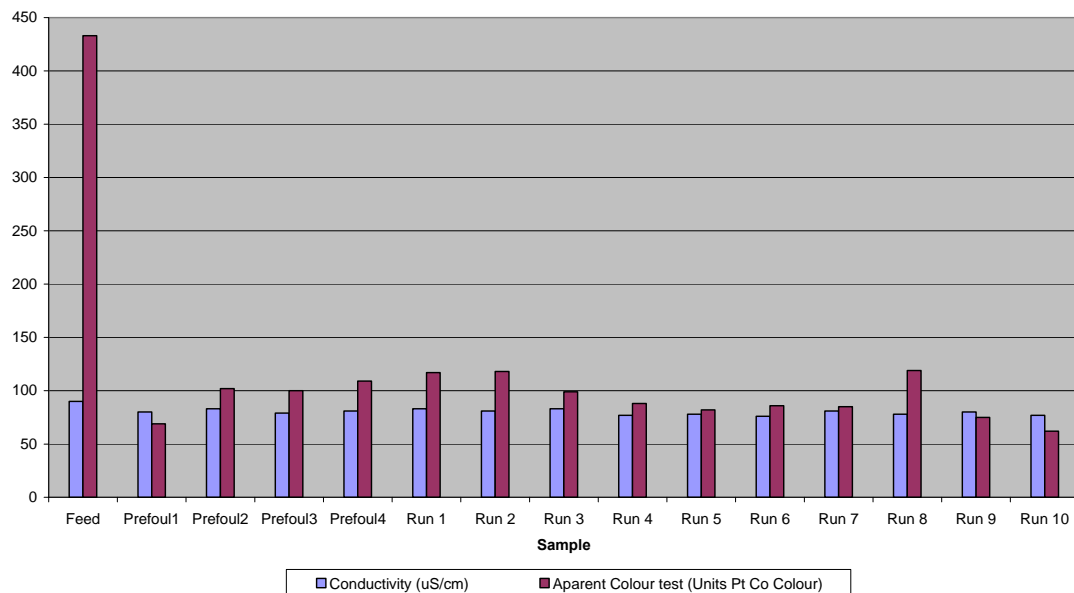


Figure 4-17. Permeate Quality Analysis – Conductivity and Apparent Colour test

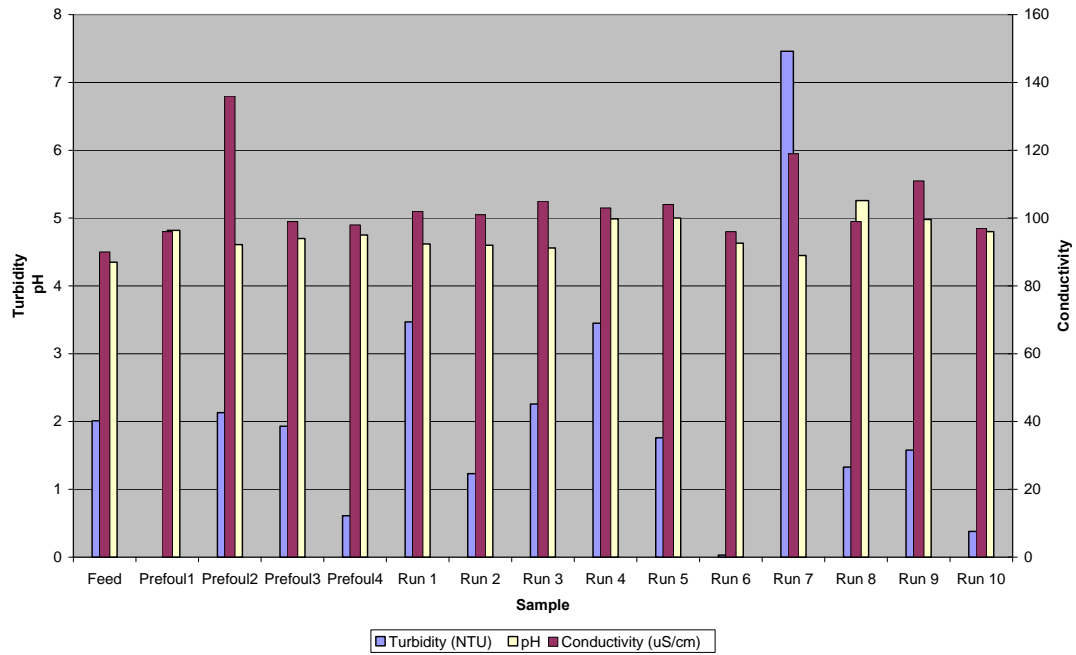


Figure 4-18. Retentate Quality Analysis – Turbidity, pH and Conductivity

At the end of each interval of the experimental run the permeate and retentate was sampled. Analyses were carried out to monitor the quality of the permeate and retentate. The objective of the sampling process was to determine whether sonication has an impact on the product water quality. Turbidity, absorbency, pH, conductivity and apparent colour in units platinum cobalt (Pt Co) colour were measured. In the above quality graphs the odd-numbered runs were sonicated and correlate with the shaded areas on the flux-curve. (See Appendix A for tabular data.)

The turbidity of the permeate is close to zero except for three runs of which all three are sonicated. The conductivity measurements for the sonicated runs are slightly higher (1-3 $\mu\text{S/cm}$). This difference is very small and is not considered as indicative of a degradation in permeate quality. All the other analyses displayed no trend whereby sonicated intervals could be distinguished from non-sonicated intervals. No conclusive proof was found that sonication has a negative impact on permeate quality.

The absorbency and apparent colour could not be measured for the retentate as it was too dark and the degree of dilution required was very high. These measurements were also regarded as optional in the case of the retentate, as the focus was on product (permeate) quality. The conductivity measurements for the sonicated intervals are higher than for the non-sonicated intervals. The highest turbidity measurements occur mostly during sonicated intervals. This phenomenon is in line with the expected behaviour during sonication: the fouling layer is scrubbed off the membrane surface; increased turbulence prevents re-

deposition of the foulant-particles and holds it in suspension and the foulant is removed with the retentate flow.

4.3.2. Second Experimental Run

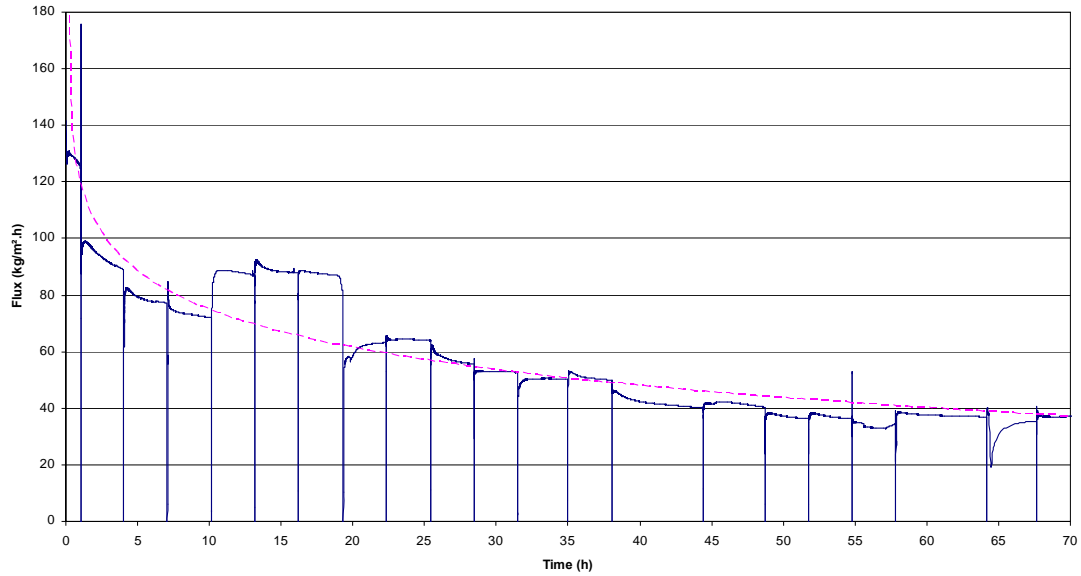


Figure 4-19. Membrane Preparation with Milli-Q Water

The CWF was obtained from the membrane preparation process and has a value of 37 kg/m².h.

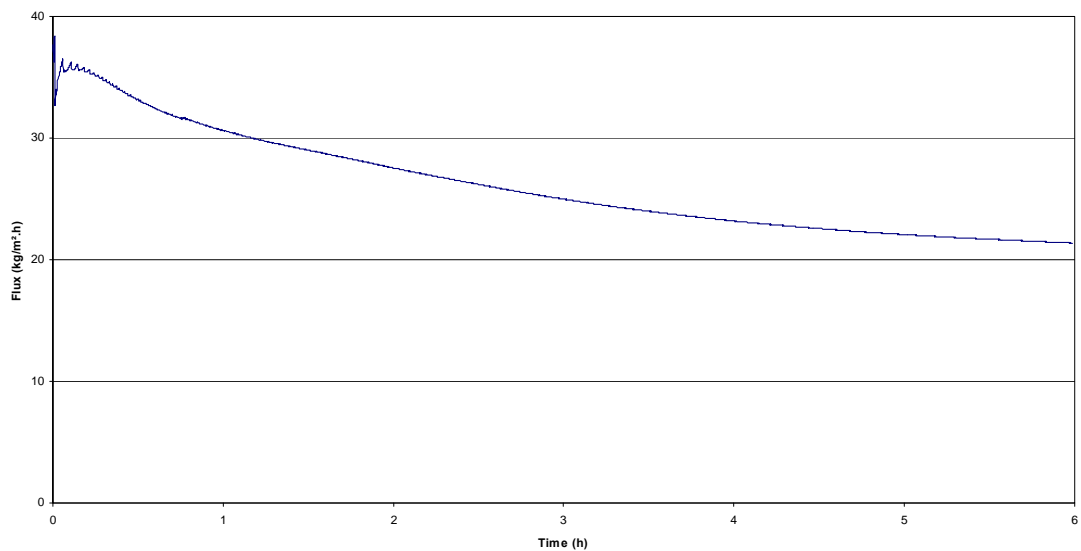


Figure 4-20. Prefouling with coloured ground water from the George region.

After the previous experiment a pre-fouling period of 6 hours was deemed sufficient. The flux curve started flattening out at 21 kg/m².h.

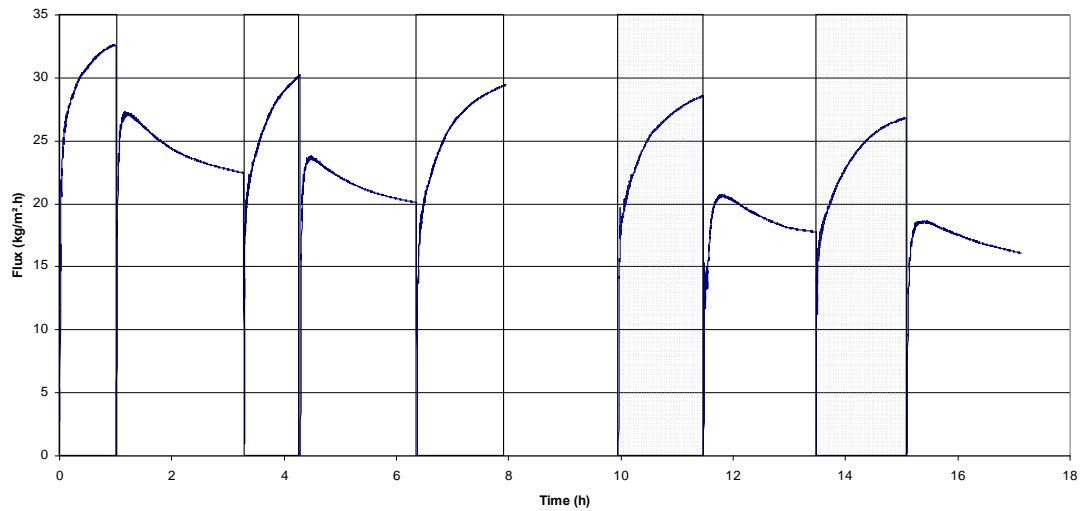


Figure 4-21. Effect of sonication on the permeate flux

During periods of sonication the flux increased by 35-55%. In no instance could the flux be restored to the CWF via sonication and the flux obtained at the end of a sonication period has a decreasing trend. This indicates that the defouling phenomenon caused by sonication is not 100% efficient.

Also, when the sonotrode was switched off, the flux decreased again, indicating that the effect of the ultrasound does not last after the sonotrode is switched off. The flux in the absence of sonication also shows a decreasing trend – decreases below the flux-value obtained at the end of the pre-fouling period. This indicates that the introduction of sonication does not stop overall flux decline, but is effective in delaying it.

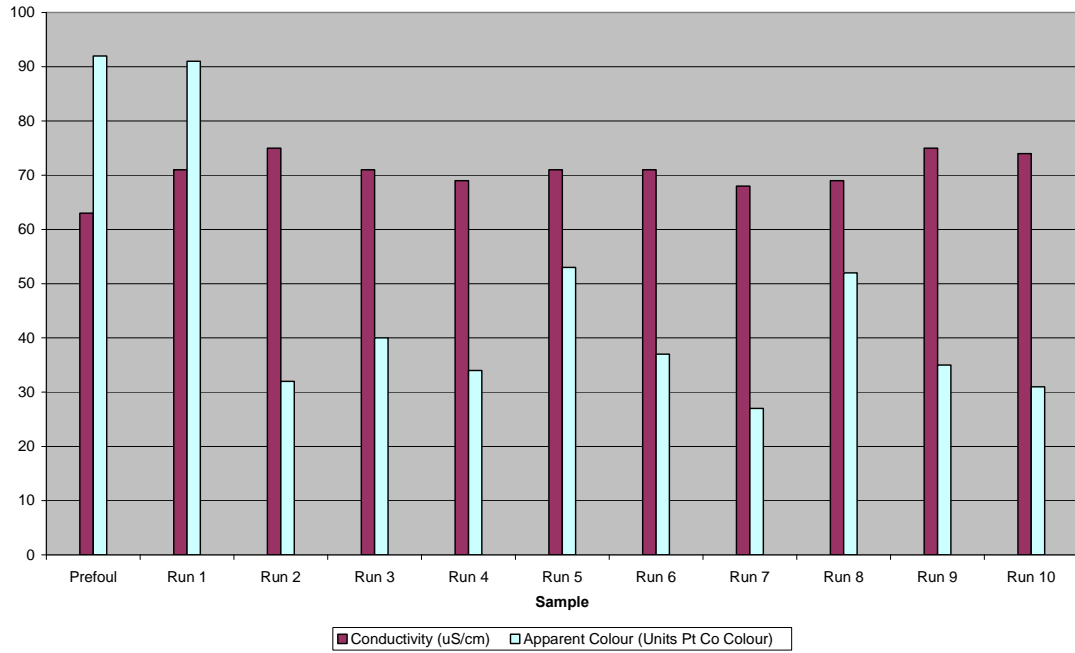


Figure 4-22. Permeate Quality Analysis – Conductivity and Apparent Colour

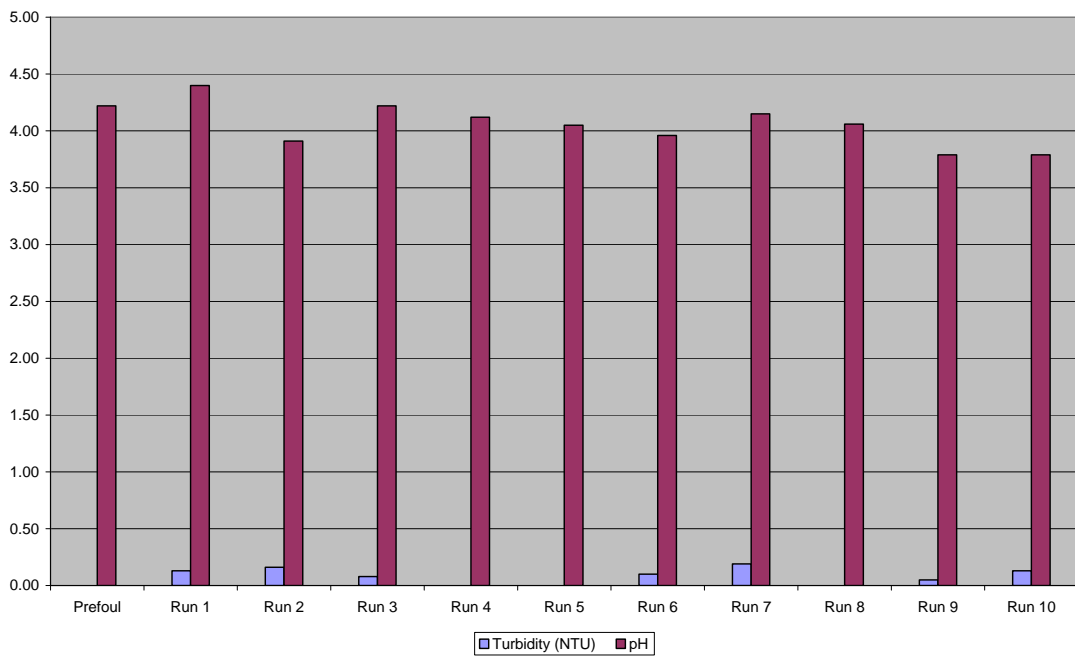


Figure 4-23. Permeate Quality Analysis – Turbidity and pH

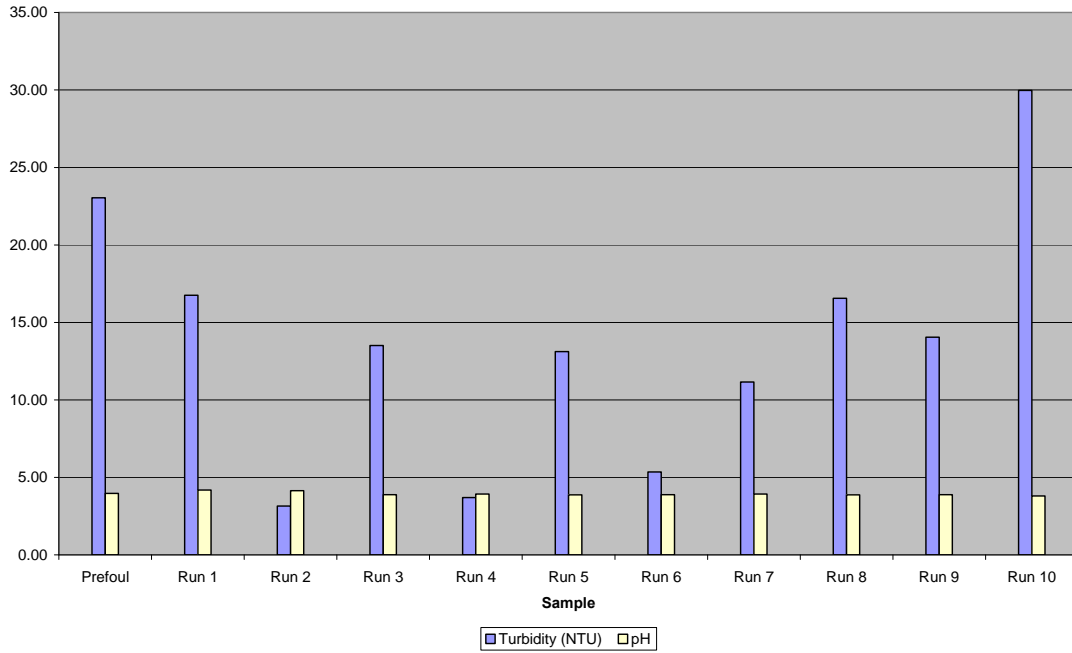


Figure 4-24. Retentate Quality Analysis – Turbidity and pH

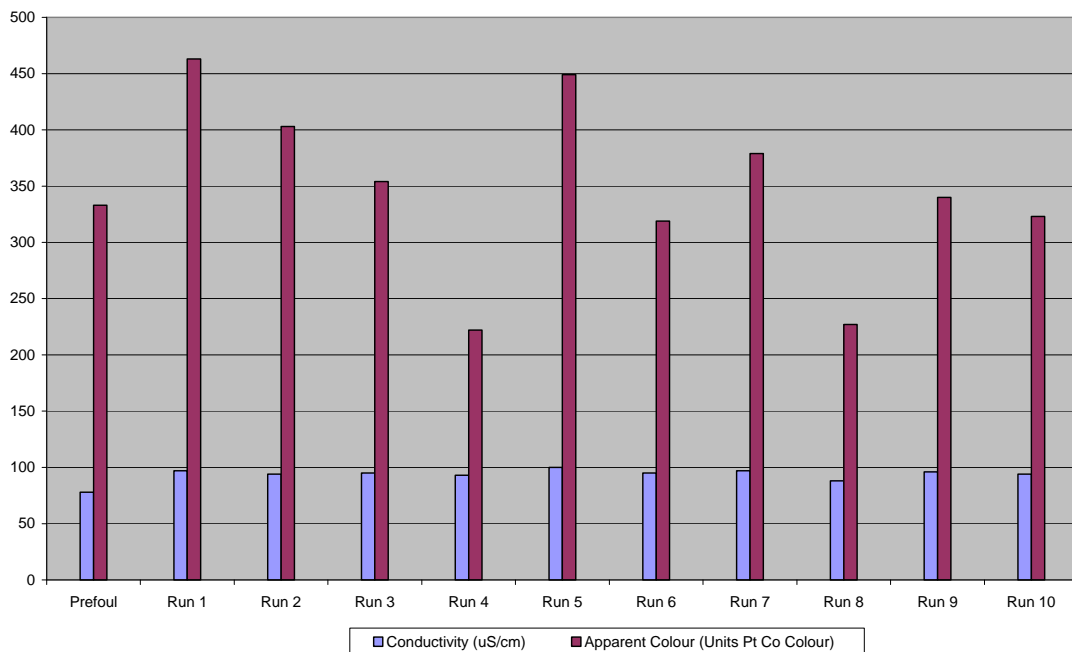


Figure 4-25. Retentate Quality Analysis – Conductivity and Apparent Colour

Samples were taken again at the end of each interval of the experiment to monitor the quality of the permeate and retentate. Turbidity, pH, conductivity and apparent colour in units Pt Co colour were measured. The apparent colour for the retentate was measured after dilution of 3 ml sample with 27 ml demineralised water. In the above graphs concerning quality the odd-numbered

runs were sonicated and correlate with the shaded areas on the flux-curve. (See Appendix A for tabular data.)

No relationship between any of the measured physical properties and the sonication intervals could be established. It appears that sonication has little or no impact on the permeate quality.

The conductivity, most of the turbidity and the apparent colour measurements for the sonicated intervals are higher than for the non-sonicated intervals. This phenomenon is as expected: during sonication the fouling layer is removed via micro-streaming and exits the module via the retentate stream.

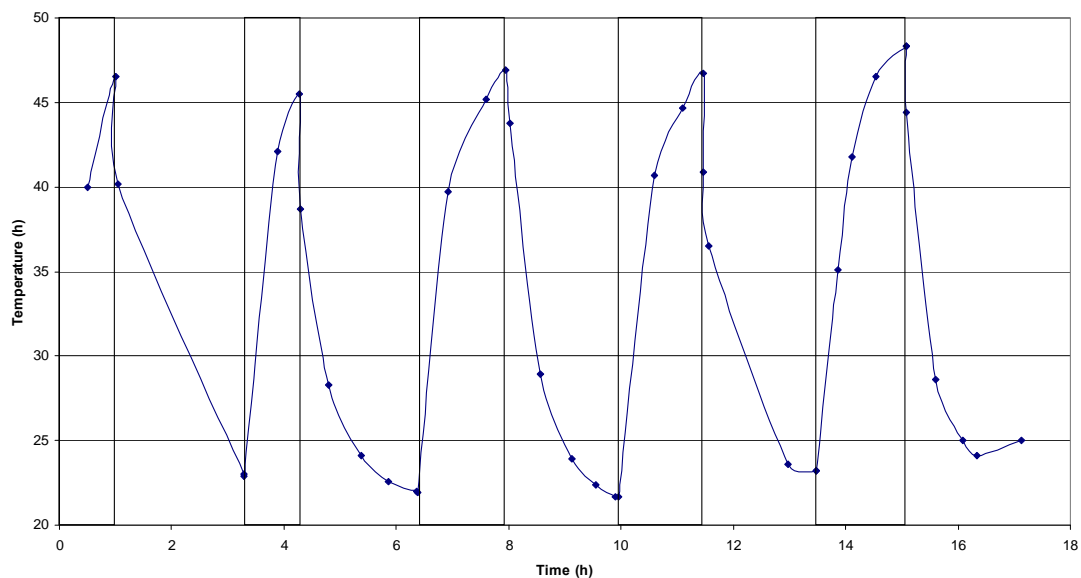


Figure 4-26. Effect of sonication on temperature.

For the experiments with coloured ground water from the George region a significant increase in the water temperature inside the membrane module was observed – up to 25 °C. The maximum temperature at 48 °C is still deemed as safe for the membrane type.

The temperature increase causes a decrease in the viscosity which leads to an increase in membrane flux. Therefore the flux increase during periods of ultrasonication cannot be attributed solely to the defouling and/or mass transfer enhancement effects.

There is the probability that the almost instantaneous and fast drops in the flux after ending the sonication can be due to the lowering of the temperature of the feed value (See figure 4.21 and figure 4.26).

4.4. Tests with Water from the Steenbras Dam

4.4.1. First Experimental Run

The membranes were prepared by pumping ultrapure water through the module for 7.65 hours. The CWF was measured as 80 kg/m².h, as indicated by Figure 4-20. After 22 hours of filtering the water of the Steenbras Dam, the flux curve started flattening out at 41 kg/m².h, as shown in Figure 4-21.

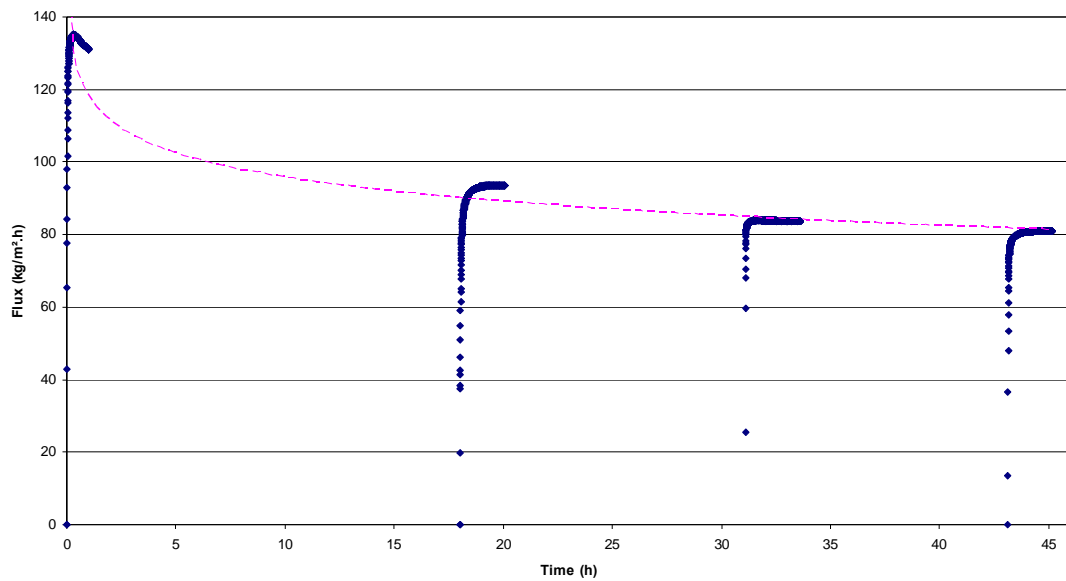


Figure 4-27. Membrane preparation with distilled water

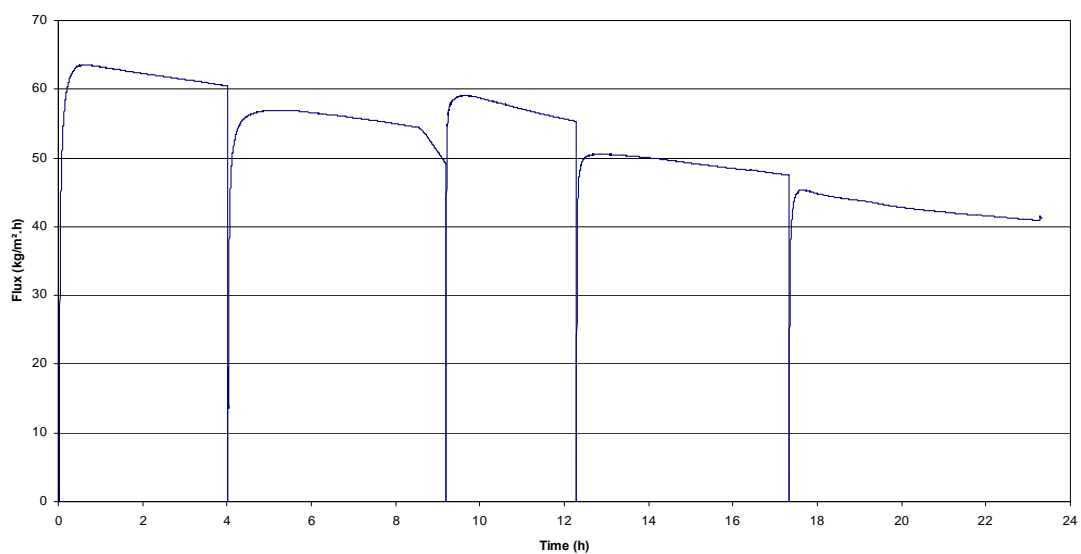


Figure 4-28. Prefouling with Steenbras dam water.

Sonication caused a flux-enhancement of 21-48%. As with the experiments with George ground water, in no instance could the flux be restored to the CWF via sonication. The flux obtained at the end of a sonication period also has a decreasing trend. Again, this indicates that the defouling via sonication is not majorly efficient.

In the absence of sonication the flux decreased again, indicating that the effect of the ultrasound does not last after the sonotrode has been switched off.

For the non-sonicated periods following the first two sonicated periods, the flux was higher than the value at the end of the prefouling run. This indicates that sonication defouled the membrane.

The flux in the absence of sonication also shows a decreasing trend – and in the last half of the experimental run it decreases below the flux-value obtained at the end of the prefouling period. This indicates that the introduction of ultrasonication does not stop overall flux decline, but is effective in delaying it.

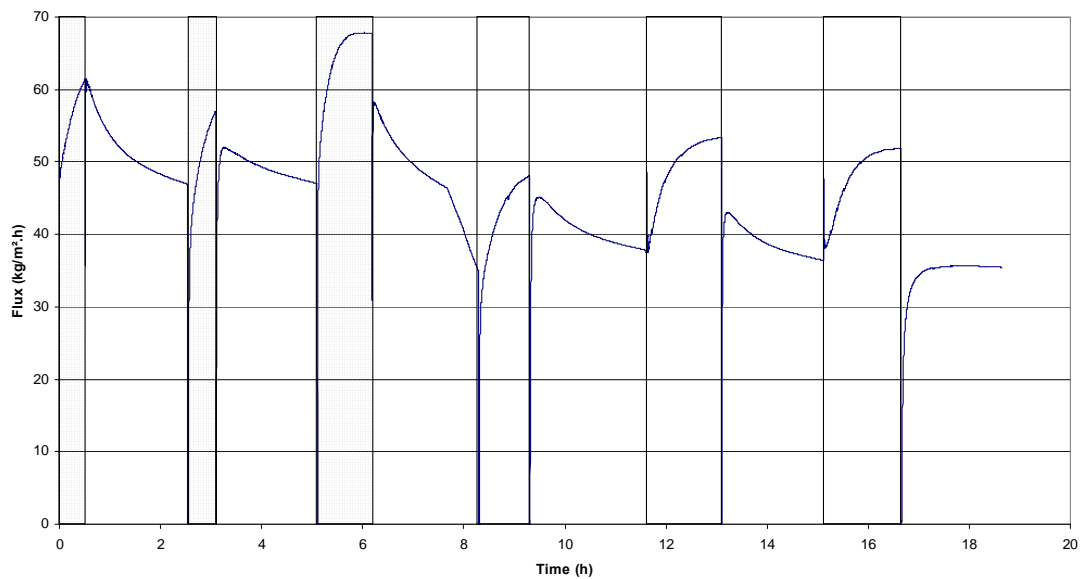


Figure 4-29. Effect of sonication on the permeate flux

Table 4-1. Effect of sonication on temperature

Time (h)	Temperature (°C)	Time Interval (h)	Sonication On/Off
0	23.7		
0.5	39.9	0-0.5	On
2.54	25.3	0.5-2.54	Off
3.1	41.6	2.54-3.1	On
5.1	24.1	3.1-5.1	Off
6.2	43.6	5.1-6.2	On
8.3	25.1	6.2-8.3	Off
9.3	44.2	8.3-9.3	On
11.6	23.9	9.3-11.6	Off
13.1	43.9	11.6-13.1	On
15.1	24.3	13.1-15.1	Off
16.6	44.8	15.1-16.6	On
18.6	26	16.6-18.6	Off

As in the case for the George water, for the experiments with Steenbras dam water a significant increase in the water temperature inside the membrane module was observed – up to 20.5 °C. Again, the maximum temperature at 44.8 °C is still deemed as safe for the membrane type.

The decrease in viscosity due to the temperature increase leads to an increase in membrane flux. As in the case of the George water, the flux increase during periods of sonication cannot be attributed solely to the defouling and/or mass transfer enhancement effects.

4.4.2. Second Experimental Run

The membranes were prepared by pumping ultrapure water through the module for 7.75 hours. The CWF was measured as 51 kg/m².h, as indicated in Figure 4-24.

The discontinuities are the result of pausing the experiment. After 18 hours the flux curve flattened out at 18 kg/m².h. The sharp flux decline and increase in the last hour of the fouling run is considered as faulty readings.

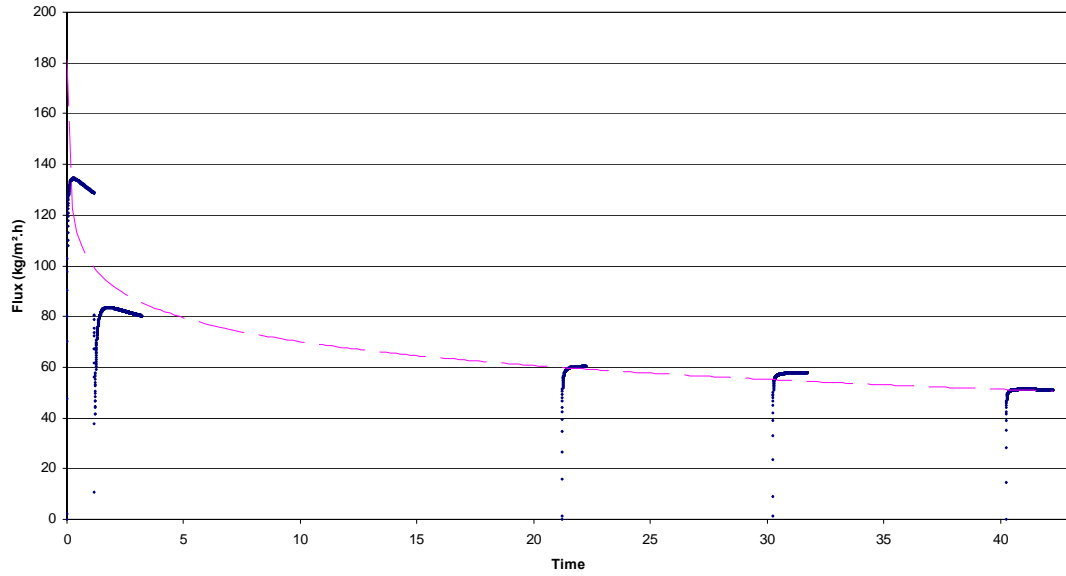


Figure 4-30. Membrane preparation with distilled water.

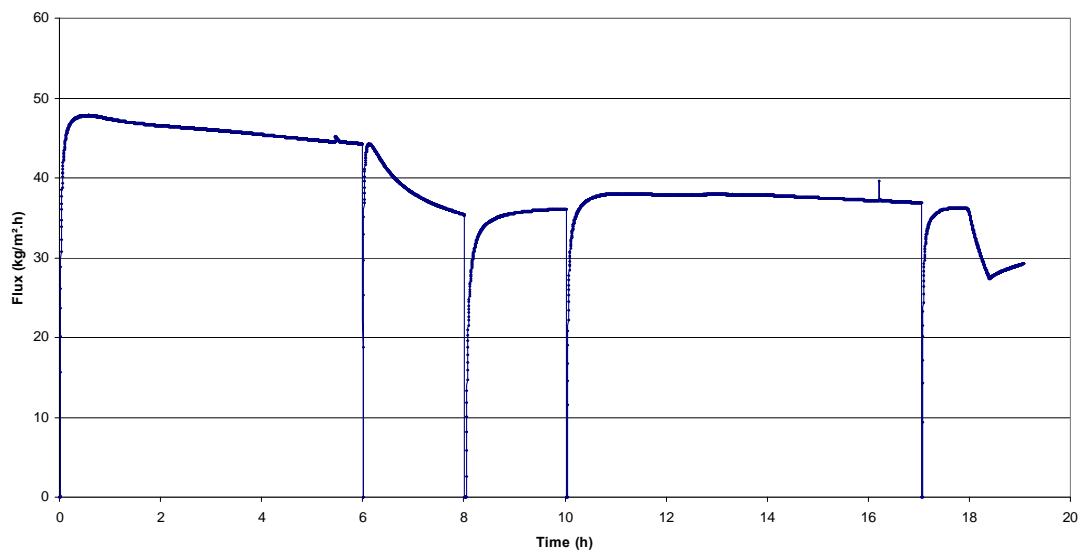


Figure 4-31. Prefouling with Steenbras dam water

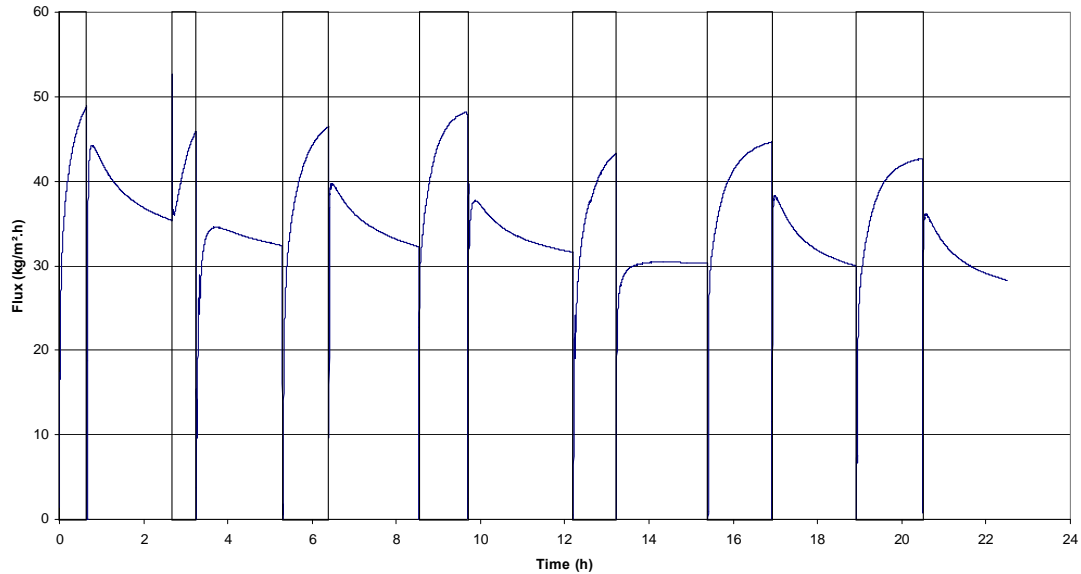


Figure 4-32. Effect of sonication on the permeate flux

The first sonication period caused a flux increase from the flux value obtained at the end of the prefouling run of 166%. In the subsequent runs the flux increases ranged from 30-47%. In no instant could the flux be restored to the CWF value. The flux obtained at the end of each sonication interval (a maximum value) also showed a decreasing trend. This indicates the occurrence of irreversible fouling and that the defouling via sonication is not majorly efficient.

In the absence of sonication the flux decreased again, indicating that the effect of the ultrasound does not last after the sonotrode has been switched off.

In each instant the flux value at the end of the non-sonicated periods was higher than the flux-value at the end of the prefouling run. This indicates that sonication defouled the membrane.

The flux in the absence of sonication also shows a decreasing trend, although remaining higher than the value obtained at the end of the prefouling run. This shows that some defouling has occurred, but also indicates that the introduction of sonication does not stop overall flux decline.

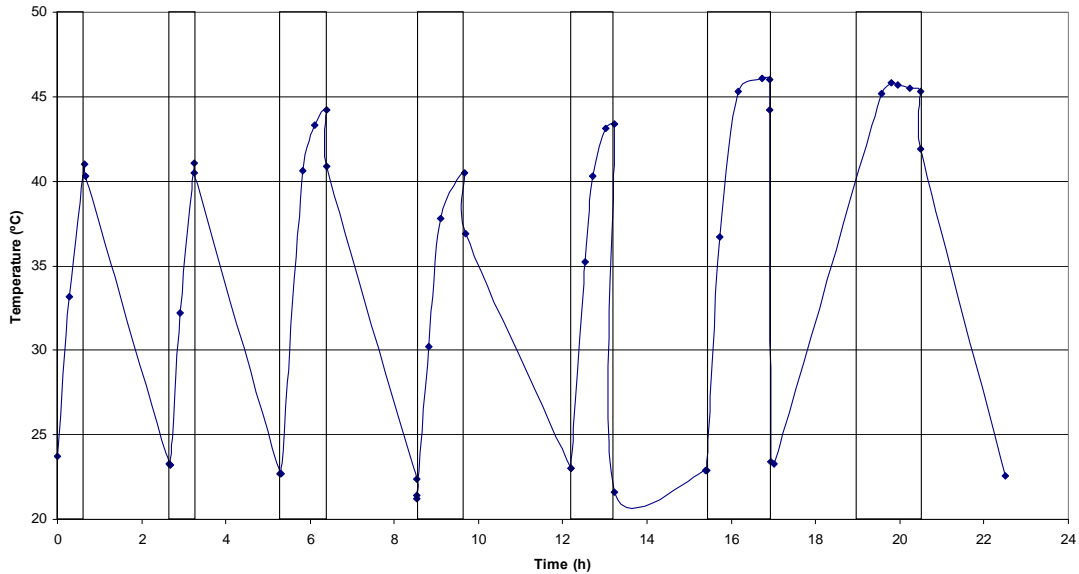


Figure 4-33. Effect of sonication on temperature.

As in the previous experiments, a significant increase in the water temperature inside the membrane module was observed – up to 23 °C. The maximum temperature, 46 °C, is still deemed as safe for the membrane type.

The decrease in viscosity due to the temperature increase leads to an increase in membrane flux. As in the previous experiments, the flux increase during periods of sonication cannot be attributed solely to the defouling and/or mass transfer enhancement effects.

4.5. Tests with Dextran

The membranes were prepared by pumping ultrapure water through the module for 13.4 hours. The CWF was measured as 51 kg/m².h (see Figure 4-28).

The membrane was prefouled with a 1 wt% Dextran solution for 2 hours. The flux declined sharply during the first 15 minutes and then gradually declined further to 9.4 kg/m².h at the end of the 2 hours.

The sonotrode was switched on and almost immediately a marked increase in the flux could be observed. The flux by sonication increase from the previously measured value of the prefouling was 73%. However, the flux could not be restored to the CWF value.

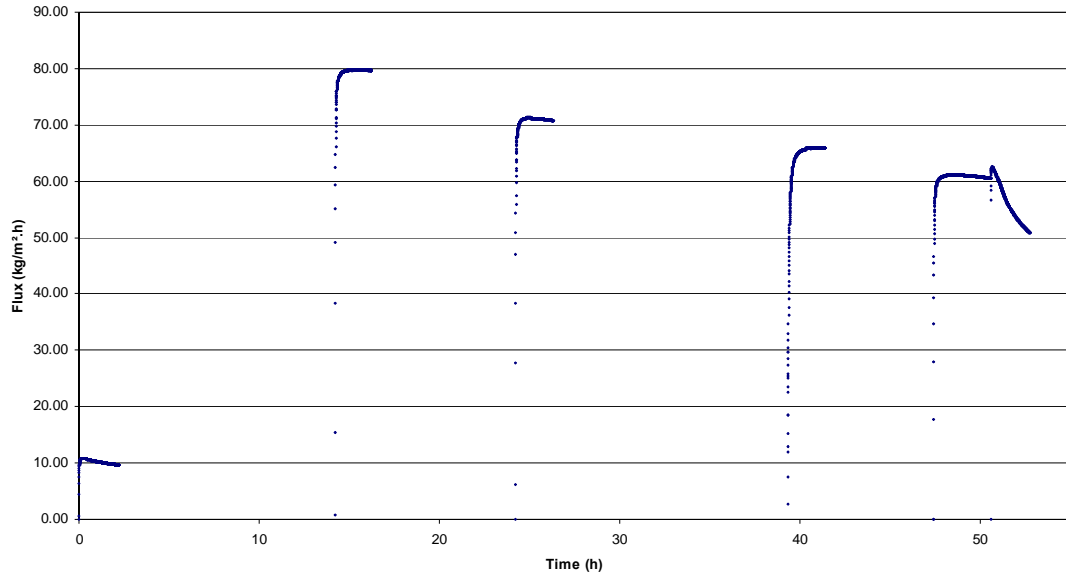


Figure 4-34. Membrane preparation with distilled water.

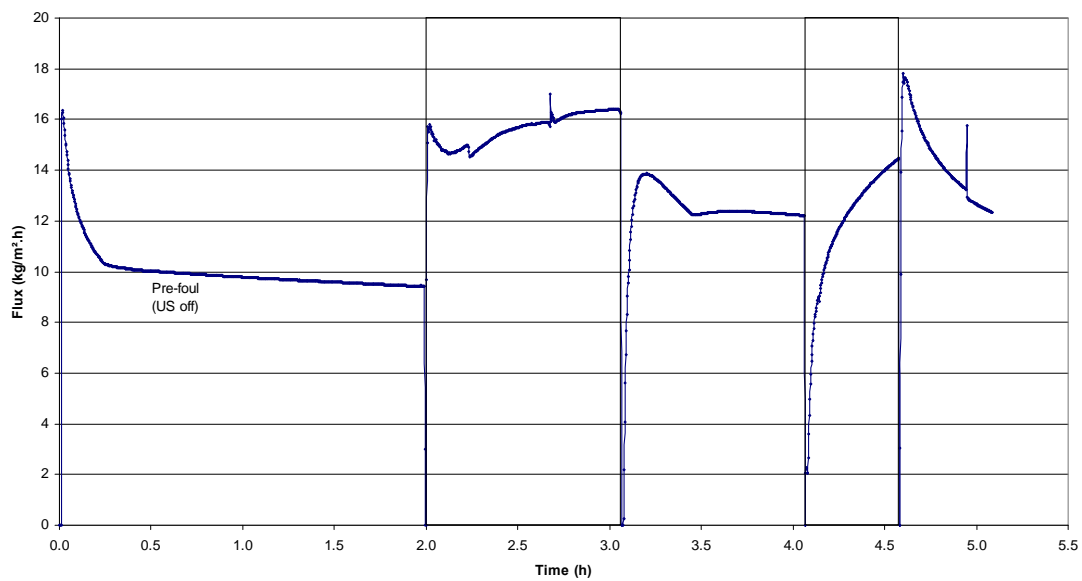


Figure 4-35. Effect of sonication on the permeate flux for dextran solution.

After the sonotrode was switched off, the flux decreased again and then stabilized at a value higher than the value at the end of the prefouling run. This indicates that the sonication period had a defouling effect on the membranes.

After 2 hours without sonication, the sonotrode was switched on again for an hour. A flux increase was observed, but the increase was less than the previous run.

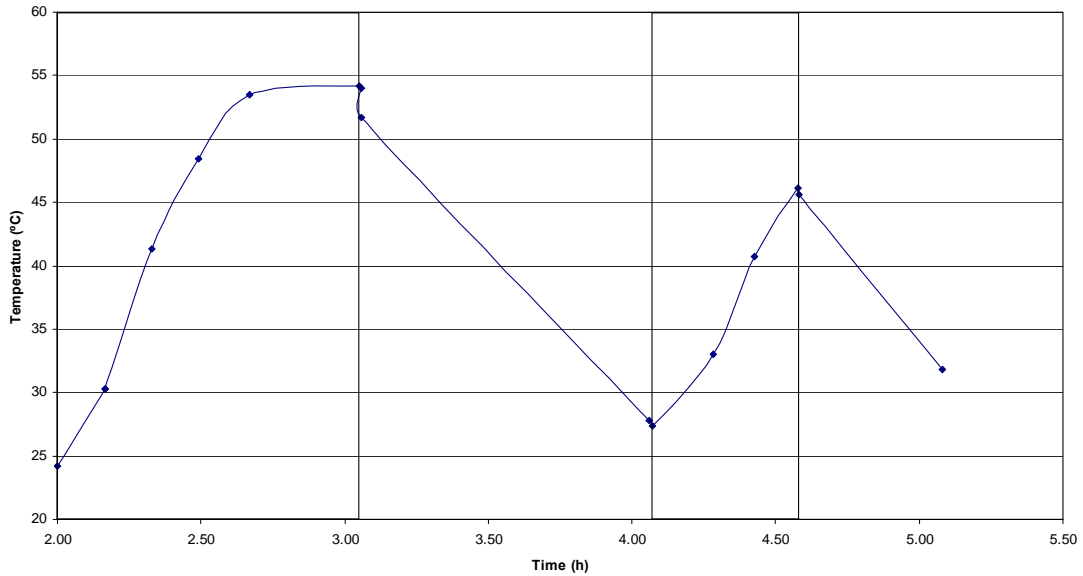


Figure 4-36. Effect of sonication on temperature.

After the sonotrode had been switched off the recorded initial flux readings were higher than the flux readings at the end of the sonicated period. It may be that the backpressure valve was closed more than for the previous run. This unsonicated run does show a decreasing flux trend indicating that the effect of the sonications stops once the sonotrode is switched off.

In the experiment with Dextran solution a significant increase in the water temperature inside the membrane module was observed – up to 27.4 °C. Again, the maximum temperature at 54 °C is still deemed as safe for the membrane type (must be less than 60°C).

The decrease in viscosity due to the temperature increase leads to an increase in membrane flux. As in the case of the George water, the flux increase during periods of sonication cannot be attributed solely to the defouling and/or mass transfer enhancement effects.

A summary of the experimental results are given in Figure 4-38. These results show the increase in temperature (Delta T) with an increase in the nominal ultrasound energy input per unit mass of fluid.

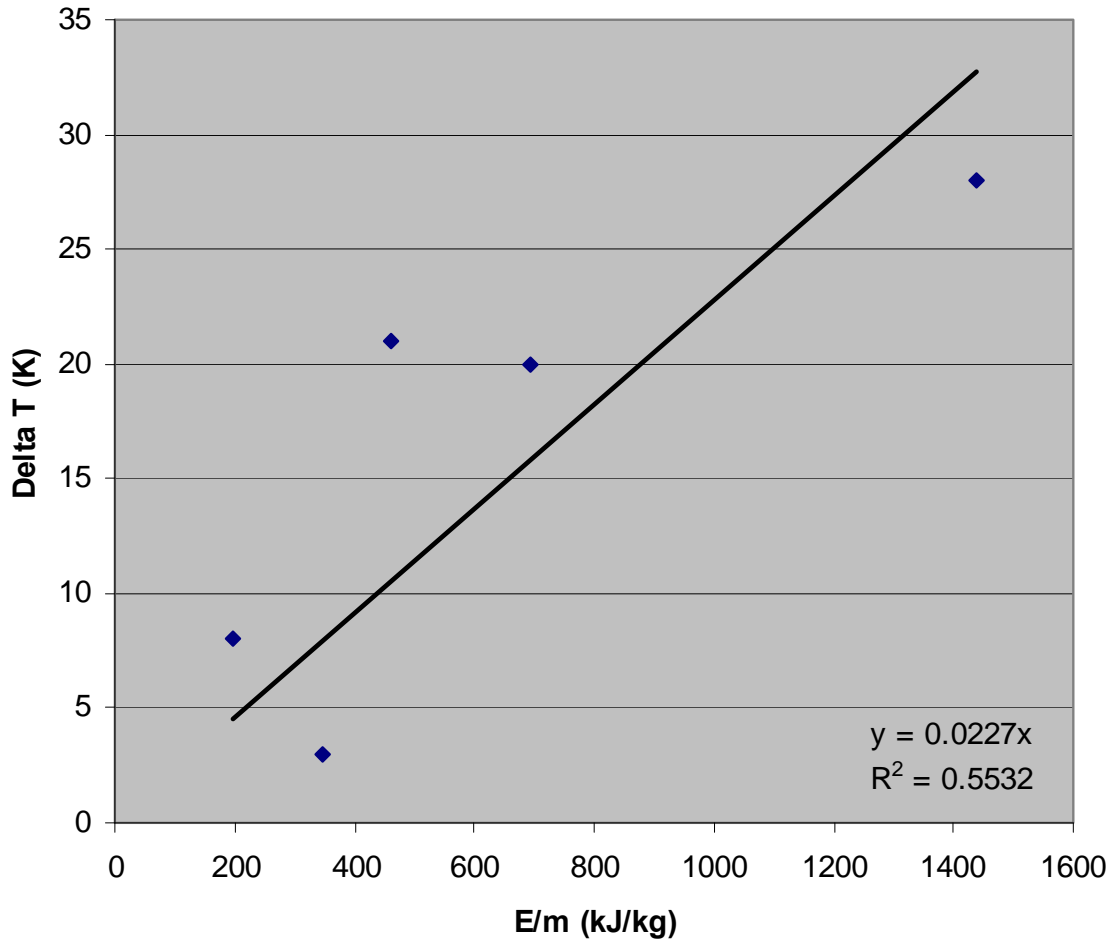


Figure 4-37. Increase in temperature of the systems studied, as a function of nominal ultrasonic energy input per kg of fluid.

4.6. Relationship between flux and temperature

Membrane flux (J_w) is expressed in volume or mass per area per unit time:

$$J_w = \frac{\text{Volume}}{A \cdot t} = \frac{Q}{A}$$

Where Q is the volumetric flow-rate.

If we assume the flow is laminar and we approach the flow through a membrane pore as through a straight channel (pipe) the volumetric flow-rate through the pore can be approximated from the Hagen-Poiseuille equation:

$$Q = \frac{P_1 - P_2}{\Delta x} \cdot \frac{\pi \cdot r_0^4}{\mu \cdot 8}$$

For flow through a "pore-channel":

P_1 = pressure inside the module = 100 kPa (g)

P_2 = atmospheric pressure, since the module is open to atmosphere

Δx = membrane thickness = length of flow-channel

μ = viscosity of the fluid, temperature dependent

r_0 = pore radius

To determine the relationship between the flux at two temperatures, T_1 and T_2 :

$$\frac{J_{w,T2}}{J_{w,T1}} = \frac{Q_{T2}/A}{Q_{T1}/A} = \frac{Q_{T2}}{Q_{T1}}$$

Since all variables in the Hagen-Poiseuille equation remains the same for T_1 and T_2 except the viscosity:

$$\frac{J_{w,T2}}{J_{w,T1}} = \frac{\mu_{T1}}{\mu_{T2}}$$

If T_2 and T_1 is arbitrarily chosen as 50 °C and 25 °C, and the viscosity of pure water is used then $J_{w,T2}/J_{w,T1} = 1.65$ – this indicates that at higher temperature and its corresponding lower viscosity the flux will increase.

From figures 4.21 and 4.26 a composite graph can be compiled.

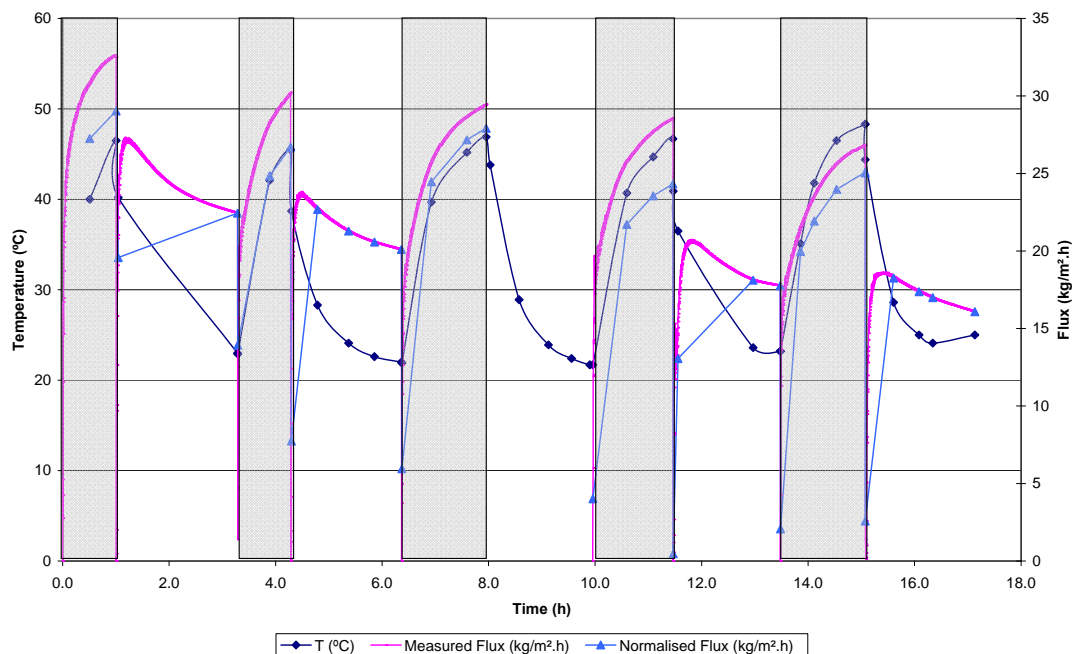


Figure 4-38. Contribution of temperature effect to flux enhancement

If the instantaneous and fast drops in temperature corresponding with the drops in flux after ending the sonication is considered as the contribution of the

temperature effect (via the decrease in viscosity) on the flux enhancement, a normalised flux-curve can be constructed.

$$J_{w,Normalised} = \frac{\mu_{T,Measured} \cdot J_{w,Measured}}{\mu_{T,Normalised}}$$

The normalised temperature was obtained by subtracting the instantaneous temperature drop (ΔT) from the temperature values for a sonication interval. During unsonicated intervals the normalised temperature is the same as the measured temperature. The viscosity of pure water at atmospheric pressure was used to approach the viscosity of the ground water. The viscosity at the normalised temperature was used to calculate the normalised flux. This was only done for sonicated intervals.

The measured flux shows a 35-55% increase in flux during sonication. For the normalised curve the flux increase is 16-38%. It therefore appears that roughly 18% of the overall flux increase can be attributed to the temperature effect. The peak values on the normalised curve still exceed the flux value obtained at the end of the pre-fouling run (21 kg/m².h) indicating that some defouling occurred.

4.7. Observations on the Dynamics of Fouling

A much larger number of flux measurements were made in the experiments with the ground water obtained from George, than with the other systems and it is interesting to examine these data further. For example, consider the increments in the flux in Figure 4-20 (pre-fouling of the membranes with the water containing natural organic matter) as indicated in Figure 4-39. These increments are not random, but appear to be cyclical, as can be more clearly seen from Figure 4-40.

In theory, analysis of the dynamics of the flux through the membrane may yield valuable insights into fouling mechanisms of membranes, but an in-depth analysis of these data was considered beyond the scope of the present work.

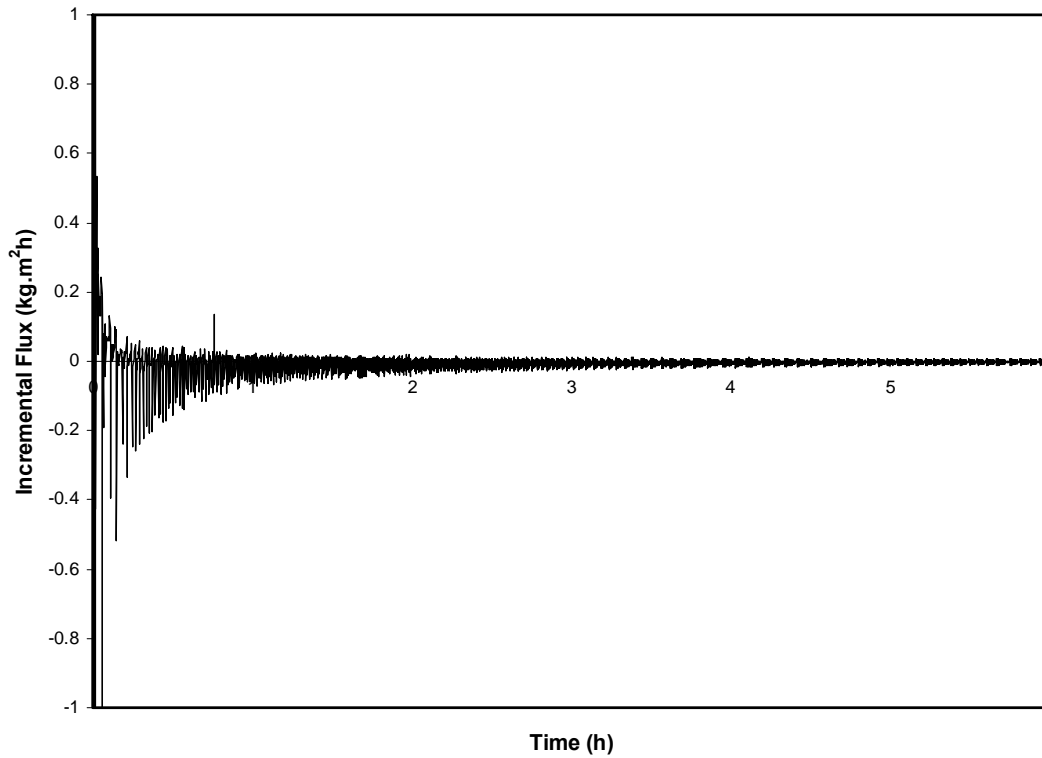


Figure 4-39. Incremental flux of George mountain water, corresponding to the data in Figure 4-20.

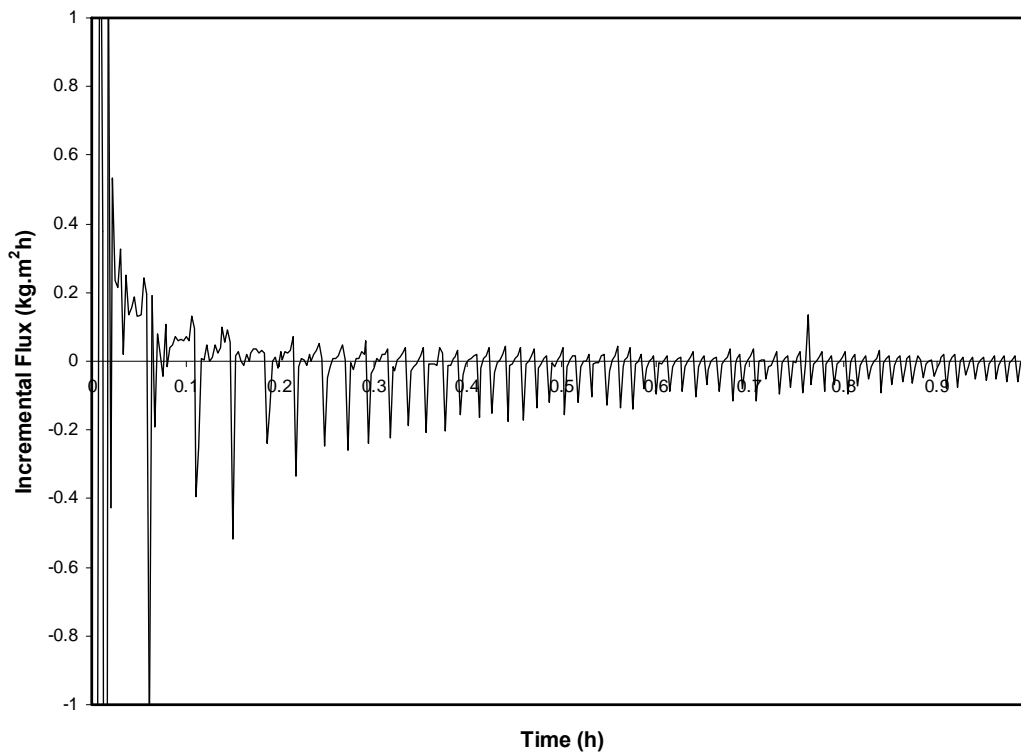


Figure 4-40. Incremental flux of George mountain water, corresponding to the data in Figure 4-20 – first hour only.

Chapter 5

Conclusions

The most important barrier to cost-effective membrane filtration is the reduced permeate flux attributed to fouling of the membranes caused by pore plugging and adsorption of rejected macromolecules or other solutes in the membrane system. This requires periodic cleaning of membranes, which can add considerably to the overall cost of plant operation owing to lost productivity related to down-time, the cost of the chemicals used in cleaning, higher pressures and associated pumping costs to maintain membrane productivity, as well as reduced lifetime of the membranes.

In this study, the use of ultrasound to mitigate the fouling of membranes with organic foulants was studied on a laboratory scale. Ultrasound has recently been identified as a promising approach to combating fouling in membranes. The study has shown that in principle it can be used on-line and may even eliminate the use of chemical cleaning or alternative measures completely, which could lead to major advances in the development and implementation of membrane technology. Specifically,

- No membrane damage was apparent during the crossflow filtration experiments with water containing Congo Red dye and ultrapure water, except where the sonotrode of the sonicator was in contact with the membrane fibres.
- With ultrapure water as feed, the flux was not enhanced significantly. This was expected, as there were no or very little foulant that could be removed. The slight flux enhancement (6% for Milli-Q test 2 and 4% for test 3) could possibly be attributed to enhanced mass transfer, owing to microstreaming associated with the ultrasound. The fact that the flux kept declining during the Milli-Q water tests suggested that a possible increase in the pore size of the membranes was also unlikely, as was the effects associated with a rise in the temperature of the flux. The flux behaviour also indicated that the ultrasound did not damage the membranes, either by increasing the pore size or by creating holes in the membrane material and thereby elevating the apparent membrane flux. When the sonotrode was switched off, the flux decreased sharply – indicating that the defouling effect of the sonication is not permanent.

- In distilled water containing approximately 0.11 wt% Congo Red dye, sonication enhanced the permeate flux with approximately 30-40%. This improvement could not be explained completely in terms of the defouling of the membranes and some other phenomenon must also have occurred.
- In every visual test with the Congo Red dye, the sonication led to increased permeate and retentate temperatures, but since these temperature increases were not excessive, the flux enhancement could also not be explained in full in terms of the increased temperatures (lower viscosities).
- Two of the five systems that were studied, were obtained from water bodies containing natural organic matter. During periods of sonication the flux increased by 21% up to 55%. In no instance could the flux could be restored to the CWF via sonication. The flux obtained at the end of a sonication period had a decreasing trend. When the sonotrode was switched off, the flux decreased again, indicating that the effect of the ultrasound did not last after the sonotrode is switched off. The flux in the absence of sonication also showed a decreasing trend – in some cases it decreased below the flux-value obtained at the end of the pre-fouling period. This indicates that the defouling phenomenon caused by sonication is not 100% efficient. The introduction of sonication does not stop overall flux decline, but is effective in delaying it. In some of the experimental intervals sonication was able to restore the flux to a value higher than that obtained at the end of the pre-fouling run – this is where sonication was successful in defouling the membrane.
- A sampling process was conducted during the experiments with ground water from the George region to determine whether sonication has an impact on the product water quality. Turbidity, absorbency, pH, conductivity and apparent colour in units Pt Co colour were measured. No distinct trend could be obtained from the analyses whereby sonicated intervals could be distinguished from non-sonicated intervals. No conclusive proof could be found that sonication has a negative impact on permeate quality. If damage had occurred to the membrane material, or the pore size had increased during sonication a degradation in permeate quality was expected. Since no evidence was found to conclude that sonication has a negative impact on permeate quality, it is concluded that sonication did not damage the membrane material. If the pore-size was increased during sonication it was not increased to such an extent where by product quality was impacted.

- Sampling of the retentate of the experiment with ground water from the George region displayed higher conductivity, turbidity and apparent colour measurements for the sonicated intervals. This phenomenon is in line with the mechanical effects associated with sonication, specifically micro-streaming: the fouling layer is scrubbed off the membrane surface; increased turbulence prevents re-deposition of the foulant-particles and holds it in suspension. During sonicated intervals the retentate carries the foulant-particles out of the module and the resultant retentate is expected to have higher turbidity and conductivity than during a non-sonicated interval.
- For the experiments with coloured ground water from the George region as well as the experiments with Steenbras dam water a significant increase in the water temperature inside the membrane module was observed – up to 25 °C. This temperature increase is expected behaviour in line with the temperature effect associated with bubble collapse during cavitation. (In all instances the maximum temperature of the liquid inside the module was still within the safe limits.) Since viscosity is temperature dependent, the rise in temperature corresponds with a decrease in the viscosity which leads to an increase in membrane flux. Therefore the flux increase during periods of sonication cannot be attributed solely to defouling and/or mass transfer enhancement effects.
- The experiment with Dextran showed definite defouling of the membrane via sonication, but the flux could not be restored to the CWF flux. The temperature increase during sonication as observed for the ground water and the dam water was also present in this experiment. The significant flux increase in this experiment cannot be attributed solely to the defouling and /or enhanced mass-transfer effects of sonication.
- Further study is recommended to quantify the contributions of enhanced mass and energy transfer due to sonication and the decrease in viscosity due to the increase in temperature (due to sonication) to the increase in permeate flux.

References

- Agranat, B.A. *et al.*, (1969) UI 'trazvuk v hidro-metallurgii, Russia.
- Band, M., Gutman, M., Faerman, V., Korngold, E., Kost, J., Plath, P.J. and Gontar, V. (1997) Influence of specially modulated ultrasound on the water desalination process with ion-exchange hollow fibres, Desalination, **109**, 303-313.
- Chai, X., Kobayashi, T. and Fujii, N. (1998) Ultrasound effect on crossflow filtration of polyacrylonitrile ultrafiltration membranes, Journal of Membrane Science, **148**, 1998.
- Chai, X., Kobayashi, T. And Fujii, N. (1999) Ultrasound-associated cleaning of polymeric membranes, Separation and Purification Technology, **15(2)**, 139-146.
- Cheryan, M. (1986) Ultrafiltration Handbook, Technomics. Lancaster: Technomics.
- Crabb, C. and D'Aquino, R. (1999) Ultrasound makes waves in the CPI. Chemical Engineering, August, 26-27.
- Dekker, M. and Boom, R. (1995) Improving membrane filtration processes, Trends in Biotechnology, **13**, 129-131
- Doktycz, S.J. and Suslick, K.S. (2 March 1990) Interparticle Collisions Driven by Ultrasound. Science, **247**, 1067-1069.
- Glater, J. (1998). The early history of reverse osmosis membrane development. Desalination, **117**, 297-309.
- Harvey, R. (1965) US Patent No. 3 206 397.
- Hoffmann, U., Horst, C., Wietelmann, U., Bandelin, S. and Jung, R. (2005) Sonochemistry, Ullmann's Encyclopedia of Industrial Chemistry, Wiley-VCH Verlag GmbH & Co.KGaA
- Howkins, S.D. (1969) Diffusion rates and the effect of ultrasound, Ultrasonics, April, 129-130.
- Kobayashi, T., Chai, X. and Fujii, N. (1999) Ultrasound enhanced cross-flow membrane filtration, Separation and Purification Technology, **17**, 31-40.
- Kost, J. and Langer, R. (1988) Ultrasound enhancement of membrane permeability, US Patent No. 4 780 212.
- Lenart, I. and Auslander, D. (1980) Ultrasonics, **9**, 216.

- Li, H., Ohdaira, E. and Ide, M. (1995) Enhancement in diffusion of electrolyte through membrane using ultrasonic dialysis equipment with plane membrane, Japanese Journal of Applied Physics, 35(5B), 2725-2729.
- Li, H., Ohdaira, E. and Ide, M. (1996) Effect of ultrasonic irradiation on permeability of dialysis membrane, Japanese Journal of Applied Physics, 35(5B), 3255-3258.
- Li, J., Sanderson, R.D. and Jacobs, E.P. (2002) Ultrasonic cleaning of nylon microfiltration membranes fouled by Kraft paper mill effluent, Journal of Membrane Science, 205, 247-257
- Mason, T.J. and Cordemans, E.D. (1996) Ultrasonic Intensification of Chemical Processing and Related Operations: A review. Transactions of the Institution of Chemical Engineers, 74, Part A, 511-516.
- Masselin, I., Chasseray, X., Durand-Bourlier, L., Lainé, J.-M., Syzaret, P.-Y., and Lemordant, D. (2001) Effect of sonication on polymeric membranes, Journal of Membrane Science, 181, 213-220.
- Muralidhara, H.S., Senapati, N., Ensminger, D. and Chauhan, S.P. (1986) Electro-Acoustic Separation Process for Fine Particle Suspension, Filtration & Separation, November/December, 351-353.
- Nosov, V.A. (1965) Ultrasonics in the Chemical Industry, New York.
- Pandit, A.B. and Moholkar, V.S. (1996) Harness Cavitation to Improve Processing. Chemical Engineering Progress, July, 57-69.
- Peterson, M.N.A. (1967) Ultrasonic Sieving, U.S. Patent 3 305 481, February 21.
- Reith, C. and Birkenhead, B. (1998) Membranes enabling the affordable and cost effective reuse of wastewater as an alternative water source. Desalination, 117, 203-210.
- Semmelink, A. (1970) Application of ultrasonic energy to filtering of liquids, paper read at IEEE Ultrasonics Symposium, 1970.
- Semmelink, A. (1973) Ultrasonically enhanced liquid filtering, Ultrasonics International Conference Proceedings, 1973.
- Simon, A., Penpenic, L, Gondrexon, N., Taha, S and Dorange, G. (2000) A comparative study between classical stirred and ultrasonically-assisted dead-end ultrafiltration, Ultrasonics Sonochemistry, 7, 183-186.
- Suslick, K.S. (1989) The chemical effects of ultrasound. Scientific American, February, 62-68.

Tarleton, E.S. (1988) How electric and ultrasonic fields assist membrane filtration. Filtration & Separation, 25(6), 402-406.

Tarleton, E.S. and Wakeman, R.J. (1990) Microfiltration enhancement by electrical and ultrasonic force fields, Filtration & Separation, 27(3), 192-194.

Tarleton, E.S. and Wakeman, R.J. (1992) Electro-Acoustic Crossflow Microfiltration, Filtration & Separation, 29(5), 425-431.

University of Pretoria. Department of Chemical Engineering, Water Utilisation Division. (2004). Membrane Processes and Ion Exchange (for desalination and industrial water treatment). Short Course Notes. University of Pretoria – Continuing Education, 23-25 August 2004.

Wakeman, R.J. and Tarleton, E.S. (1991) An experimental study of electroacoustic crossflow microfiltration, Chemical Engineering Research and Design, 69, 386-397,

Wakeman, R.J. and Smythe, M.C. (2000) Clarifying filtration of fine particle suspensions aided by electrical and acoustic fields, Chemical Engineering Research and Design, 78(A1), 125-135.

Wakeman, R.J. and Smythe, M.C. (2000) The use of acoustic fields as a filtration and dewatering aid, Ultrasonics, 38, 657-661.

Williams, C. and Wakeman, R.J. (2000) Membrane fouling and alternative techniques for its alleviation. Membrane Technology, 124, 4-14.

Appendices

A. Experimental Data

A.1 Visual Tests with Congo Red

A.1.1 Visual Test 1

Table A-1. Experimental data

Sonicated (Y/N)	Date	Run nr.	Time (h)	flowrate (ℓ/h)	Flux (LMH)	Pump speed (rpm)	Permeate Sample (Y/N)	Permeate coloured (Y/N)	
N	14/02/2002	1	1	0.79	60.74	95-96	N	N	
N	15/02/2002	2	1	0.798	61.36	97-98	N	N	
N	15/02/2002	3	1	0.778	59.82	98-99	N	N	
N	15/02/2002	4	1	0.727	55.90	98-99	N	N	
N	15/02/2002	5	1	0.705	54.20	98-99	N	N	
Y	18/02/2002	6	10 min after switching on US, HF ruptured - probe tip touched HF's						

A.1.2 Visual Test 2

Table A-2. Experimental data

Sonicated (Y/N)	Date	Run nr.	Time (h)	flowrate (ℓ/h)	Flux (LMH)	Pump speed (rpm)	Permeate Sample (Y/N)	Permeate coloured (Y/N)
N	19/02/2002	1	1h	0.357	27.45	97-98	N	N
N	19/02/2002	2	1h	0.355	27.29	80-81	N	N
N	19/02/2002	3	1h	0.34	26.14	80-81	N	N
N	19/02/2002	4	1h	0.335	25.76	80-81	N	N
N	20/02/2002	5	1h	0.33	25.37	80-81	N	N
Y	20/02/2002	6	9min26 s			80-81	N	Yes

Two hollow fibres ruptured after 9 minutes 26 seconds of sonication due to contact with the ultrasonic probe.

A.1.3 Visual Test 3

Table A-3. Experimental data

Sonicated (Y/N)	Date	Run nr.	Time (h)	Σ Time (h)	flowrate (ℓ/h)	Flux (LMH)	Pump speed (rpm)	Permeate Sample (Y/N)	Permeate coloured (Y/N)	Retentate flowrate (ℓ/h)
N	20/02/2002	1	1	1	0.829	63.74	99-100	N	N	-
N	20/02/2002	2	1	2	0.7	53.82	99-100	N	N	-
N	20/02/2002	3	1	3	0.65	49.98	99-100	N	N	-
N	20/02/2002	4	1	4	0.625	48.05	99-100	N	N	-
N	20/02/2002	5	1	5	0.615	47.29	99-100	N	N	-
Y	21/02/2002	6	1	6	0.777	59.74	99-100	N	N	0.02
Y	21/02/2002	7	1	7	0.715	54.97	99-100	Y	N	0.377
Y	21/02/2002	8	1	8	0.706	54.28	99-100	Y	N	0.111
Y	21/02/2002	9	1	9	0.709	54.51	99-100	Y	N	0.1
Y	22/02/2002	10	1	10	0.689	52.97	99-100	Y	N	0.11
Y	22/02/2002	11	1	11	0.649	49.90	99-100	Y	N	-
Y	22/02/2002	12	1	12	0.656	50.44	99-100	Y	N	0.139

A.1.4 Visual Test 4

Table A-4. Experimental data

Sonicated (Y/N)	Date	Run nr.	Time (h)	Σ Time (h)	flowrate (ℓ/h)	Flux (LMH)	Pump speed (rpm)	Permeate Sample (Y/N)	Permeate coloured (Y/N)	Retentate flowrate (ℓ/h)
N	27/02/2002	1	1.0	1.0	0.733	56.36	109-110	N	N	0.338
N	27/02/2002	2	1.0	2.0	0.770	59.20	109-110	N	N	0.311
N	27/02/2002	3	1.0	3.0	0.728	55.97	109-110	N	N	0.45
N	27/02/2002	4	1.0	4.0	0.737	56.67	109-110	N	N	0.43
N	27/02/2002	5	1.0	5.0	0.719	55.28	109-110	N	N	0.295
Y	28/02/2002	6	1.0	6.0	1.030	79.19	108-109	N	N	0.632
N	28/02/2002	7	0.5	6.5	0.934	71.81	108-109	N	N	-
Y	28/02/2002	8	1.0	7.5	1.020	78.42	109-110	Y	N	0.151
N	28/02/2002	9	0.6	8.1	0.826	63.49	109-110	N	N	0.782 (??)
Y	2002/01/03	10	1	9.1	0.991	76.19	108-109	Y	N	1.12 (??)
N	2002/01/03	11	0.5	9.6	0.836	64.28	108-109	N	N	0.16
Y	2002/01/03	12	1	10.6	1.019	78.35	109-110	N	N	0.23
N	2002/01/03	13	0.5	11.1	0.804	61.82	109-110	N	N	0.854
Y	2002/01/03	14	1	12.1	1.111	85.42	109-110	N	YES	0.22

A.1.5 Visual Test 5

Table A-5. Experimental data

Run nr.	Date	Sonicated (Y/N)	Time (h)	flowrate (ℓ/h)	Flux (LMH)	Pump speed (rpm)	Permeate Sample (Y/N)	Permeate coloured (Y/N)	Retentate flowrate (ℓ/h)
1	2002/08/03	N	1	0.858	65.97	108-109	N	N	-
2	2002/08/03	N	1.25	0.815	62.68	99-100	N	N	0.544
3	2002/08/03	N	1	0.799	61.43	102-103	N	N	0.127
4	2002/08/03	N	1	0.798	61.36	104-105	N	N	0.24
5	2002/08/03	N	1	0.79	60.74	104-105	N	N	0.632
6	2002/08/03	N	1	0.788	60.59	104-105	N	N	0.468
7	2002/11/03	Y	1	1.09	83.81	103-104	Y	N	0.312
8	2002/11/03	N	0.5	0.514	79.04	103-104	N	Yes	1.28

A.1.6 Visual Test 6

Table A-6. Experimental data

Run nr.	Date	Sonicated (Y/N)	Time (h)	Σ Time (h)	Volume collected	flowrate (ℓ/h)	Flux (LMH)	Pump speed (rpm)	Permeate Sample (Y/N)	Permeate coloured (Y/N)	Retentate flowrate (ℓ/h)	LMH as % of CWF
1	15/03/2002	N	1.6	1.6	0.949	0.599	46.08	124	N	N	0.06	53
2	15/03/2002	N	1	2.6	0.558	0.558	42.90	124	N		0.13	49
3	19/03/2002	N	1	3.6	0.749	0.749	57.59	123-124	N	N	242	66
4	19/03/2002	N	1.1	4.7	0.671	0.619	47.62	123-124	N	N	-	55
5	19/03/2002	N	1	5.7	0.591	0.591	45.44	123-124	N	N	0.085	52
6	19/03/2002	N	1.9	7.6	1.085	0.566	43.52	123-124	N	N	< 0.05	50
7	19/03/2002	N	0.9	8.5	0.569	0.621	47.73	123-124	N	N	0.261	55
8	20/03/2002	Y	1	9.5	0.762	0.762	58.59	122-123	Y	N	480	68
9	20/03/2002	N	0.5	10.0	0.32	0.640	49.21	123-124	N	N	-	57
10	20/03/2002	Y	1	11.0	0.775	0.775	59.59	123-124	Y	N	0.1	69
11	20/03/2002	N	0.5	11.5	0.331	0.662	50.90	123-124	N	N	0.11	59
12	20/03/2002	Y	1	12.5	0.817	0.817	62.82	123-124	Y	N	0.134	72
13	20/03/2002	N	0.5	13.0	0.331	0.662	50.90	123-124	N	N	0.05	59
14	21/03/2002	Y	1	14.0	0.818	0.818	62.89	122-123	Y	N	0.129	73
15	22/03/2002	N	0.54	14.5	0.34	0.633	48.64	122-123	N	N	-	56
16	22/03/2002	Y	1	15.5	0.778	0.778	59.82	123-124	Y	N	0.166	69
17	22/03/2002	N	0.5	16.0	0.302	0.604	46.44	123-124	N	N	1.558	54
18	22/03/2002	Y	1	17.0	0.811	0.811	62.35	123-124	Y	N	0.04	72

A.2 Tests with Ultrapure Water

A.2.1 Milli-Q Water Test 1

Table A-7. Experimental data

Run nr.	Date	Sonicated (Y/N)	Time (h)	Σ Time (h)	Volume Collected (L)	flowrate (ℓ/h)	Flux (LMH)	Pump speed (rpm)
1	2002/08/04	N	1.02	1.02	1.709	1.681	129.24	122-123
2	2002/08/04	N	1	1.00	1.479	1.479	113.72	122-123
3	2002/09/04	N	1.03	2.03	1.425	1.379	106.03	122-123
4	2002/09/04	N	1	3.03	1.242	1.242	95.49	122-123
5	2002/09/04	N	1	4.03	1.17	1.170	89.96	123-124
6	2002/09/04	N	1.75	5.78	1.949	1.114	85.63	123
7	2002/09/04	N	1.17	6.95	1.25	1.071	82.38	123-124
8	2002/10/04	N	1.5	8.45	1.589	1.059	81.45	122-123
9	2002/10/04	N	3.5	11.95	3.442	0.983	75.61	123-124
10	2002/10/04	N	1	12.95	0.955	0.955	73.43	123-124
11	2002/10/04	N	1	13.95	0.95	0.950	73.04	123-124
12	2002/11/04	N	1.03	14.98	0.932	0.902	69.35	122-123
13	15/04/2002	N	1.5	16.48	1.267	0.845	64.94	123-124
14	16/04/2002	N	1.03	17.52	0.858	0.830	63.84	142-143
15	16/04/2002	N	1	18.52	0.76	0.760	58.43	138-139
16	22/04/2002	N	1	19.52	0.699	0.699	53.74	138
17	22/04/2002	N	1.25	20.77	0.83	0.664	51.05	138-139
18	23/04/2002	N	1	21.77	0.648	0.648	49.82	131
19	2002/06/05	N	1	22.77	0.519	0.519	39.90	97-98
20	2002/06/05	N	2.08	24.85	1.038	0.498	38.31	97-98
21	2002/06/05	Y	1	25.85	0.629	0.629	48.36	97-98
22	2002/07/05	N	0.67	26.52	0.3	0.450	34.60	97-98
23	2002/07/05	Y	1	27.52	0.539	0.539	41.44	97-98
24	2002/07/05	N	0.67	28.18	0.294	0.441	33.91	97-98
25	2002/07/05	Y	1.17	29.35	0.583	0.500	38.42	98-99
26	2002/09/05	N	0.67	30.02	0.29	0.435	33.45	96-97
27	2002/09/05	Y	1	31.02	0.5	0.500	38.44	98-99
28	2002/09/05	N	1	32.02	0.435	0.435	33.45	98-99
29	2002/09/05	Y	1.03	33.05	0.544	0.526	40.48	98-99
30	2002/09/05	N	0.5	33.55	0.22	0.440	33.83	98-99
31	2002/09/05	Y	1	34.55	0.519	0.519	39.90	98-99

A.2.2 Milli-Q Water Test 2

Table A-8. Experimental data

Run nr.	Date	Sonicated (Y/N)	Time (h)	Σ Time (h)	Volume Collected (L)	flowrate (ℓ/h)	Flux (LMH)	Pump speed (rpm)
1	13/5/2002	N	2	2.00	1.45	0.725	55.74	98-99
2	13/5/2002	N	1.02	3.02	0.68	0.669	51.43	98-99
3	13/5/2002	N	2	5.02	1.312	0.656	50.44	99-100
4	13/5/2002	N	1.67	6.68	1.078	0.647	49.73	99-100
5	14/5/2002	N	1	7.68	0.617	0.617	47.44	98-99
6	14/5/2002	N	1.03	8.72	0.628	0.608	46.73	99-100
7	14/5/2002	N	1	9.72	0.6	0.600	46.13	99-100
8	15/5/2002	N	1.1	10.82	0.71	0.645	49.63	98-99
9	15/5/2002	N	1	11.82	0.637	0.637	48.98	98-99
10	15/5/2002	N	1	12.82	0.635	0.635	48.82	99-100
11	15/5/2002	N	1.57	14.38	1.005	0.641	49.32	99-100
12	15/05/2002	Y	1	15.38	0.691	0.691	53.13	99-100
13	16/05/2002	N	0.55	15.93	0.37	0.673	51.72	97-98
14	16/05/2002	Y	1.02	16.95	0.709	0.697	53.62	98-99
15	16/05/2002	N	0.67	17.62	0.44	0.660	50.75	99-100
16	16/05/2002	Y	1.05	18.67	0.72	0.686	52.72	99-100
17	16/05/2002	N	1.07	19.73	0.687	0.644	49.52	99-100
18	17/05/2002	Y	1	20.73	0.69	0.690	53.05	99-100
19	17/05/2002	N	0.5	21.23	0.278	0.556	42.75	99-100
20	17/05/2002	Y	1	22.23	0.608	0.608	46.75	99-100
21	17/05/2002	N	0.52	22.75	0.28	0.542	41.67	99-100
22	17/05/2002	Y	1	23.75	0.55	0.550	42.29	99-100

A.2.3 Milli-Q Water Test 3

Table A-9. Experimental data

Run nr.	Date	Sonicated (Y/N)	Time (h)	Σ Time (h)	Volume Collected (L)	flowrate (ℓ/h)	Flux (LMH)	Pump speed (rpm)
1	22/05/2002	N	1	1.02	0.907	0.907	69.74	99-100
2	22/05/2002	N	1	1.00	0.928	0.928	71.35	100-101
3	22/05/2002	N	1.05	2.05	0.868	0.827	63.56	100-101
4	22/05/2002	N	1	3.05	0.803	0.803	61.74	100
5	22/05/2002	N	1.08	4.13	0.825	0.762	58.55	100
6	22/05/2002	N	1.05	5.18	0.751	0.715	54.99	100
7	23/05/2002	N	1.08	6.27	0.817	0.754	57.98	99-100
8	23/05/2002	N	1.02	7.28	0.721	0.709	54.53	99-100
9	23/05/2002	N	1	8.28	0.7	0.700	53.82	99-100
10	23/05/2002	N	1	9.28	0.71	0.710	54.59	99-100
11	23/05/2002	Y	1.03	10.32	0.84	0.813	62.50	99-100
12	27/05/2002	N	1.5	11.82	0.99	0.660	50.75	97-98
13	28/05/2002	Y	1	12.82	0.69	0.690	53.05	99-100
14	28/05/2002	N	0.5	13.32	0.33	0.660	50.75	99-100
15	28/05/2002	Y	1	14.32	0.66	0.660	50.75	99-100
16	28/05/2002	N	1.5	15.82	0.91	0.607	46.64	99-100
17	29/05/2002	Y	1	16.82	0.605	0.605	46.52	99-100
18	29/05/2002	N	0.67	17.48	0.398	0.597	45.90	99-100
19	29/05/2002	Y	1	18.48	0.627	0.627	48.21	99-100
20	31/05/2002	N	1	19.48	0.576	0.576	44.29	98-99
21	31/05/2002	Y	1	20.48	0.59	0.590	45.36	99-100

A.3 Tests with Coloured Ground Water from the George Region

A.3.1 First Experimental Run

For flux-data see: [George Water\Flux-data Experimental Run 1.xls](#), [George Water\Prefoul - Experimental Run 1.xls](#), [George Water\Membrane Prep - Experimental Run1.xls](#)

Table A-10. Permeate Quality Analysis for Experimental Run 1

Date	Sample	US/No US	Run Duration	Turbidity	Absorbancy	Conductivity	pH	T for pH	Apparent Colour Test
			(h)	(NTU)		µS/cm		(°C)	Units Pt Co Colour
-	Feed	N/A	N/A	2.01		90	4.35		433
26-Aug	Prefoul1	No US	5.5	0.00	0.423	80	5.09	18.7	69
26-Aug	Prefoul2	No US	5.5	0.00	0.604	83	5.02	18.5	102
28-Aug	Prefoul3	No US	5.5	0.00	0.53	79	5.07	18.4	100
29-Aug	Prefoul4	No US	5.5	0.00	0.564	81	5.11	18.7	109
04-Sep	Run 1	US	1	0.68	0.552	83	4.87	19	117
04-Sep	Run 2	No US	2	0.00	0.461	81	4.84	18.8	118
04-Sep	Run 3	US	1	0.00	0.462	83	4.84	19.2	99
05-Sep	Run 4	No US	2	0.00	0.32	77	5.31	19.1	88
05-Sep	Run 5	US	1	0.00	0.285	78	5.2	19.4	82
05-Sep	Run 6	No US	2	0.00	0.285	76	5.01	19.5	86
05-Sep	Run 7	US	1.5	0.19	0.433	81	4.91	19.6	85
09-Sep	Run 8	No US	2	0.00	0.475	78	5.7	19.5	119
09-Sep	Run 9	US	1.5	0.54	0.367	80	5.41	19.8	75
09-Sep	Run 10	No US	2	0.00	0.368	77	5.18	20.1	62

Table A-11. Retentate Quality Analysis for Experimental Run 1

Date	Sample	US/No US	Run Duration	Turbidity	Absorbancy	Conductivity	pH	T for pH	Apparent Colour Test
			(h)	(NTU)		µS/cm		(°C)	Units Pt Co Colour
-	Feed	N/A	N/A	2.01		90	4.35		433
26-Aug	Prefoul1	No US	5.5	0.00	>3.5	96	4.82	20.3	Too Dark even after diluting 15 ml sample with 10 ml demin water. Values > 500
26-Aug	Prefoul2	No US	5.5	2.13	>3.5	136	4.61	20.5	
28-Aug	Prefoul3	No US	5.5	1.93	>3.5	99	4.7	20.1	
29-Aug	Prefoul4	No US	5.5	0.61	>3.5	98	4.75	20.1	
04-Sep	Run 1	US	1	3.47	>3.5	102	4.62	20.4	
04-Sep	Run 2	No US	2	1.23	>3.5	101	4.6	20.4	
04-Sep	Run 3	US	1	2.26	>3.5	105	4.56	20.4	
05-Sep	Run 4	No US	2	3.45	>3.5	103	4.99	20.5	
05-Sep	Run 5	US	1	1.76	>3.5	104	5	20.5	
05-Sep	Run 6	No US	2	0.03	3.05	96	4.63	20.6	
05-Sep	Run 7	US	1.5	7.46	>3.5	119	4.45	20.7	
09-Sep	Run 8	No US	2	1.33	>3.5	99	5.26	20.7	
09-Sep	Run 9	US	1.5	1.58	>3.5	111	4.98	20.7	
09-Sep	Run 10	No US	2	0.38	>3.5	97	4.8	20.9	

A.3.2 Second Experimental Run

For detailed flux and temperature data see: [George Water\Flux-data Experimental Run 2.xls](#), [George Water\Prefoul - Experimental Run2.xls](#), [George Water\Membrane Prep - Experimental Run2.xls](#)

Table A-12. Membrane preparation with distilled water

Date	Feed material	Run nr	Duration (h)	Back P (kPa(g))	Pump speed (rpm)
16-Sep	Dist Water	1	1	100	70
18-Sep	Dist Water	2	3	100	70
18-Sep	Dist Water	3	3	100	71
18-Sep	Dist Water	4	3	100	70
18-Sep	Dist Water	5	3	100	70
19-Sep	Dist Water	6	3	100	70
19-Sep	Dist Water	7	3	100	70
20-Sep	Dist Water	8	3	100	80
20-Sep	Dist Water	9	3	100	80
26-Sep	Dist Water	10	3	100	80
26-Sep	Dist Water	11	3	100	80
26-Sep	Dist Water	12	3	100	80
27-Sep	Dist Water	13	3	100	80
30-Sep	Dist Water	14	6	100	80
03-Oct	Dist Water	15	4	100	80
04-Oct	Dist Water	16	3	100	80
04-Oct	Dist Water	17	3	100	80
07-Oct	Dist Water	18	6	100	105
07-Oct	Dist Water	19	6	100	105
08-Oct	Dist Water	20	3	100	105
Total Duration:			68	h	

Table A-13. Operating Data

Date	Feed material	Interval nr	Duration (h)	US On/Off	Back P (kPa(g))	Pump speed (rpm)	Retentate Volume (ml)
09-Oct	George	Prefoul	6.00	Off	100	105	150
10-Oct	George	Run 1	1	On	100	90	39
10-Oct	George	Run 2	2	Off	100	100	140
10-Oct	George	Run 3	1	On	100	100	90
10-Oct	George	Run 4	2	Off	100	100	145
10-Oct	George	Run 5	1.5	On	100	100	120
10-Oct	George	Run 6	2	Off	100	100	140
11-Oct	George	Run 7	0.5	On	100	100	120
11-Oct	George	Run 8	2	Off	100	100	140
11-Oct	George	Run 9	0.5	On	100	100	140
11-Oct	George	Run 10	2	Off	100	100	100

Table A-14. Permeate Quality Analysis for Experimental Run 2

Date	Sample	US/No US	Run Duration	Turbidity	Conductivity	pH	T for pH	Apparent Colour Test
			(h)	(NTU)	$\mu\text{S/cm}$		($^{\circ}\text{C}$)	Units Pt Co Colour
09-Oct	Prefoul	No US	6	0.00	63	4.22	23.3	92
10-Oct	Run 1	US	1	0.13	71	4.4	23.4	91
10-Oct	Run 2	No US	2	0.16	75	3.91	23.6	32
10-Oct	Run 3	US	1	0.08	71	4.22	23.8	40
10-Oct	Run 4	No US	2	0.00	69	4.12	23.8	34
10-Oct	Run 5	US	1.5	0.00	71	4.05	23.3	53
10-Oct	Run 6	No US	2	0.10	71	3.96	23.3	37
11-Oct	Run 7	US	1.5	0.19	68	4.15	23.9	27
11-Oct	Run 8	No US	2	0.00	69	4.06	24.5	52
11-Oct	Run 9	US	1.5	0.05	75	3.79	24.2	35
11-Oct	Run 10	No US	2	0.13	74	3.79	24.5	31

Table A-15. Retentate Quality Analysis for Experimental Run

Date	Sample	US/No US	Run Duration	Turbidity	Conductivity	pH	T for pH	Apparent Colour Test
			(h)	(NTU)	µS/cm		(°C)	Units Pt Co Colour
09-Oct	Prefoul	No US	6	23.04	78	3.97	21.6	333
10-Oct	Run 1	US	1	16.75	97	4.18	22.8	463
10-Oct	Run 2	No US	2	3.15	94	4.14	23.1	403
10-Oct	Run 3	US	1	13.51	95	3.88	21.9	354
10-Oct	Run 4	No US	2	3.7	93	3.93	22.7	222
10-Oct	Run 5	US	1.5	13.12	100	3.87	22.7	449
10-Oct	Run 6	No US	2	5.35	95	3.89	22.8	319
11-Oct	Run 7	US	1.5	11.16	97	3.93	23.0	379
11-Oct	Run 8	No US	2	16.56	88	3.87	23.1	227
11-Oct	Run 9	US	1.5	14.04	96	3.88	23.6	340
11-Oct	Run 10	No US	2	29.97	94	3.8	23.5	323
								3 ml sample 27 ml demin water

Table A-16. Temperature data

Time (h)	T (°C)
0.5	40
1.0	46.5
1.0	40.2
3.3	23
3.3	22.9
3.9	42.1
4.3	45.5
4.3	38.7
4.8	28.3
5.4	24.1
5.9	22.6
6.4	22
6.4	21.9
6.9	39.7
7.6	45.2
8.0	46.9
8.0	43.8
8.6	28.9
9.1	23.9
9.6	22.4
9.9	21.7
10.0	21.7
10.6	40.7
11.1	44.7
11.5	46.7
11.5	40.9
11.6	36.5
13.0	23.6
13.5	23.2
13.5	23.2
13.9	35.1
14.1	41.8
14.5	46.5
15.1	48.3
15.1	48.3
15.1	44.4
15.6	28.6
16.1	25
16.3	24.1
17.1	25

Table A-17. Temperature statistics

T (°C)	
Mean	33.965
Median	35.8
Mode	46.5
Range	26.6
Minimum	21.7
Maximum	48.3
Count	40

A.4 Tests with Water from the Steenbras Dam

A.4.1 First Experimental Run

Table A-18. Membrane preparation with distilled water

Date	Feed material	Run	Duration (h)	Back P (kPa(g))	Pump speed (rpm)
24-Mar	Dist Water	1	1	100	115
24-Mar	Dist Water	2	17	100	115
25-Mar	Dist Water	3	2	100	125
25-Mar	Dist Water	4	11	100	125
25-Mar	Dist Water	5	2.5	100	125
25-Mar	Dist Water	6	9.5	100	125
25-Mar	Dist Water	7	2	100	125
Total duration:			45h		

Table A-19. Prefouling of the membranes

Date	Feed material	Interval nr	Duration (h)	US On/Off	Back P (kPa(g))	Pump speed (rpm)	Retentate Volume (ml)
26-Mar	Steenbras	1	4	Off	100	130	130
26-Mar	Steenbras	2	5	Off	100	130	30
27-Mar	Steenbras	3	3	Off	100	130	30
27-Mar	Steenbras	4	5	Off	100	138	45
27-Mar	Steenbras	5	6	Off	100	140	240

Table A-20. Operating Data

Date	Feed material	Interval nr	Duration (h)	US On/Off	Back P (kPa(g))	Pump speed (rpm)	Retentate Volume (ml)	T _{tank(begin)} (°C)	T _{tank(end)} (°C)	T _{module(begin)} (°C)	T _{module(end)} (°C)	ΔT _{tank} (°C)	ΔT _{module} (°C)
28-Mar	Steenbras	1	0.5	On	100	135	20	20	20.5	23.7	39.9	0.5	16.2
28-Mar	Steenbras	2	2	Off	100	135	70	20.5	21	39	25.3	0.5	-13.7
28-Mar	Steenbras	3	0.5	On	100	135	30	21	21.5	25.3	41.6	0.5	16.3
30-Mar	Steenbras	4	2	Off	100	135	90	12	15	25	24.1	3	-0.9
01-Apr	Steenbras	5	1	On	100	135	80	21	21	24.6	43.6	0	19
01-Apr	Steenbras	6	2	Off	100	135	70	21	21	41.5	25.1	0	-16.4
01-Apr	Steenbras	7	1	On	100	110	50	11	10	25	44.2	-1	19.2
01-Apr	Steenbras	8	2.25	Off	100	108	90	10	13.5	40.3	23.9	3.5	-16.4
01-Apr	Steenbras	9	1.5	On	100	110	180	14	16	24	43.9	2	19.9
01-Apr	Steenbras	10	2	Off	100	115	110	16	19	42.1	24.3	3	-17.8
01-Apr	Steenbras	11	1.5	On	100	118	50	19	20	24.2	44.8	1	20.6
02-Apr	Steenbras	12	2	Off	100	118	60	20	21.5	25.1	26	1.5	0.9

Table A-21. Temperature data

Time (h)	T (°C)	abs ΔT (°C)
0	23.7	
0.5	39.9	16.2
2.54	25.3	14.6
3.1	41.6	16.3
5.1	24.1	17.5
6.2	43.6	19.5
8.3	25.1	18.5
9.3	44.2	19.1
11.6	23.9	20.3
13.1	43.9	20
15.1	24.3	19.6
16.6	44.8	20.5
18.6	26	18.8

Table A-22. Temperature Statistics

T (°C)	
Mean	33.11
Median	26
Range	21.1
Minimum	23.7
Maximum	44.8
Count	13

A.4.2 Second Experimental Run

Table A-23. Membrane preparation with distilled water

Date	Feed material	Run nr	Duration (h)	Back P (kPa(g))	Pump speed (rpm)
03-Apr	Dist Water	1	1	100	125
03-Apr	Dist Water	2	2	100	110
05-Apr	Dist Water	3	18	100	110
05-Apr	Dist Water	4	1	100	111
05-Apr	Dist Water	5	8	100	111
05-Apr	Dist Water	6	1.5	100	111
05-Apr	Dist Water	7	2.7	100	111
07-Apr	Dist Water	8	5.8	100	120
07-Apr	Dist Water	7	2	100	120
Total Duration:			42 h		

Table A-24. Prefouling with Steenbras dam water

Date	Feed material	Interval nr	Duration (h)	Back P (kPa(g))	Pump speed (rpm)	Retentate Volume (ml)
08-Apr	Steenbras	1	6	100	125	275
08-Apr	Steenbras	2	7	100	128	140
08-Apr	Steenbras	3	2	100	128	-
09-Apr	Steenbras	4	7	100	128	180
09-Apr	Steenbras	5	2	100	130	120
Total Duration:			24 h			

Table A-25. Operating data

Date	Feed material	Interval no	Duration (h)	US On/Off	Back P (kPa(g))	Pump speed (rpm)	Retentate Volume (ml)	T _{tank(begin)} (°C)	T _{tank(end)} (°C)	T _{module(begin)} (°C)	T _{module(end)} (°C)	ΔT _{module} (°C)
09-Apr	Steenbras	1	0.65	On	100	130	50	14	16	23.7	41	17.3
09-Apr	Steenbras	2	2	Off	100	130	-	16	17.5	40.3	23.3	-17
09-Apr	Steenbras	3	0.57	On	100	130	40	17.5	18.5	23.2	41.1	17.9
09-Apr	Steenbras	4	2	Off	100	130	40	18.5	19	40.5	22.7	-17.8
09-Apr	Steenbras	5	1	On	100	130	50	19	20	22.7	44.2	21.5
09-Apr	Steenbras	6	2	Off	100	130	40	20	19.5	40.9	22.4	-18.5
10-Apr	Steenbras	7	1	On	100	130	40	19	19	21.2	40.5	19.3
10-Apr	Steenbras	8	2.5	Off	100	114	70	19	19.5	36.6	23	-13.6
10-Apr	Steenbras	9	1	On	100	115	60	19.5	20	23	43.5	20.5
11-Apr	Steenbras	10	2	Off	100	120	70	19	19	21.6	22.9	1.3
11-Apr	Steenbras	11	1.5	On	100	120	40	19	19.5	22.9	46	23.1
11-Apr	Steenbras	12	2	Off	100	120	40	19.5	20	44.2	23.6	-20.6
11-Apr	Steenbras	13	1.5	On	100	120	50	20	20	23.5	45.3	21.8
11-Apr	Steenbras	14	2	Off	100	120	50	20	20.5	41.9	22.6	-19.3

Table A-26. Temperature data

Time (h)	T (°C)	abs ΔT (°C)
0.00	23.7	-
0.28	33.2	9.5
0.65	41	7.8
0.67	40.3	0.7
2.66	23.3	17
2.67	23.2	0.1
2.93	32.2	9
3.24	41.1	8.9
3.26	40.5	0.6
5.30	22.7	17.8
5.30	22.7	0
5.83	40.6	17.9
6.10	43.3	2.7
6.40	44.2	0.9
6.40	40.9	3.3
8.53	22.4	18.5
8.54	21.4	1
8.54	21.2	0.2
8.81	30.2	9
9.09	37.8	7.6
9.67	40.5	2.7
9.69	36.9	3.6
12.20	23	13.9
12.20	23	0
12.53	35.2	12.2
12.71	40.3	5.1
13.02	43.1	2.8
13.22	43.4	0.3
13.22	21.6	21.8
15.40	22.9	1.3
15.40	22.9	0
15.71	36.7	13.8
16.17	45.3	8.6
16.72	46.1	0.8
16.92	46	0.1
16.92	44.2	1.8
16.93	23.4	20.8
17.01	23.3	0.1
19.57	45.2	21.9
19.80	45.8	0.6
19.95	45.7	0.1
20.24	45.5	0.2
20.49	45.3	0.2
20.50	41.9	3.4
22.51	22.6	19.3

Table A-27. Temperature statistics

T (°C)	
Mean	34.57
Median	37.8
Mode	40.3
Range	24.9
Minimum	21.2
Maximum	46.1
Count	45

A.5 Tests With Dextran**Table A-28.** Membrane preparation with distilled water

Date	Feed material	Run nr	Duration (h)	Back P (kPa(g))	Pump speed (rpm)
14-Apr	Dist Water	1	2	100	118
14-Apr	Dist Water	2	12	100	125
15-Apr	Dist Water	3	2	100	125
15-Apr	Dist Water	4	8	100	125
15-Apr	Dist Water	5	2	100	125
15-Apr	Dist Water	6	13	100	125
16-Apr	Dist Water	7	2.0	100	110
16-Apr	Dist Water	8	6.0	100	110
16-Apr	Dist Water	9	3.0	100	115
29-Apr	Dist Water	10	2.0	100	115
Total Duration:			52	h	

Table A-29. Operating Data

Date	Feed material	Interval nr	Duration (h)	US On/Off	Back P (kPa(g))	Pump speed (rpm)	Retentate Volume (ml)	T _{tank(begin)} (°C)	T _{tank(end)} (°C)	T _{module(begin)} (°C)	T _{module(end)} (°C)	ΔT _{module} (°C)
29-Apr	Dextran	Prefoul	2	Off	100	115	50	21	21.5	21	21	0
30-Apr	Dextran	1	1	On	100	115	10	21	21.5	24.2	54.2	30
30-Apr	Dextran	2	1	Off	100	114	40	21.5	22	51.4	27.8	-23.6
30-Apr	Dextran	3	0.5	On	100	115	10	22	22	27.4	46.1	18.7
30-Apr	Dextran	4	0.5	Off	100	115	5	22	22	45.6	31.8	-13.8

Table A-30. Temperature data

Time (h)	T (°C)	abs ΔT (°C)
2.00	24.2	
2.17	30.3	6.1
2.17	30.3	0
2.33	41.3	11
2.49	48.4	7.1
2.67	53.5	5.1
3.05	54.2	0.7
3.06	54	0.2
3.06	51.7	2.3
4.06	27.8	23.9
4.07	27.4	0.4
4.28	33	5.6
4.43	40.7	7.7
4.58	46.1	5.4
4.58	45.6	0.5
5.08	31.8	13.8

Table A-31. Temperature statistics

T (°C)	
Mean	40.02
Median	41
Mode	30.3
Range	30
Minimum	24.2
Maximum	54.2
Count	16

A.6 Relationship between Temperature and Viscosity

Table A-32. Density and Viscosity of pure water as a function of temperature at 100 kPa

T (°C)	Density kg/m³	Viscosity mPa.s
0	999.84	1.793
10	999.7	1.307
20	998.21	1.002
25	996.93	0.89985
30	995.65	0.7977
40	992.22	0.6532
50	988.03	0.547
60	983.2	0.4665
70	977.78	0.404
80	971.82	0.3544
90	965.35	0.3145
100	958.4	0.2818

Table A-33. Calculation of normalised temperature and flux

Time (h)	T (°C)	μ @ T ($\mu\text{Pa}\cdot\text{s}$)	Measured Flux ($\text{kg}/\text{m}^2\cdot\text{h}$)	Normalised T (°C)	μ @ T ($\mu\text{Pa}\cdot\text{s}$)	Normalised Flux ($\text{kg}/\text{m}^2\cdot\text{h}$)		ΔT (°C)
0.5	40	653.2	30.81	33.7	738.50	27.25		
1.0	46.5	581	32.51	40.2	650.60	29.03		6.5
1.0	40.2	650.6	22.12	33.9	735.50	19.57		6.3
3.3	23	933	22.44	23.0	933.00	22.44		17.2
3.3	22.9	935.2	13.93	22.9	935.20	13.93		0.1
3.9	42.1	627.9	28.32	35.3	715.50	24.85		19.2
4.3	45.5	591	30.25	38.7	669.60	26.70		3.4
4.3	38.7	669.6	8.87	31.9	766.60	7.74		6.8
4.8	28.3	827.6	22.68	28.3	827.60	22.68		10.4
5.4	24.1	909	21.29	24.1	909.00	21.29		4.2
5.9	22.6	941.8	20.58	22.6	941.80	20.58		1.5
6.4	22	955	20.10	22.0	955.00	20.10		0.6
6.4	21.9	957.4	5.95	21.9	957.40	5.95		0.1
6.9	39.7	662.1	25.77	36.6	697.20	24.47		17.8
7.6	45.2	594.6	28.70	42.1	627.90	27.17		5.5
8.0	46.9	577	29.48	43.8	609.20	27.92		1.7
8.0	43.8	609.2		40.7	644.60			3.1
8.6	28.9	816.8		28.9	816.80			14.9
9.1	23.9	913.2		23.9	913.20			5
9.6	22.4	946.2		22.4	946.20			1.5
9.9	21.7	962.2		21.7	962.20			0.7
10.0	21.7	962.2	4.01	21.7	962.20	4.01		0
10.6	40.7	644.6	25.77	32.0	765.00	21.71		19
11.1	44.7	599.3	27.72	36.0	705.00	23.57		4
11.5	46.7	579	28.48	38.0	678.00	24.32		2
11.5	40.9	642.2	0.55	32.2	761.80	0.47	8.7	5.8
11.6	36.5	695.5	15.71	27.8	836.80	13.06		4.4
13.0	23.6	919.8	18.12	23.6	919.80	18.12		12.9
13.5	23.2	928.6	17.75	23.2	928.60	17.75		0.4
13.5	23.2	928.6	2.08	23.2	928.60	2.08		0
13.9	35.1	718.5	21.62	31.2	777.80	19.97		11.9
14.1	41.8	631.4	23.60	37.9	679.40	21.93		6.7
14.5	46.5	581	25.69	42.6	622.40	23.98		4.7
15.1	48.3	563	26.84	44.4	602.60	25.08		1.8
15.1	48.3	563	26.79	44.4	602.60	25.03		0
15.1	44.4	602.6	2.77	40.5	647.00	2.58		3.9
15.6	28.6	822.2	18.26	28.6	822.20	18.26		15.8
16.1	25	891	17.38	25.0	891.00	17.38		3.6
16.3	24.1	909	17.00	24.1	909.00	17.00		0.9
17.1	25	891	16.09	25.0	891.00	16.09		0.9

Cells highlighted in green indicate sonicated intervals; cells highlighted in blue indicate the ΔT for the instantaneous temperature drop associated with switching off the sonotrode.

B.Experimental Set-up



Figure B-1. Close-up of membrane module with ultrasonic probe



Figure B-2. The capillary ultrafiltration membranes – ends were epoxied into the 10 mm stainless steel tubing



Figure B-3. Close-up of the hollow fibres



Figure B-4. Lab-scale setup showing permeate collection and measurement via scale.